NOVEL ROLE OF THE *Agrobacterium* VIRULENCE EFFECTOR PROTEIN VirE2 IN MODULATING PLANT GENE EXPRESSION

by

Rachelle Lapham

A Dissertation

Submitted to the Faculty of Purdue University

In Partial Fulfillment of the Requirements for the degree of

Doctor of Philosophy

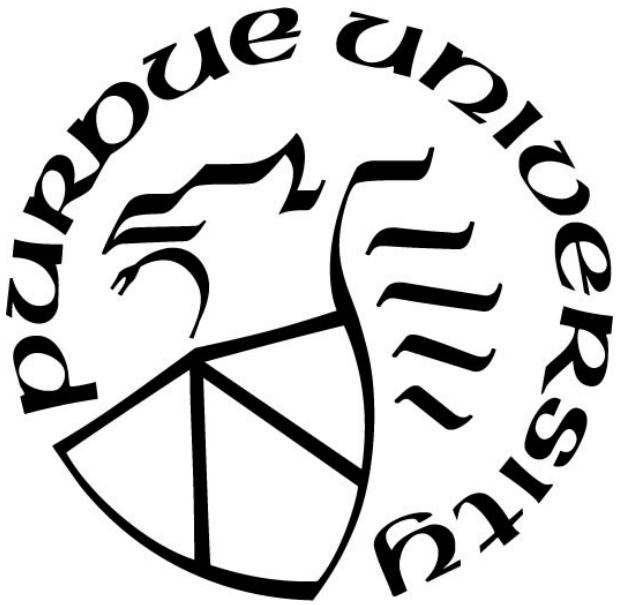

Department of Biological Sciences

West Lafayette, Indiana

August 2019

THE PURDUE UNIVERSITY GRADUATE SCHOOL
STATEMENT OF COMMITTEE APPROVAL

Dr. Stanton B. Gelvin, Chair
Department of Biological Sciences
Dr. Zhao-Qing Luo
Department of Biological Sciences
Dr. Chris Staiger
Department of Biological Sciences
Department of Botany and Plant Pathology
Dr. Jianxin Ma
Department of Agronomy

Approved by:

Dr. Janice Evans
Head of the Graduate Program

For my husband who is my greatest inspiration, support, and distraction when I need it the most

ACKNOWLEDGMENTS

CHAPTER 2

We would like to thank Dr. Xiao-Hung Zhu and Ms. Wen-Shan Liu for their help in constructing the single-guide RNA (sgRNA) vectors. Dr. Lan-Ying Lee cloned the sgRNA vectors along with some of the vectors used for confocal imaging. Dr. Lan-Ying Lee also performed all the confocal imaging and protoplast preparations (Figures 2.2, 2.7, and 2.8). Confocal imaging was performed using the Bindley Bioscience Imaging Facility at Purdue University. Sequence analysis was performed by the Purdue Genomics Core Facility. Dr. Sanghun Lee performed the *Botrytis cinerea* and *Pseudomonas syringae* disease assays (Figure 2.10). Dr. Daisuke Tsugama contributed reagents. Undergraduate researchers Eder Xhako, Laurel Jahn, Lauren Huemmer, Emily Traxler, and Erica Wolfe helped with the genotyping of the mutant lines used in the study. Dr. Stanton Gelvin, Dr. Lan-Ying Lee, Dr. Tesfaye Mengiste, and Dr. Daisuke Tsugama provided suggestions and advice during the writing of the manuscript.

CHAPTER 3

The VirE2-Venus, VirE2-Venus-NLS, and VirE2-Venus-sNLS plasmids were cloned by Dr. Lan-Ying Lee, Fang-Yu Hsu, and Eder Xhako. The overexpression vectors were constructed by Dr. Lan-Ying Lee. Inducible transgenic VirE2-Venus and VirE2-Venus-NLS plants were generated by Fang-Yu Hsu and Eder Xhako. Confocal images of plant roots were taken by Dr. Lan-Ying Lee (Figure 3.2). All confocal imaging was performed at the Purdue Bindley Imaging Facility and Dr. Andy Schaber provided valuable advice. Eder Xhako performed the transformation assays on inducible VirE2-Venus and VirE2-Venus-NLS plants (Figure 3.3). Esteban Ganan-Gomez assisted in performing the transformation assays of constitutive overexpression lines (Figure 3.12). RNA-seq was performed by the Purdue Genomics Core and the Cornell University Institute of Biotechnology Genomics Facility. Analysis of the RNA-seq data was performed in part by the Purdue Bioinformatics Core (Second Study). Protein extraction and proteomics were performed by the Purdue Proteomics Core Facility. Proteomics Core leader Dr. Uma Aryal assisted with the analysis and interpretation of the proteomics data.

TABLE OF CONTENTS

LIST OF TABLES

LIST OF FIGURES

ABSTRACT

Author: Lapham, Rachelle, A. PhD
Institution: Purdue University
Degree Received: August 2019
Title: Novel Role of The *Agrobacterium* Virulence Effector Protein VirE2 in Modulating Plant Gene Expression
Committee Chair: Stanton Gelvin

Agrobacterium tumefaciens transfers virulence effector proteins to infected host plants to facilitate the transfer and trafficking of a piece of its tumor inducing (Ti) plasmid, (T-[transfer] DNA), into and through plant cells. T-DNA integrates into the host genome where it uses the host's gene expression machinery to express transgenes. Scientists have used this process to insert beneficial genes into plants by replacing native T-DNA in the bacteria with engineered T-DNA, making *Agrobacterium*-mediated transformation the preferred method for crop genetic engineering. In spite of its wide-spread use in research and agriculture, we still do not have a complete understanding of the transformation process. Consequently, many important crop species remain highly resistant to transformation. One of my lab's major goals is to define the molecular interactions between *Agrobacterium* and its host plants which mediate transformation. I study the role of the *Agrobacterium* effector protein, VirE2, which is important for plant transformation. VirE2 likely coats the transferred DNA (T-DNA) after it enters the plant cell and protects it from degradation. VIP1 is a host transcription factor that interacts with VirE2 and is involved in activating plant defense responses. VIP1 localizes to both the cytoplasm and the nucleus. Under stress, VIP1 localizes to the nucleus where it activates expression of defense response genes. This observation led to the model that T-DNA-bound VirE2 binds VIP1 and uses VIP1 nuclear localization to deliver T-DNA into the nucleus (the "Trojan Horse" model). In contrast to this model, our lab has obtained data showing that VirE2 holds at least a portion of the VIP1 pool outside the nucleus. We also showed that VIP1 and its homologs are not necessary for transformation. VirE2 interacts with several host proteins in addition to VIP1, and these interactions could lead to changes in host gene expression and protein levels, possibly facilitating transformation. We investigated this model by placing VirE2 under the control of an inducible promoter in *Arabidopsis* and performing RNA-seq and proteomics under non-induced and

induced conditions, and in the presence of *Agrobacterium* to determine its individual effect on plant RNA and protein levels during infection. Some genes differentially expressed after VirE2 induction are known to be important for transformation. Knockout mutant lines of some VirE2 differentially expressed genes showed altered transformation phenotypes. Protein levels of genes known to be important for transformation were also increased in response to VirE2 induction, and overexpression of some of these genes resulted in increased transformation susceptibility. We therefore conclude that VirE2 modulates both plant RNA and protein levels to facilitate transformation.

CHAPTER 1: INTRODUCTION

Virulent strains of the soil bacterium *Agrobacterium tumefaciens* cause the plant tumorous disease crown gall. *A. tumefaciens* transfers five virulence effector proteins (VirD2, VirD5, VirE2, VirE3, and VirF) to infected host plants to facilitate the transfer and trafficking of a piece of its tumor inducing (Ti) plasmid, T-(transfer) DNA. T-DNA molecules travel into and traffic within plant cells and may eventually integrate into the host genome. Integrated T-DNA uses the host's gene expression machinery to express transgenes. Scientists have used this process to insert genes into plants by replacing native T-DNA in the bacteria with engineered T-DNA. *Agrobacterium*-mediated genetic transformation is the preferred method for plant genetic engineering (Gelvin, 2003, 2012).

VirE2 is an *Agrobacterium* effector protein that is important for plant transformation (Gelvin, 2003, 2012), and *virE2* mutant *Agrobacterium* strains are highly attenuated in virulence (Stachel and Nester, 1986). As a single-strand DNA binding protein, VirE2 likely coats T-DNA after it enters the plant cell to protect it from degradation (Yusibov et al., 1994; Rossi et al., 1996) and may assist in its nuclear import (Ziemienowicz et al., 2001; Tzfira et al., 2001). VIP1 and VIP2 (VirE2-interacting proteins 1 and 2) are two host transcription factors that interact with VirE2 (Tzfira et al., 2001; Pitzschke et al., 2009; Anand et al., 2007). Under stress, VIP1 localizes to the nucleus (Pitzschke et al., 2009; Tsugama et al., 2012, 2013, 2014, 2016a, 2016b) where it activates expression of defense response genes (Pitzschke et al., 2009). This observation led to the model that T-DNA-bound VirE2 binds VIP1 and uses VIP1 nuclear localization to deliver T-DNA into the nucleus (the "Trojan Horse" model; Djamei et al., 2007). In contrast to this model, our laboratory showed that VirE2 holds at least a portion of the VIP1 pool outside the nucleus (Shi et al., 2014). We hypothesized that in addition to VirE2's proposed structural role in T-DNA trafficking, VirE2 also prevents localization of VIP1, VIP2, and/or other transcription factors to the nucleus during *Agrobacterium* infection. This could result in changes in expression of their respective downstream target genes and suppression of defense responses, facilitating transformation. As detailed in later chapters, this hypothesis may not fully explain the effect of VirE2 on host gene expression.

The importance and role of VIP1 in *Agrobacterium*-mediated transformation are controversial (Tzfira et al., 2001; Shi et al., 2014; Lapham et al., 2018). Previous studies showed

that transgenic tobacco lines expressing antisense constructs targeting *VIP1,* and the *A. thaliana* T-DNA insertion mutant *vip1-1*, had decreased susceptibility to stable transformation compared to that of wild-type plants (Tzfira et al., 2001; Li et al., 2005). Overexpression of *VIP1* resulted in increased transformation susceptibility in tobacco (Tzfira et al., 2001). Taken together, these results suggested that VIP1 plays a role in transformation (Tzfira et al., 2001). Conversely, Shi et al. (2014) performed quantitative transformation assays with the *vip1-1* mutant and with 59 *A. thaliana VIP1* overexpressing lines and observed no effect on transformation susceptibility, suggesting that VIP1 is not important for *Agrobacterium*-mediated transformation.

The *vip1-1* mutant still produces ~80% of the VIP1 protein, including its bZIP DNA binding domain (Li et al., 2005). Because this domain may be important for VIP1 function, we used CRISPR technology to generate a homozygous mutant, *vip1-2,* that produces a smaller protein lacking the bZIP DNA binding domain. Transient and stable transformation assays showed no effect of this mutation on *Agrobacterium*-mediated transformation. In addition, transformation assays of single and multiple null mutant lines of *VIP1* homologs, and transgenic lines overexpressing VIP1 fused to a SRDX repression domain (Hiratsu et al., 2002), also had no major effect on transformation. We therefore concluded that *VIP1* and its homologs are not necessary for *Agrobacterium*-mediated transformation. However, *VIP1* may play a role in defense responses against the fungus *Botrytis cinerea*, in abscisic acid (ABA) signaling, and growth under salt stress conditions (Lapham et al., 2018; Chapter 2 of this dissertation) as well as regulate osmosensory and touch responses in roots (Tsugama et al. 2012, 2014, 2016).

Expression of VirE2 in a plant can restore transformation by a *virE2* mutant *Agrobacterium* strain (Citovsky et al., 1992; Simone et al., 2001). These data suggest that VirE2's major function in transformation occurs in the plant, but where VirE2 functions within the plant cell remains unclear. Some studies showed that N-terminally tagged VirE2 localized to the nucleus (Citovsky et al., 1992, 1994, 2004; Tzfira and Citovsky, 2001; Tzfira et al., 2001; Li et al., 2005), whereas other studies showed that both N-terminally and C-terminally tagged VirE2 localized to the cytoplasm (Bhattacharjee et al., 2008; Shi et al., 2014). Bhattacharjee et al. (2008) showed that only C-terminally tagged VirE2, but not the N-terminally tagged protein, could complement a *virE2* mutant strain to restore efficient transformation. VirE2 internally tagged with a small fragment of GFP could be delivered from bacteria into plant cells and would form filamentous structures (Li et al., 2014; Li and Pan, 2017). The majority of these structures

localized to the cytoplasm, but some were also found in the nucleus (Li et al., 2014; Li and Pan, 2017). Li and Pan (2017) also observed that bacterial-delivered VirE2 associated with the host plasma membrane and endomembrane compartments, and could bind clatherin-associated sorting proteins. Similarly, Roushan et al. (2018) used phiLOV2.1 to tag VirE2 internally. phiLOV2.1 has improved fluorescence and photostability compared to the LOV domain from which it is derived (Christie et al., 2012a,b) and has been used to visualize protein translocation from *Shigella flexneri* into mammalian cells (Gawthorne et al., 2016). The fluorescent LOV domain of plant blue-light receptor kinases, or phototropins, is regulated by **L**ight, **O**xygen, or **V**oltage (Huala et al., 1997; Buckley et al., 2015). phiLOV2.1-tagged VirE2 localized to the cytoplasm of *A. thaliana* roots and *Nicotiana tabacum* leaves after being transferred from *Agrobacterium* (Roushan et al., 2018). A summary of the VirE2 subcellular localization results from previous studies can be found in Table 1.1.

Table 1.1 Summary of subcellular localization results of VirE2 in previous studies

Study [Figure]	**Localization Result**	**Tagging Method [Tag]**	**VirE2 Expression Method**
Citovsky et al., 1992 [Figure 2]	Nuclear	N-terminal [β-glucuronidase: GUS]	Transiently expressed in *N. tabacum* BY-2 protoplasts after transfecting with DNA encoding the fused protein
Citovsky et al., 1994 [Figure 1]	Nuclear	N-terminal [GUS]	Transiently expressed in *Zea mays* leaves after delivering the DNA encoding the fused protein via particle bombardment
Citovsky et al., 2004 [Figure 1]	Nuclear	N-terminal [Lissamine rhodamine or fluorescein isothiocyanate]	Purified protein expressed in *E.coli* and microinjected into *N. benthamiana* leaves
Tzfira and Citovsky, 2001 [Figures 1 and 2]	Nuclear	N-terminal [GUS]	Transiently expressed in *N. tabacum* leaves and epidermal onion cells after delivering the DNA encoding the fused protein via particle bombardment

Table 1.1 continued

Study [Figure]	Localization Result	Tagging Method [Tag]	VirE2 Expression Method
Tzfira et al., 2001 [Figure 8]	Nuclear	N-terminal [GUS]	Transiently expressed in *N. tabacum* leaves after delivering the DNA encoding the fused protein via particle bombardment
Bhattacharjee et al., 2008 [Figure 10 and 11]	Cytoplasmic	N-terminal and C-terminal [YFP]; VirE2-VirE2 BiFC, C-terminally tagged [half YFP]	Stably expressed in transgenic *A. thaliana* roots and transiently expressed in *N. tabacum* BY-2 protoplasts after transfecting with DNA encoding the fused proteins
Grange et al., 2008 [Figure 4]	Cytoplasmic	C-terminal [Hemaglutinin: HA]	Transiently expressed in *N. tabacum* BY-2 protoplasts after delivering the DNA encoding the fused protein via particle bombardment
Lee et al., 2008 [Figures 3, 4, and 5]	Cytoplasmic	C-terminal [half cyan fluorescent protein (CFP) VirE2-VirE2 BiFC]	Transiently expressed in *N. tabacum* BY-2 protoplasts after transfecting with DNA encoding the fused protein and transiently expressed in epidermal onion cells after delivering the DNA encoding the fused protein via particle bombardment
Gelvin, S.B., 2010 [Figure 2]	Cytoplasmic	C-terminal [YFP]	Stably expressed in transgenic *A. thaliana* roots and leaves
Lee et al., 2012 [Figure 1]	Cytoplasmic	C-terminal [VirE2-VirE2 BiFC using half Venus/YFP, half CFP tags]	Transiently expressed in *A. thaliana* protoplasts after transfecting with DNA encoding the fused proteins

Table 1.1 continued

Study [Figure]	Localization Result	Tagging Method [Tag]	VirE2 Expression Method
Lee, L.-Y. and Gelvin, S.B., 2014 [Figure 1]	Cytoplasmic	C-terminal [VirE2-VirE2 BiFC using half YFP tags]	Transiently expressed in *N. tabacum* BY-2 protoplasts transfected with DNA encoding the fused proteins
Shi et al., 2014 [Figures 4, 5 and 7]	Cytoplasmic	C-terminal [Venus, VirE2-VirE2 BiFC using half Cerulean and half CFP]	Transiently expressed in *N. tabacum* BY-2 and *A. thaliana* protoplasts transfected with DNA encoding the fused protein, transgenic *A. thaliana* roots stably overexpressing tagged VirE2, and transiently expressed Agro-infiltrated *N. benthamiana* leaves
Lapham et al., 2018 [Figure 8D]	Cytoplasmic	C-terminal [Venus]	Transiently expressed in *N. tabacum* BY-2 protoplasts transfected with DNA encoding the fused protein
Li et al., 2014 [Figures 1D, 2, 3, and 4A	Mostly cytoplasmic with some nuclear-localized filamentous structures observed	Internal [Split green fluorescent protein: GFP11]	Expressed in *Agrobacterium* before infiltrating *N. benthamiana* leaves
Li and Pan, 2017 [Figure 1, 2, and 3]	Mostly cytoplasmic with some nuclear-localized filamentous structures observed	Internal [Split GFP]	Expressed in *Agrobacterium* before infiltrating *N. benthamiana* leaves
Roushan et al., 2018 [Figures 4 and 5]	Cytoplasmic	Internal [phiLOV2.1]	Expressed in *Agrobacterium* before infecting *A. thaliana* roots and *N. benthamiana* leaves

To determine where VirE2 must localize within the plant cell to facilitate transformation, we generated plants which expressed either C-terminally tagged VirE2-Venus (cytoplasmic localized) or VirE2-Venus plus a nuclear localization signal (NLS; nuclear localized) and

infected them with a *virE2* mutant *Agrobacterium* strain. Cytoplasmic, but not nuclear, localized VirE2 was able to complement the *virE2* mutant strain to effect transformation, indicating that VirE2's major function in transformation occurs in the cytoplasm.

We investigated possible functions of VirE2 in transformation other than its proposed role in T-DNA binding. VirE2 interacts with various plant proteins (Lee et al., 2008, 2012) in addition to VIP1 and VIP2 (Tzfira et al., 2001; Anand et al., 2007; Pitzschke et al., 2009). We hypothesized that these interactions could lead to changes in plant gene expression or plant protein levels, perhaps facilitating transformation. In addition to the effector protein VirE2, the *Agrobacterium* effector proteins VirD5, VirE3, and VirF interact with plant proteins, resulting in changes to plant gene expression (Lacroix et al., 2005; García-Rodríguez et al., 2006; Niu et al., 2015) or protein levels (Schrammeijer et al., 2001; Tzfira et al., 2004; Magori and Citovsky, 2011; Wang et al., 2014; García-Cano et al., 2015; Wang et al., 2018).

VirD5 is a putative transcriptional activator which interacts with several plant proteins, including VIP2 (Wang et al., 2018), to prevent degradation of the proteins which coat the T-DNA (Wang et al., 2014) and to inhibit the action of some host proteins, thus facilitating transformation (Wang et al., 2018). VirD5 may also prevent the degradation of VirF via the plant proteasome (Magori and Citovsky, 2011).

The *Agrobacterium* effector protein VirE3 was proposed to act as a transcriptional activator in plants (García-Rodríguez et al., 2006). Inducible overexpression of VirE3 in *A. thaliana* plantlets resulted in differential expression of more than 900 genes (Niu et al., 2015). Some of these changes may result from VirE3's interaction with the plant general transcription factor IIB (TFIIB)-related protein pBrp (García-Rodríguez et al., 2006) which, under certain forms of stress, moves from the surface of plastids to the nucleus to activate transcription of its target genes (Lagrange et al., 2003). Niu et al. (2015) showed that VirE3 expression caused some molecules of pBrp to relocalize from the plastid to the nucleus, and that pBrp was required for VirE3-induced changes in expression of several genes.

VirF interacts with ARABIDOPSIS SKP1-LIKE PROTEIN (ASK1) which is involved in targeted proteolysis (Schrammeijer et al., 2001), and is a subunit of the Skp1-Cdc53-cullin-F-box (SCF) complex. VIP1 is destabilized in the presence of VirF in both yeast and plant cells (Tzfira et al., 2004), and VirF may function in uncoating VirE2 from T-strands prior to T-DNA integration (Tzfira et al. 2004; Zaltsman et al., 2013). Both VirF and VIP1-BINDING F-BOX

PROTEIN (VBF), a plant protein which functionally complements VirF, interact with the SCF complex and promote the degradation of VIP1 and VirE2, perhaps helping facilitate T-DNA integration and transformation (Zaltsman et al., 2010; Zaltsman et al., 2013). VirF also interacts with two *Arabidopsis* trihelix-domain transcription factors, VBF3 and VBF5, which could also lead to changes in plant gene expression to facilitate transformation (García-Cano et al., 2015).

Other bacterial plant pathogens, such as *Pseudomonas syringae* and *Xanthomonas spp.*, manipulate plant gene expression and protein levels to promote infection (Dodds and Rathjen, 2010). *P. syringae* effectors target host signaling proteins to suppress defense responses (Xiang et al., 2008; Göhre et al., 2008) and inhibit stomatal closure to promote virulence (Axtell and Staskawicz, 2003; Mackey et al., 2003; Liu et al., 2009; Wilton et al., 2010). *P. syringae* can also manipulate host hormone signaling pathways (Cui et al., 2005; de Torres-Zabala et al., 2007) and systemic plant defenses to promote secondary infections (Cui et al., 2005). *Xanthomonas* effector proteins directly bind to the promoters of plant genes either to enhance or repress their transcription (Schornack et al., 2005; Römer et al., 2007; Kim et al., 2008) as well as to destabilize plant transcription factors involved in promoting senescence and bacterial defense responses (Kim et al., 2013).

We propose that VirE2 interacts with plant proteins to alter plant gene expression or protein levels, thereby facilitating transformation. To investigate this possibility, we performed RNA-seq and proteomics analyses on transgenic *Arabidopsis thaliana* roots inducibly expressing VirE2 in the presence of an avirulent *Agrobacterium* strain. Defense response genes and genes known to be important for transformation were differentially expressed in the presence of VirE2. Knockout mutant lines of some of these genes exhibited altered transformation phenotypes. In addition, proteins known to be important for transformation were more prevalent after VirE2 induction. Taken together, our results suggest that VirE2 alters the steady-state levels of specific plant genes and proteins to facilitate transformation.

References

Anand, A., Krichevsky, A., Schornack, S., Lahaye, T., Tzfira, T., Tang, Y., Citovsky, V., and Mysore K.S. (2007) *Arabidopsis* VirE2 INTERACTING PROTEIN 2 is required for *Agrobacterium* T-DNA integration in plants. *Plant Cell* 19, 1695-1708.

Axtell, M.J., and Staskawicz, B.J. (2003) Initiation of RPS2-specified disease resistance in *Arabidopsis* is coupled to the AvrRpt2-directed elimination of RIN4. *Cell* 112, 369-377.

Bhattacharjee, S., Lee, L.-Y., Oltmanns, H., Cao, H., Veena, Cuperus, J., and Gelvin, S.B. (2008) AtImpa-4, an *Arabidopsis* importin α isoform, is preferentially involved in *Agrobacterium*-mediated plant transformation. *Plant Cell* 20, 2661–2680.

Buckley, A.M., Petersen, J., Roe, A.J., Douce, G.R., and Christie, J.M. (2015) LOV-based reporters for fluorescence imaging. *Curr. Opin. Chem. Biol.* 27, 39-45.

Christie, P.J., Ward, J.E., Winans, S.C., and Nester, E.W. (1988) The *Agrobacterium tumefaciens* virE2 gene product is a single-stranded-DNA-binding protein that associates with T-DNA. *J. Bacteriol.* 170, 2659–2667.

Christie, J.M., Gawthorne, J.A., Young, G., Fraser, N.J., and Roe A.J. (2012a) LOV to BLUF: flavoprotein contributions to the optogenetic toolkit. *Mol. Plant.* 5, 533-544.

Christie, J.M., Hitomi, K., Arvai, A.S., Harfield, K.A., Mettlen, M., Pratt, A.J., Tainer, J.A., and Getzoff, E.D. (2012b) Structural tuning of the fluorescent protein iLOV for improved photostability. *J. Biol. Chem.* 287, 22295-22304.

Citovsky, V., Zupan, J., Warnick, D., and Zambryski, P. (1992) Nuclear localization of *Agrobacterium* VirE2 protein in plant cells. *Science* 256, 1802–1805.

Citovsky, V., Warnick, D., and Zambryski, P. (1994) Nuclear import of *Agrobacterium* VirD2 and VirE2 proteins in maize and tobacco. *Proc. Natl. Acad. Sci. USA* 91, 3210-3214.

Citovsky, V., Kapelnikov, A., Oliel, S., Zakai, N., Rojas, M.R., Gilbertson, R.L., Tzfira, T., and Loyter, A. (2004) Protein interactions involved in nuclear import of the *Agrobacterium* VirE2 protein *in vivo* and *in vitro*. *J. Biol. Chem.* 279, 29528–29533.

Cui, J., Bahrami, A.K., Pringle, E.G., Hernandez-Guzman, G., Bender, C.L., Pierce, N., and Ausubel, F.M. (2005) *Pseudomonas syringae* manipulates systemic plant defenses against pathogens and herbivores. *Proc. Natl. Acad. Sci. USA* 102, 1791-1796.

De Torres-Zabala, M., Truman, W., Bennet, M.H., Lafforgue, G., Mansfield, J.W., Rodriguez-Egea, P., Bögre, L., and Grant, M. (2007) *Pseudomonas syringae* pv. *tomato* hijacks the *Arabidopsis* abscisic acid signaling pathway to cause disease. *EMBO J.* 26, 1434-1443.

Dodds, P.N., and Rathjen, J.P. (2010) Plant immunity: Towards an integrated view of plant-pathogen interactions. *Nat. Rev. Gen.* 11, 539-548.

Djamei, A., Pitzschke, A., Nakagami, H., Rajh, I., and Hirt, H. (2007) Trojan horse strategy in *Agrobacterium* transformation: Abusing MAPK defense signaling. *Science* 318, 453–456.

García-Cano, E., Magori, S., Sun, Q., Ding, Z., Lazarowitz, S.G., and Citovsky, V. (2015) Interaction of *Arabidopsis* trihelix-domain transcription factors VFP3 and VFP5 with *Agrobacterium* virulence protein VirF. *PLOS ONE* 10, e0142128.

García-Rodríguez, F.M., Schrammeijer, B., and Hooykaas, P.J.J. (2006) The *Agrobacterium* VirE3 effector protein: A potential plant transcriptional activator. *Nucleic Acids Res.* 34, 6494-6504.

Gawthorne, J.A., Audry, L., McQuitty, C., Dean, P., Christie, J.M., Enninga, J., and Roe, A.J. (2016) Visualizing the translocation and localization of bacterial type III effector proteins by using a genetically encoded reporter system. *Appl. Environ. Microbiol.* 82, 2700-2708.

Gelvin, S.B. (2003) *Agrobacterium*-mediated plant transformation: the biology behind the "gene-jockeying" tool. *Microbiol. Mol. Biol. Rev.* 67, 16-37.

Gelvin, S.B. (2010) Finding a way to the nucleus. *Curr. Opin. Microbiol.* 13: 53–58.

Gelvin, S.B. (2012) Traversing the cell: *Agrobacterium* T-DNA's journey to the host genome. *Front. Plant Sci.* 3, 1-11.

Göhre, V., Spallek, T., Häweker, H., Mersmann, S., Mentzel, T., Boller, T., de Torres, M., Mansfield, J.W., and Robatzek, S. (2008) Plant pattern-recognition receptor FLS2 is directed for degradation by the bacterial ubiquitin ligase AvrPtoB. *Curr. Biol.* 18, 1824-1832.

Grange, W., Duckely, M., Husale, S., Jacob, S., Engel, A., and Hegner, M. (2008) VirE2: a unique ssDNA-compacting molecular machine. *PLoS Biol.* 6, e44.

Hiratsu, K., Ohta, M., Matsui, K., and Ohme-Takagi, M. (2002) The SUPERMAN is an active repressor whose carboxy-terminal repression domain is required for the development of normal lowers. *FEBS Lett.* 514, 351-354.

Huala, E., Oeller, P.W., Liscum, E., Han, I.S., Larsen, E., and Briggs, W.R. (1997) *Arabidopsis* NPH1: a protein kinase with a putative redox-sensing domain. *Science* 278, 2120-2123.

Kim, J.-G., Taylor, K.W., Hotson, A., Keegan, M., Schmelz, E.A., and Mudgett, M.B. (2008) XopD SUMO protease affects host transcription, promotes pathogen growth, and delays symptom development in *Xanthomonas*-infected tomato leaves. *Plant Cell* 20, 1915-1929.

Kim, J.-G., Stork, W., and Mudgett, M.B. (2013) *Xanthomonas* type III effector XopD desumoylates tomato transcription factor SIERF4 to suppress ethylene responses and promote pathogen growth. *Cell Host Micro.* 13, 143-154.

Lacroix, B., Vaidya, M., Tzfira, T., and Citovsky, V. (2005) The VirE3 protein of *Agrobacterium* mimics a host cell function required for plant genetic transformation. *EMBO J.* 24, 428-437.

Lagrange, T., Hakimi, M.A., Pontier, D., Courtois, F., Alcaraz, J.P., Grunwald, D., Lam, E., and Lerbs-Mache, S. (2003) Transcription factor IIB (TFIIB)-related protein (pBrp), a plant-specific member of the TFIIB-related protein family. *Mol. Cell Biol.* 23, 3274-3286.

Lapham, R., Lee L.-Y., Tsugama D., Lee S., Mengiste T., and Gelvin S.B. (2018) *VIP1* and its homologs are not required for *Agrobacterium*-mediated transformation, but play a role in *Botrytis* and salt stress responses. *Frontiers Plant Sci*. 9, 1-15.

Lee, L.-Y., Fang, M.-J., Kuang, L.-Y., and Gelvin, S. B. (2008) Vectors for multi-color bimolecular fluorescence complementation to investigate protein-protein interactions in living plant cells. *Plant Methods* 4, 24.

Lee, L.-Y., Wu, F.-H., Hsu, C.-T., Shen, S.-C., Yeh, H.-Y., Liao, D.-C., Fang, M.-J., Liu, N.-T., Yen, Y.-C., Dokládal, L., Sýkorová, E., Gelvin, S.B., and Lin, C.-S. (2012) Screening of a cDNA library for protein-protein interactions directly *in planta*. *Plant Cell*. 24, 1746-1759.

Lee, L.Y., and Gelvin, S.B. (2014) Bimolecular fluorescence complementation for imaging protein-protein interactions in plant hosts of microbial pathogens. In Methods in Molecular Biology: Host-Bacteria Interactions. (A.C. Vergunst and D. O'Callaghan, eds.). *Springer, Humana Press.* 1197, 185-208.

Li, J., Krichevsky, A., Vaidya, M., Tzfira, T., and Citovsky, V. (2005) Uncoupling of the functions of the *Arabidopsis* VIP1 protein in transient and stable plant genetic transformation by *Agrobacterium*. *Proc. Natl. Acad. Sci. USA* 102, 5733–5738.

Li, X., Yang, Q., Tu, H., Lim, Z., and Pan, S.Q. (2014) Direct visualization of *Agrobacterium*-delivered VirE2 in recipient cells. *Plant J*. 77, 487-495.

Li, X., and Pan, S.Q. (2017) *Agrobacterium* delivers VirE2 protein into host cells via clatherin-mediated endocytosis. *Sci. Adv.* 3, e1601528.

Liu, J., Elmore, J.M., Fuglsang, A.T., Palmgren, M.G., Staskawicz, B.J., and Coaker, G. (2009) RIN4 functions with plasma membrane H^+ -ATPases to regulate stomatal apertures during pathogen attack. *PLOS Biol.* 7, e1000139.

Mackey, D., Belkhadir, Y., Alonso, J.M., Ecker, J.R., and Dangl, J.L. (2003) *Arabidopsis* RIN4 is a target of the type III virulence effector AvrRpt2 and modulates RPS2-mediated resistance. *Cell* 112, 379-389.

Magori, S. and Citovsky, V. (2011) *Agrobacterium* counteracts host-induced degradation of its effector F-box protein. *Sci. Signal* 4, ra69.

Niu, X., Zhou, M., Henkel, C.V., van Heusden, G.P.H., and Hooykaas, P.J.J. (2015) The *Agrobacterium tumefaciens* virulence protein VirE3 is a transcriptional activator of the F-box gene *VBF*. *Plant J.* 84, 914-924.

Pitzschke, A., Djamei, A., Teige, M., Hirt, H. (2009) VIP1 response elements mediate mitogen-activated protein kinase 3-induced stress gene expression. *Proc. Natl. Acad. Sci. USA* 106, 18414-18419.

Römer, P., Hahn, S., Jordan, T., Strauβ, T., Bonas, U., and Lahaye, T. (2007) Plant pathogen recognition mediated by promoter activation of the pepper *Bs3* resistance gene. *Science* 318, 645-648.

Rossi, L., Hohn, B., and Tinland, B. (1996) Integration of complete transferred DNA units is dependent on the activity of virulence E2 protein of *Agrobacterium tumefaciens. Proc. Natl. Acad. Sci. USA* 93, 126-130.

Roushan, M.R., de Zeeuw, M.A.M., Hooykaas, P.J.J., and van Heusden, G.P.H. (2018) Application of phiLOV2.1 as a fluorescent marker for visualization of *Agrobacterium* effector protein translocation. *Plant J.* 96, 685-699.

Schornack, S., Meyer, A., Römer, P., Jordan, T., and Lahaye, T. (2006) Gene-for-gene-mediated recognition of nuclear-targeted AvrBs3-like bacterial effector proteins. *J. Plant Physiol.* 163, 256-272.

Shi, Y., Lee L.-Y., and Gelvin S.B. (2014) Is VIP1 important for *Agrobacterium*-mediated transformation? *Plant J.* 79, 848-860.

Simone, M., McCullen, C.A., Stahl, L.E., and Binns, A.N. (2001) The carboxy-terminus of VirE2 from *Agrobacterium tumefaciens* is required for its transport to host cells by the *virB*-encoded type IV transport system. *Mol. Microbiol.* 41, 1283–1293.

Schrammeijer, B., Risseeuw, E., Pansegrau, W., Regensburg-Tuïnk, T.J., Crosby, W.L., and Hooykaas, P.J.J. (2001) Interaction of the virulence protein VirF of *Agrobacterium tumefaciens* with plant homologs of the yeast protein Skp1 protein. *Curr. Biol.* 11, 258-262.

Stachel, S.E., and Nester, E.W. (1986) The genetic and transcriptional organization of the *vir* region of the A6 Ti plasmid of *Agrobacterium tumefaciens*. *EMBO J.* 5, 1445-1454.

Tenea, G.N., Spantzel, J., Lee L.-Y., Zhu, Y., Lin, K., Johnson, S.J., and Gelvin, S.B. (2009) Over-expression of several *Arabidopsis* histone genes increases *Agrobacterium*-mediated transformation and transgene expression in plants. *Plant Cell* 21, 3350-3367.

Tsugama, D., Liu, S., and Takano, T. (2012) A bZIP protein, VIP1, is a regulator of osmosensory signaling in *Arabidopsis*. *Plant Physiol.* 159, 144-155.

Tsugama, D., Liu, S., and Takano, T. (2013) A bZIP protein, VIP1, interacts with *Arabidopsis* heterotrimeric G protein β subunit, AGB1. *Plant Physiol. & Biochem.* 71, 240-246.

Tsugama, D., Liu, S., and Takano, T. (2014) Analysis of functions of VIP1 and its close homologs in osmosensory responses of *Arabidopsis thaliana*. *PLOS ONE* 9, e103930.

Tsugama, D., Liu, S., and Takano, T. (2016a) The bZIP protein VIP1 is involved in touch responses in *Arabidopsis* roots. *Plant Physiol.* 171, 1355-1365.

Tsugama, D., Liu, S., and Takano, T. (2016b) VIP1 is very important/interesting protein 1 regulating touch responses of *Arabidopsis*. *Plant Sig, & Behav.* 11, e1187358.

Tzfira, T., Vaidya, M., and Citovsky, V. (2001) VIP1, an *Arabidopsis* protein that interacts with *Agrobacterium* VirE2, is involved in VirE2 nuclear import and *Agrobacterium* infectivity. *EMBO J.* 20, 3596–3607.

Tzfira, T., Vaidya, M., and Citovsky, V. (2004) Involvement of targeted proteolysis in plant genetic transformation by *Agrobacterium*. *Nature* 431, 87-92.

Wang, Y., Peng, W., Zhou, X., Huang, F., Shao, L., and Luo, M. (2014) The putative *Agrobacterium* transcriptional activator-like virulence protein VirD5 may target T-complex to prevent the degradation of coat proteins in the plant cell nucleus. *New Phytol.* 203, 1266-1281.

Wang, Y., Zhang, S., Huang, F., Zhou, X., Chen, Z., Peng, W., and Luo, M. (2018) VirD5 is required for efficient *Agrobacterium* infection and interacts with *Arabidopsis* VIP2. *New Phytol.* 217, 726-738.

Wilton, M., Subramaniam, R., Elmore, J., Felsensteiner, C., Coaker, G., Desveaux, D. (2010) The type III effector HopF2Pto targets *Arabidopsis* RIN4 protein to promote *Pseudomonas syringae* virulence. *Proc. Natl. Acad. Sci. USA* 107, 2349-2354.

Xiang, T., Zong, N., Zou, Y., Wu, Y., Zhang, J., Xing, W., Li, Y., Tang, X., Zhu, L., Chai, J., and Zhou, J.M. (2008) *Pseudomonas syringae* effector AvrPto blocks innate immunity by targeting receptor kinases. *Curr. Biol.* 18, 74-80.

Yusibov, V.M., Steck, T.R., Gupta, V., and Gelvin, S.B. (1994) Association of single-stranded transferred DNA from *Agrobacterium tumefaciens* with tobacco cells. *Proc. Natl. Acad. Sci. USA* 91, 2994–2998.

Zaltsman, A., Krichevsky, A., Loyter, A., and Citovsky, V. (2010) *Agrobacterium* induces expression of a host -box protein required for tumorgenicity. *Cell Host Microbe.* 7, 197-209.

Zaltsman, A., Lacroix, B., Gafni, Y. and Citovsky, V. (2013) Disassembly of synthetic *Agrobacterium* T-DNA—protein complexes via the host SCF^{VBF} ubiquitin-ligase complex pathway. *Proc. Natl. Acad. Sci. USA* 110, 169-174.

Ziemienowicz, A., Merkle, T., Schoumacher, F., Hohn, B., and Rossi, L. (2001) Import of *Agrobacterium* T-DNA into plant nuclei: Two distinct functions of VirD2 and VirE2 proteins. *Plant Cell* 13, 369-383.

Zuo, J., Niu, Q.-W., and Chua, N.-H. (2000) An estrogen receptor-based system transactivator XVE mediates highly inducible gene expression in transgenic plants. *Plant J.* 24, 265–273.

CHAPTER 2: VIP1 AND ITS HOMOLOGS ARE NOT REQUIRED FOR AGROBACTERIUM-MEDIATED TRANSFORMATION, BUT PLAY A ROLE IN BOTRYTIS AND SALT STRESS RESPONSES

Introduction

Virulent strains of the soil bacterium *Agrobacterium tumefaciens* cause the tumorigenic disease crown gall. *Agrobacterium*-mediated plant genetic transformation involves mobilization of transferred-DNA (T-DNA) and five virulence proteins (VirD2, VirE2, VirE3, VirD5, and VirF) from the bacterium into a plant cell (Gelvin, 2003, 2012).

The effector protein VirE2 has non-specific single-stranded DNA binding activity and is thought to coat single-stranded T-DNA (T-strands) after entry into the plant cell (Citovsky et al., 1992), protecting T-strands from nucleolytic degradation (Yusibov et al., 1994; Rossi et al., 1996). In addition to this structural role, VirE2 interacts with a number of plant proteins including VirE2-interacting protein 1 (VIP1; Tzfira et al., 2001) and VIP2 (Anand et al., 2007). VIP1, a bZIP transcription factor which is a target of the mitogen-activated protein kinase 3 (MPK3), is thought to be involved in plant defense responses (Djamei et al., 2007; Pitzschke et al., 2009). Phosphorylation of VIP1 on serine 79 by MPK3 results in the import of VIP1 into the plant nucleus (Djamei et al., 2007). VIP1 may subsequently bind to VIP1 response elements (VREs) to activate transcription of its target genes (Pitzschke et al., 2009). VIP1 may also be involved in sulfur utilization, starch accumulation, osmosensory signaling, and touch-induced root waving (Wu et al., 2010; Chen et al*.,* 2015; Ishida et al., 2004; Tsugama et al., 2012, 2014, 2016).

The importance and role of VIP1 in *Agrobacterium*-mediated transformation are controversial (Tzfira et al., 2001; Shi et al., 2014). Previous studies using transgenic tobacco lines expressing antisense constructs targeting *VIP1,* and the *Arabidopsis thaliana* T-DNA insertion mutant *vip1-1*, found that these plants showed decreased stable transformation compared to that of wild-type plants (Tzfira et al., 2001; Li et al., 2005). Overexpression of *VIP1* in tobacco resulted in increased transformation susceptibility, suggesting that VIP1 plays a role in transformation (Tzfira et al., 2001). However, quantitative transformation assays with the *vip1-1* mutant and with 59 *A. thaliana VIP1* overexpressing lines showed no effect on

transformation susceptibility (Shi et al., 2014), suggesting that VIP1 is not important for *Agrobacterium*-mediated transformation.

Previous studies indicated that β-glucoronidase- (GUS) or YFP-tagged VirE2 localizes to the plant nucleus (Citovsky et al., 1992, 1994; Tzfira and Citovsky, 2001). However, other studies showed exclusively cytoplasmic localization of VirE2 (Bhattacharjee et al., 2008; Grange et al., 2008; Lee et al., 2008; Sakalis et al., 2013; Shi et al., 2014). VirE2 possesses a weak putative nuclear localization signal (NLS) sequence which does not bind strongly to importin α protein (Citovsky et al., 1994; Chang et al., 2014). Early work indicated that VirE2 does not interact with *Arabidopsis* importin alpha-1 (IMPa-1, also known as AtKAPα) in yeast (Ballas and Citovsky, 1997), although Bhattacharjee et al. (2008) subsequently detected such interactions in yeast, *in planta,* and *in vitro.* However, VirE2-IMPa-1 complexes remained cytoplasmic in plants (Lee et al., 2008). VirE2 nuclear import has been attributed to its interaction with VIP1 (Tzfira et al., 2001), a protein that localizes to both the cytoplasm and to the nucleus (Djamei et al., 2007; Shi et al., 2014). Activation of VIP1 by MPK3 and subsequent binding of phosphorylated VIP1 to VirE2 may facilitate nuclear localization of VIP1-VirE2-T-strand complexes (the Trojan-horse model; Djamei et al., 2007).

The *vip1-1* mutant still produces ~80% of the VIP1 protein, including the crucial bZIP DNA binding domain (Li et al., 2005). Because this domain may be important for function, we used CRISPR technology to generate a homozygous mutant, *vip1-2,* that produces a smaller protein lacking the bZIP domain. Transient and stable transformation assays indicated no effect of this mutation on *Agrobacterium*-mediated transformation. Furthermore, transformation assays of single and multiple null mutant lines of *VIP1* homologs, and transgenic lines overexpressing VIP1 fused to a modified EAR-like motif repression domain (SRDX; Hiratsu et al., 2003), also failed to show any major effect on transformation. We therefore conclude that *VIP1* and its homologs are not required for *Agrobacterium*-mediated transformation. However, *VIP1* may be important for defense responses against the fungus *Botrytis cinerea*, for abscisic acid (ABA) signaling, and for growth under salt stress conditions.

Materials and Methods

Plasmids and strain constructions

Supplemental Tables 2.1 and 2.2 list the plasmids, strains, and single-guide RNA sequences used in this study. To make *VIP1* CRISPR-Cas9 constructs, we designed three sets of sgRNA constructs targeting the *VIP1* gene within the first exon. For each set, two 20-nucleotide oligomers of target DNA sequences were synthesized with an additional GATC on the 5' end of the sense-strand and AAAC on the 5' end of the antisense-strand. After annealing, we cloned this double stranded oligomer into the *Bbs*I site of psgR-Cas9-At. A *Hin*dIII-*Kpn*I fragment from this plasmid (containing both sgRNA and Cas9 expression cassettes) was cloned into pCAMBIA1300 to make the plasmids pE4351, pE4352, and pE4353. These T-DNA binary vectors were introduced by electroporation into *A. tumefaciens* GV3101 (Van Larebeke et al., 1974) to generate *A. tumefaciens* At2115, At2116, and At2117, respectively.

To make the *vip1-2*-Venus (out of frame) fusion construct, we cloned the *vip1-2* RT-PCR product into the *Sma*I site of pBluescript KS+ to create pE4443. *Bgl*II and *Bam*HI sites were used to remove the *vip1-2* cDNA fragment, which was ligated to the *Venus* gene in pE3857 to produce pE4451 (confirmed by sequencing; Supplemental Table 2.1).

To create the *vip1-2*-GUS-Venus fusion construct, the nucleotides encoding the first 145 amino acids of *vip1-2* was amplified by PCR using the primers VIP1-*Bgl*II-FP1 and *vip1-2* peptide, flanked by *Bgl*II and *Bam*HI sites, respectively. The PCR product was cloned into the *Sma*I site of pE886 to create pE4516. The *Bgl*II-*Bam*HI fragment as made blunt with Klenow fragment of DNA polymerase (New England Biolabs) and cloned into the *Bgl*II site of pE3835 to make pE4521. A plasmid (pE4517) containing the VIP1-GUS-Venus fusion was made by cloning the *Bam*HI-*Bgl*II fragment from pE3857 into the *Bgl*II site of pE3835.

To create the inducible *VIP1* overexpression construct, we excised an *Sph*I-*Xho*I fragment, containing the LexA operator and a minimal Cauliflower Mosaic Virus 35S promoter, from pER8 (Zuo et al., 2000). The fragment, made blunt using Klenow fragment of DNA polymerase, was ligated to pE3542 digested with *Age*I and *Xho*I and made blunt. The resulting plasmid, pE4224, is a pSAT1-derived cloning vector used to generate β-estradiol-inducible gene constructions.

To generate the T-DNA binary vector into which the inducible gene constructions were placed, we ligated a blunted *Sbf*I-*Nco*I fragment containing the XVE expression cassette and a Pnos-partial *hptII* gene into the blunted *Swa*I-*Nco*I site of pE4145 (pPZP-RCS-*hptII*) to make pE4216. We then ligated a *Nco*I fragment containing part of the *hptII* gene from pER8 to the *Nco*I site of pE4216 to generate a complete *hptII* gene (pE4215). pE4215 is a T-DNA binary vector containing the XVE and *hptII* expression cassettes and a *AscI* site into which the inducible gene expression cassette can be cloned.

The *Swa*I-*Not*I fragment containing the *VIP1* gene was removed from the plasmid pE4132 and cloned into the *Sma*I and *Not*I sites of the β-estradiol inducible promoter plasmid pE4224, making pE4275. pE4275 was then digested with *Asc*I and the inducible *VIP1* fragment was cloned into the *Asc*I site of the binary vector pE4215 to create pE4288. pE4288 was introduced by electroporation into *A. tumefaciens* GV3101 (Van Larebeke et al., 1974) to generate *A. tumefaciens* At2082.

Generation and screening of VIP1 CRISPR/Cas9 and inducible VIP1 transgenic A. thaliana plants

Wild-type Col-0 ecotype *A. thaliana* plants were transformed by *A. tumefaciens* At2115, At2116, At2117, or At2082 using a flower dip protocol (Clough and Bent, 1998). T0 generation seeds harvested from transformed plants were surface sterilized for 15 min using a 50% Bleach and 0.1% sodium dodecylsulfate (SDS) before washing five times with sterile water. After incubation overnight at 4^{o}C, the seeds were plated on solidified Gamborg's B5 medium (Caisson Labs) containing 100 μg mL^{-1} Timentin and 20 μg mL^{-1} hygromycin. The seeds were incubated at 23^{o}C using a 16/8 hour light/dark cycle. Hygromycin-resistant seedlings (T1 generation) were transplanted to soil and grown under the same temperature and light conditions. Seeds were harvested from each T1 plant and T2 generation plants grown in soil. For the *VIP1* CRISPR/Cas9 plants, DNA isolated from leaves of individual T2 plants was used to PCR-amplify a region surrounding the sgRNA target site using primers listed in Supplemental Table 2.2. The PCR products were analyzed for mutations using a T7 endonuclease I (New England Biolabs) mismatch assay (Babon *et. al*, 2003). Mutations were confirmed by sequencing. For inducible *VIP1* plants, seeds were harvested from the T2 generation plants and selected on

hygromycin. Seeds from homozygous plants (100% progeny surviving on selection) were used for future experiments.

VIP1 induction in the presence and absence of Agrobacterium

T3 generation inducible *VIP1* seedlings were germinated on B5 medium containing 100 µg mL^{-1} Timentin and 20 µg mL^{-1} hygromycin. After two weeks, the seedlings were transferred to plates containing B5 medium only which were placed vertically in racks to allow for root tissue to grow on the surface of the medium. After seven days, B5 liquid medium containing 1 µM of β-estradiol suspended in DMSO (induction solution) or B5 with DMSO only (control solution) was pipetted onto the plates until a thin layer of liquid covered the root tissue. To determine differential gene expression in the presence of *Agrobacterium*, cells of *A. tumefaciens* A136 (lacking a Ti-plasmid) were suspended in either induction or control solution at a concentration of 10^8 cells mL^{-1}. The roots were incubated in the treatment solution for either 3 or 12 hours before cutting the roots from the stems using a razor blade, rinsing with sterile water, dabbing them dry with a paper towel, and freezing them in liquid nitrogen. For each treatment, the root tissue was pooled from 30 individual plants. The tissue was stored at -80^{o}C.

Preparation of samples for quantitative RT-PCR

RNA was isolated from the root tissue of untreated, non-induced, induced, non-induced in the presence of *Agrobacterium*, and induced in the presence of *Agrobacterium* after 0, 3, and 12 hours of incubation. This was done for two biological replicates of inducible *VIP1 A. thaliana* transgenic line #12 and inducible *VIP1 A. thaliana* transgenic line #8.

A total of 1.45 µg of total RNA was treated with Ambion® DNase I (Thermo Fisher Scientific) and SuperScriptIII reverse transcriptase (Thermo Fisher Scientific) was used to synthesize cDNA according to the manufacturer's protocols. Quantitative RT-PCR was performed with a Roche LightCycler 96 using the FastStart Essential Green Master reagents (Roche). Primers used to amplify the genes are described in Supplemental Table 2.2. Data were analyzed using the LightCycler 96 software, REST 2009 software (http://www.gene-quantification.de/rest-2009.html), and Microsoft Excel.

Phenotypic characterization of vip1-2 plants

Homozygous *vip1-2* and wild-type Col-0 plants were grown on soil at 23^{o}C in a chamber with a 16/8 hour light/dark cycle. After germination, plants were thinned to one plant per pot and photos were taken every two to three days throughout growth. Rosette, leaf, and flower bolt sizes were measured using image processing software and statistical analysis was performed using a Student's *t* test.

Isolation and transfection of Arabidopsis and tobacco BY-2 protoplasts

Protoplasts were isolated from leaves of wild-type (ecotype Col-0) and *vip1-2 A. thaliana* plants and tobacco BY-2 cells and transfected as described in Lee et al. (2012). pE3170 (mRFP-nuclear marker) was co-transfected into protoplasts with the appropriate clones. Protoplasts were imaged 16 hours after transfection using a Nikon A1R Confocal Laser Microscope System as described in Shi et al. (2014).

Agrobacterium-mediated transient and stable transformation assays

A. thaliana lines tested in this study are listed in Supplemental Table 2.3. Homozygous lines for the annotated T-DNA insertions were confirmed by PCR (primer sequences listed in Supplemental Table 2.2). Roots from 20-day-old *A. thaliana* plants grown in baby food jars containing sterile Gamborg's B5 medium were cut into 3-5 mm segments. Root segments were assayed as described in Tenea *et al.* (2009). *A. tumefaciens* At849 (GV3101 containing pBISN1 [Narasimhulu et al., 1996]) was used for transient transformation assays, whereas *A. tumefaciens* A208 was used for stable transformation. Three replicates were performed for each experiment and root segments were pooled from six to 10 plants for each replicate. 80 or more root segments were scored for each data point. Statistical analysis was performed using a Student's *t* test.

Quantitative RT-PCR of vip1-2

RNA was isolated from leaf tissue harvested from 3-week-old plants grown on soil using TriZol reagent (https://www.thermofisher.com). For each sample, 1 μg of total RNA was treated with Ambion® DNase I (Thermo Fisher Scientific) and SuperScriptIII reverse transcriptase

(Thermo Fisher Scientific) was used to synthesize cDNA according to the manufacturer's protocols. Real-time PCR was performed with a Roche LightCycler 96 using the FastStart Essential Green Master reagents (Roche). Primers used to amplify the 3' end of the *VIP1* transcript are described in Supplemental Table 2.2. Data were analyzed using the LightCycler 96 software, REST 2009 software (http://www.gene-quantification.de/rest-2009.html), and Microsoft Excel.

Botrytis cinerea and Pseudomonas syringae pathogenesis assays

Five-week-old *A. thaliana* wild-type (Col-0), *vip1-1*, *vip1-2*, and *VIP1-SRDX* Line #11 leaves (from plants grown on soil) were inoculated with 5 µL of *B. cinerea* at a concentration of 1.0×10^5 spores/mL. Lesion size was measured 3 days after infection and averaged over 18 leaves per genotype (36 leaves for Col-0). Standard error was calculated over two separate experiments and a Student's *t* test was used to test for significant differences.

Five-week-old *A. thaliana* wild-type (Col-0), *vip1-1*, *vip1-2*, and *VIP1-SRDX* Line #11 leaves (from plants grown on soil) were syringe-inoculated with *P. syringae pv. tomato* DC3000 (virulent) or *P. syringae pv. tomato* DC3000 *hrcC* (avirulent) at an optical density (A_{600}) of 0.001 and 0.005 respectively. Bacterial growth was determined at 0 and 4 days after infection by isolating bacteria from six leaf discs for each plant and plating a dilution series to calculate the number of colony forming units (c.f.u.) per square centimeter of leaf material. Standard error was calculated over three replicates and a Student's *t* test was used to test for significant differences.

ABA and hyper-osmotic germination and root growth assays

Seeds were plated onto ½ MS 1% sucrose medium containing 0, 0.3, or 0.5 µM abscisic acid (ABA) or onto MS 2% sucrose medium containing 0, 50, 75, or 100 mM NaCl. Twenty-five seeds per genotype were placed on each plate with two (ABA) or four (NaCl) plates prepared for each treatment. The plates were incubated in a 23^{o}C chamber with a 16/8 hour light/dark cycle. Germinated seeds were scored eight days after plating. Any seed with a radicle protruding was considered to have germinated. The number of germinated seeds was divided by the total number to calculate the percent germination and this was averaged over all the plates for each treatment. Student's *t* test was used to test for statistically significant differences.

To test the effect of exogenous ABA or hyper-osmotic conditions on root growth, seeds were germinated on ½ MS, 1% sucrose medium (ABA) or MS 2% sucrose medium (hyper-osmotic). Five-day-old seedlings with a root length of ~1 cm were transferred to ½ MS 1% sucrose containing 0, 2, or 20 μM of ABA or MS 2% sucrose with 0, 50, 75, or 100 mM of NaCl. These plates were placed vertically in racks in a 16/8 hour light/dark cycle growth chamber at 23^{o}C. Eleven plates were prepared for each treatment. Pictures were taken of each of the ABA and NaCl plates, 8 and 11 days (respectively), after the seedlings were transferred. Root length was determined using ImageJ software. Root length was averaged over 11 seedlings for each genotype for each treatment. The rate of growth was determined by subtracting the initial root length from the final root length divided by the number of days of growth. Student's *t* test was used to test for statistically significant differences.

Results

Generation of the vip1-2 mutant

Several laboratories have utilized the T-DNA insertion mutant *vip1-1* (SALK_001014.38.85.x) to study the role of VIP1 in *Agrobacterium*-mediated transformation and other cellular processes (Li et al., 2005; Pitzschke et al., 2009; Wu et al., 2010; Tsugama et al., 2012, 2016; Shi et al., 2014; Chen et al., 2015). However, *vip1-1* is not a transcriptional null mutant and still produces the first 244 amino acids of the 341 amino acid VIP1 protein (Li et al., 2005; Shi et al., 2014). The VIP1-1 protein lacks the C-terminal domain necessary for self-dimerization and interaction with histone H2A (Li et al., 2005; Lacroix et al., 2008), but still contains the transcriptional activation domain as well as the majority of the bZIP DNA binding domain (Figure 1A). We therefore used CRISPR-Cas9 technology (Feng et al., 2013) to generate a *vip1* mutant that produces a smaller VIP1 protein (Figure 1B).

We designed three guide RNAs to target multiple positions in the first exon of VIP1 (Figure 1C). T7 endonuclease analysis (Babon et al., 2003) of numerous T2 generation transgenic *Arabidopsis* lines expressing individual guide RNAs and Cas9 failed to identify mutations using constructs targeting the two most 5'-proximal regions of the *VIP1* gene. However, the third guide RNA generated several different mutations (Figure 1D). DNA sequence analysis confirmed that one of these mutations resulted in a two base pair deletion,

generating a premature stop codon. This mutant, *vip1-2*, encodes the first 140 amino acids of VIP1 plus five additional amino acids resulting from the frame-shift mutation. VIP1-2 lacks the bZIP DNA binding domain, the nuclear localization signal (NLS) sequence, and the C-terminal domain important for VIP1 dimerization or interaction with histone H2A (Figure 2.1A).

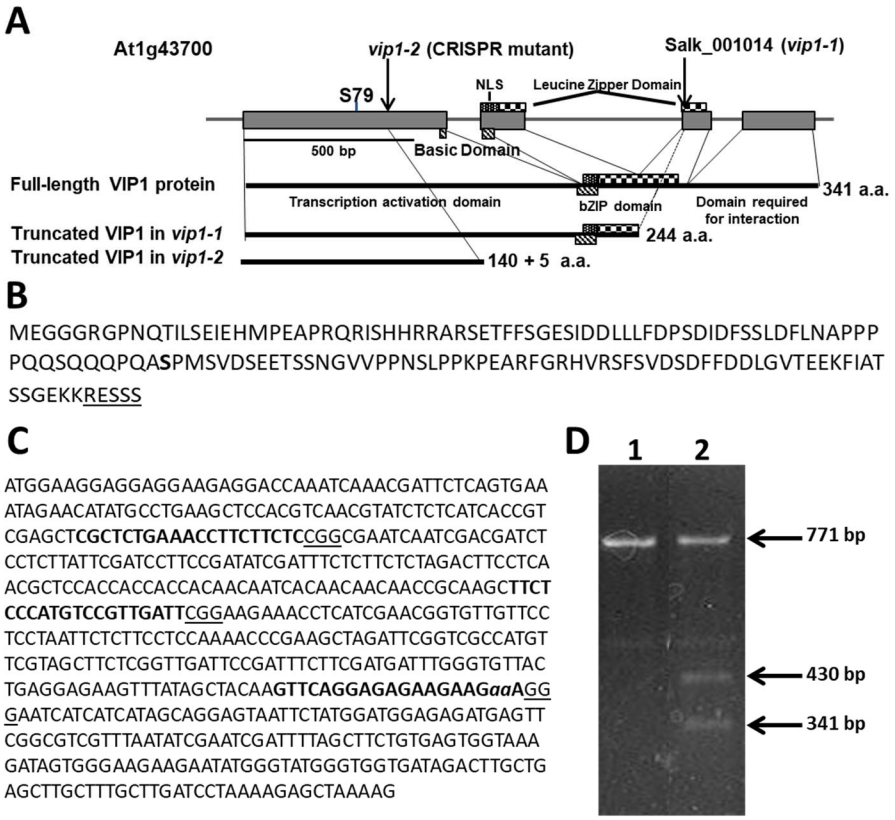

Figure 2.1. The *VIP1*, *vip1-1*, and *vip1-2* genes and coding regions.
(A) Map of the *VIP1* coding region. Important protein domains are shown for the full-length and truncated VIP1-1 and VIP1-2 proteins. The C-terminal domain absent in both mutant proteins is required for VIP1 dimerization and VIP1-Histone H2A interactions (Li et al., 2005). Serine[79], a phosphorylation site important for nuclear targeting of VIP1 (Djamei et al., 2007), is indicated. (B) Amino acid sequence of the VIP1-2 protein. The five amino acids shown underlined are not from the VIP1 protein, but result from the 2 bp deletion before a stop codon is reached. Serine[79] is indicated in bold. (C) DNA sequence of the first exon of *VIP1*. Target sites for single-guide RNAs are highlighted in bold font. The PAM sequences are underlined. The two nucleotides *aa* are deleted in the *vip1-2* mutant. (D) T7 endonuclease I digestion of *VIP1* PCR products (771 bp of gDNA surrounding the mutation in *vip1-2*) using wild-type gDNA as template (Lane 1) or a mixture of PCR products from both wild-type *and vip1-2* mutant gDNAs (Lane 2). The mutation in *vip1-2* creates a 2-bp mismatch generating two bands of 430 bp and 341 bp after T7 endonuclease cleavage.

Properties of the vip1-2 gene and VIP1-2 protein

RNA was isolated from homozygous *vip1-2* leaves and RT-PCR was performed to determine if *VIP1* transcripts were still produced (Supplemental Figure 2.1A). Despite the presence of an early stop codon within the first exon of the *vip1-2* gene, primers set at the 3' end of the gene amplified a product, indicating that the *VIP1* transcript was still produced. However, quantitative RT-PCR detected the *VIP1* transcript at 35% of the level found in wild-type plants (Supplemental Figure 2.1B). The reduced level of the *VIP1* transcripts may result from nonsense-mediated decay (Brogna and Wen, 2009). To verify that the *vip1-2* mutant cannot make full-length VIP1 protein, we fused the *vip1-2* cDNA to a Venus fluorescent protein coding sequence just before the position of the stop codon of the wild-type *VIP1* cDNA. When introduced into BY-2 cells, this cDNA should not result in fluorescence because of the premature stop codon in the *vip1-2* cDNA. Supplemental Figure 2.1C shows that a wild-type *VIP1-Venus* cDNA fusion construction could promote fluorescence in BY-2 cells. However, the *vip1-2-Venus* cDNA fusion construction could not.

Because wild-type VIP1 protein dimerizes (Li et al., 2005), we were concerned that Venus-tagged VIP1 may interact with untagged VIP1 present in cells, and that untagged full-length VIP1 may direct the subcellular localization of the dimer complex. We therefore conducted VIP1 subcellular localization experiments in both wild-type and *vip1-2* mutant protoplasts. Wild-type VIP1-Venus fusion protein localized to both the plant cytoplasm and nucleoplasm, but not the nucleolus, of wild-type and *vip1-2* mutant *Arabidopsis* protoplasts (Figures 2.2A and 2.2B; Djamei et al., 2009; Shi et al., 2014). The VIP1-2 protein is small (16,016 Da), and even when fused to Venus would produce a protein below the nuclear exclusion limit (<60kDa; Dingwall and Laskey, 1991), permitting nuclear entry of a VIP1-2-Venus fusion protein by diffusion. We therefore fused the VIP1-2 protein in-frame with a GUS-Venus protein, creating a protein (111.77 kDa) that exceeds the nuclear size exclusion limit. Transfection of a plasmid containing a VIP1-2-GUS-Venus expression cassette, together with a plasmid encoding a red fluorescence protein (RFP) nuclear marker, revealed exclusive cytoplasmic yellow fluorescence (Figure 2.2C), indicating that the VIP1-2 protein does not possess strong nuclear targeting capabilities. This result is consistent with deletion of the putative NLS from the VIP1-2 protein (Tsugama et al., 2012). Somewhat surprisingly, wild-type VIP1, when fused to GUS-Venus, also remains exclusively in the cytoplasm of both *Arabidopsis* and

tobacco BY-2 protoplasts (Figures 2.2D and 2.2E). This result suggests either that the VIP1 nuclear localization signal sequence is not strong enough to target this large fusion protein to the nucleus, or that this fusion prevents phosphorylation of VIP1 serine-79 or some other aspect of VIP1 nuclear targeting.

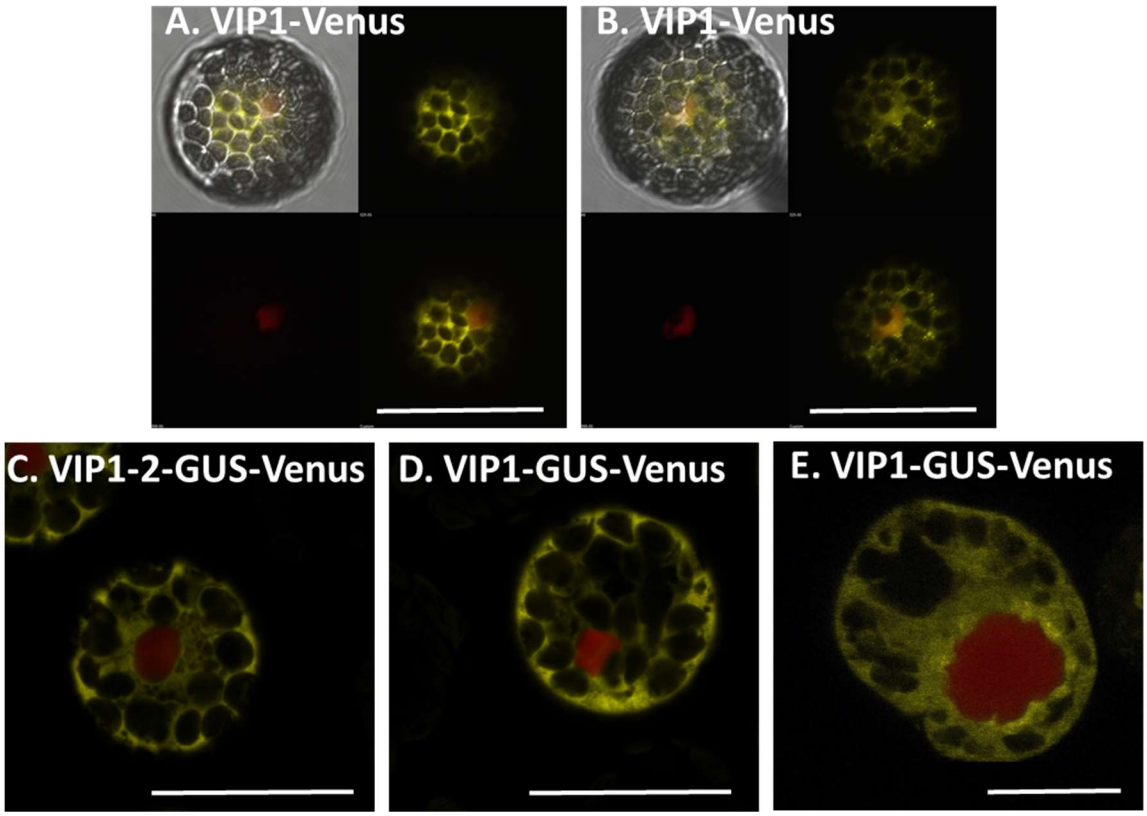

Figure 2.2. Subcellular localization of VIP1 and VIP1-2 proteins in protoplasts. Protoplasts were co-transfected with the indicated Venus-tagged constructs and a mRFP-NLS construct that marks the nucleus. 16 hours after transfection, the cells were imaged by confocal microscopy. VIP1-Venus localizes in both the cytoplasm and the nucleus of Col-0 (A) and *vip1-2* (B) protoplasts; VIP1-2-GUS-Venus localizes exclusively in the cytoplasm of Col-0 protoplasts (C); localization of VIP1-GUS-Venus is limited to the cytoplasm of Col-0 (D) and tobacco BY-2 (E) protoplasts. In A and B, four images of the same cell are presented (clockwise from top left: merged YFP, mRFP, and DIC; YFP; YFP + mRFP; mRFP). In C, D, and E, only the merged YFP and mRFP images are presented. Bars indicate 20 μm.

vip1-2 plants show altered growth characteristics

We examined *vip1-2* plants for abnormal growth or developmental phenotypes. *vip1-2* plants exhibited increased rosette and leaf size compared to wild-type plants (Figures 2.3A-C). This growth phenotype suggests a role for *VIP1* in the regulation of rosette leaf development. However, flowering time did not differ significantly from that of wild-type plants (flowering occurred 26 days after seed sowing).

Figure 2.3 Growth of wild-type and *vip1-2* mutant *Arabidopsis* plants.
(A) Mature (29 day-old) wild-type (Col-0, left) and *vip1-2* mutant (right) plants. (B) Bars represent the average diameter, ± SE, of leaf rosettes on 5-7 plants grown for the indicated number of days. (C) Bars represent the average leaf length (left) and width (right), ± SE, of the three largest leaves on five plants of each genotype grown for 29 days.
Student's t test *P-value < 0.1, **P-value < 0.05, ***P-value < 0.01

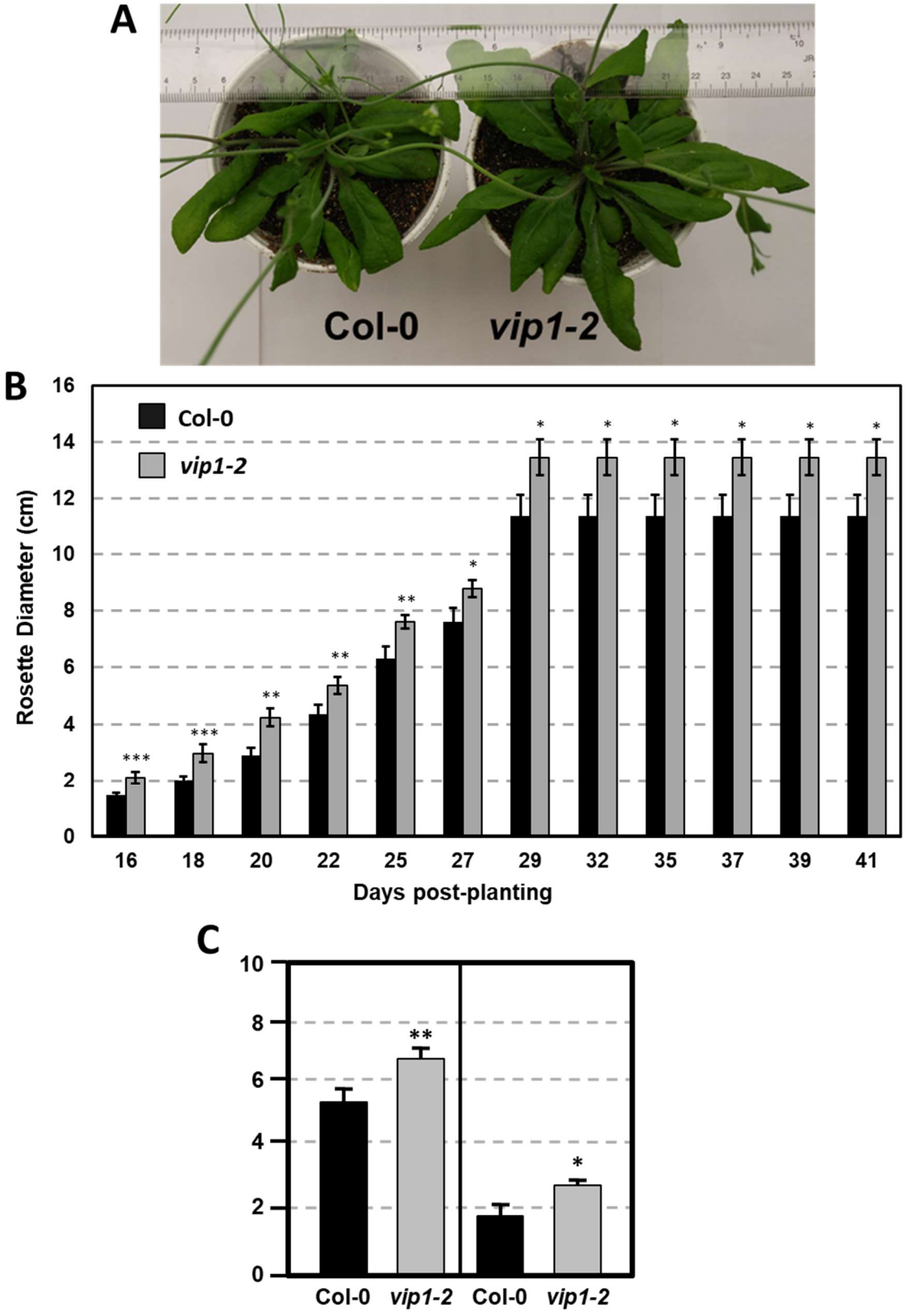
A
Col-0
vip1-2
B
Col-0
vip1-2
Rosette Diameter (cm)
0
2
4
6
8
10
12
14
16
16
18
20
22
25
27
29
32
35
37
39
41
Days post-planting
C
0
2
4
6
8
10
Col-0
vip1-2
Col-0
vip1-2

vip1-2 plants show wild-type susceptibility to Agrobacterium-mediated transformation

We tested transient and stable *Agrobacterium*-mediated transformation susceptibility of root segments from wild-type and *vip1-2* plants. Root segments were infected with a nontumorigenic *Agrobacterium* strain carrying a GUS reporter, At849 (transient transformation), or the tumorigenic strain *A. tumefaciens* A208 (stable transformation; Nam et al., 1997, 1999; Zhu et al., 2003; Shi et al., 2014) at several bacterial concentrations. Root segments of wild-type and *vip1-2* plants had similar susceptibility to both transient and stable transformation at all bacterial concentrations tested (Figure 2.4 and Supplemental Figure 2.2). These results correspond to our previous observations (Shi et al., 2014) that the *vip1-1* mutant is not deficient in transformation susceptibility.

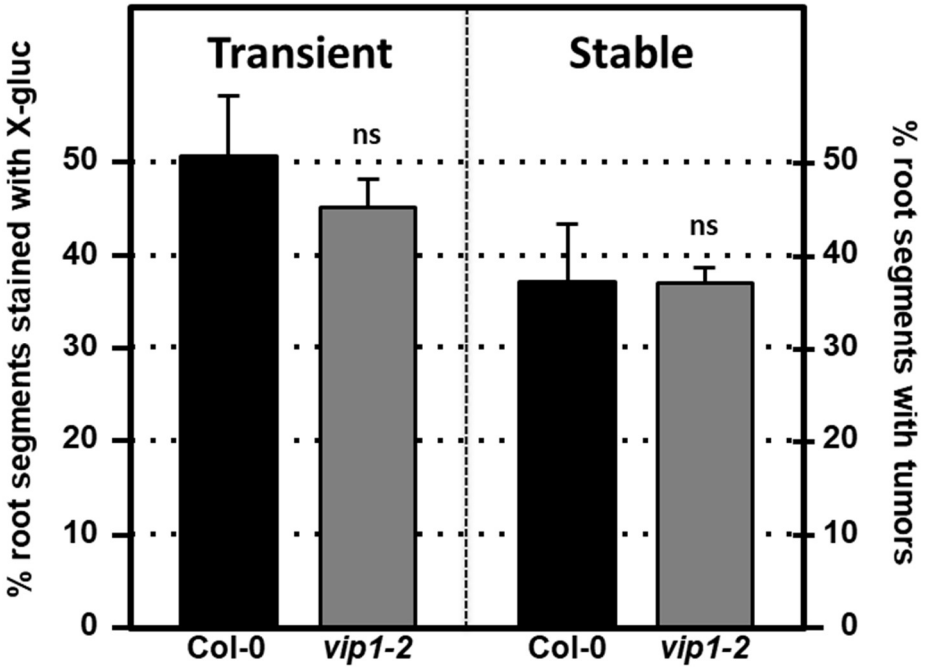

Figure 2.4. Transformation susceptibility of *Arabidopsis* wild-type and *vip1-2* mutant plants. *Agrobacterium*-mediated transient (left) or stable (right) transformation assays were conducted on wild-type and *vip1-2* mutant plants. Root segments were inoculated with 10^7 cfu/ml of the *A. tumefaciens* strains At849 (transient) or A208 (stable). For the transient assay, the root segments were stained with X-gluc 6 days after infection. For stable transformation, tumors were scored 30 days after infection. Numbers represent an average of three biological replicates (each replicate containing > 60 root segments) ± SE. Student's t test *P-value < 0.05, **P-value < 0.01, ***P-value < 0.001, ns: not significant

Individual VIP1 homologs are not essential for Agrobacterium-mediated transformation

VIP1 is one of a 12-member group (group I) of *Arabidopsis* bZIP proteins. Their C-terminal regions, which include the bZIP domain, are highly similar to each other, whereas their N-terminal regions are variable (Jakoby et al., 2002; Tsugama et al., 2014). Of the 12 genes encoding the group I bZIP proteins, *VIP1* and six other genes (*bZIP18*, *bZIP29*, *bZIP30*, *bZIP52*, *bZIP69*, and *PosF21*) are expressed at moderate levels in seedlings, roots, shoots, and flowers, whereas the other five genes (*UNE4*, *bZIP31*, *bZIP33*, *bZIP71*, and *bZIP74*) are hardly expressed in any of these tissues (Tsugama et al., 2014; Supplemental Figure 2.3). Many of these family members have similar subcellular localization, interact with each other, and can similarly bind DNA fragments with the AGCTGT/G motif (Pitzschke et al., 2009; Tsugama et al., 2014; 2016; O'Malley et al, 2016). To test the importance of individual family members for transformation susceptibility, we obtained and confirmed homozygous mutants for six of the more highly expressed *VIP1* homologs (*bZIP18*, *bZIP29*, *bZIP30*, *bZIP33, bZIP52*, and *posF21*). No aberrant phenotypes were observed in these single knockout mutants under normal growth conditions. Transient and stable root transformation assays indicated that each mutant had transformation susceptibility similar to that of wild-type plants (Figures 2.5A and B). Thus, in addition to VIP1, none of these six transcription factors are essential for *Agrobacterium*-mediated transformation.

We additionally tested a triple mutant (*vip1-1*/*posf21/ bzip29*) for transient and stable transformation susceptibility. Using two concentrations of bacterial inoculum, the *vip1-1/posf21/bzip29* mutant had a slight (1.5-fold) reduction in both transient and stable transformation efficiency (Figures 2.5C and D).

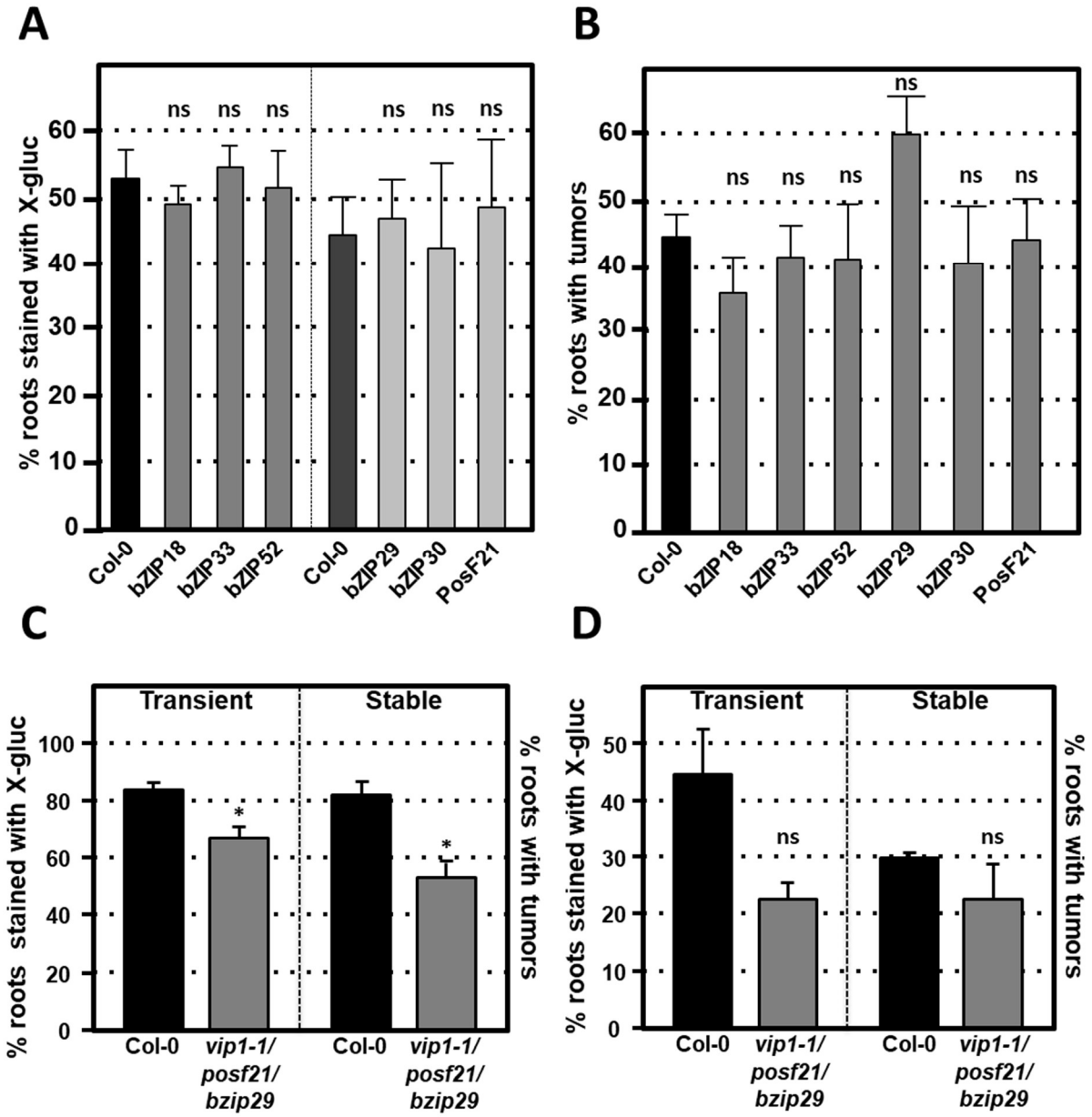

Figure 2.5. Transformation susceptibility of *Arabidopsis* VIP1 homolog mutant roots. *Agrobacterium*-mediated transient or stable transformation assays were conducted on wild-type and VIP1 homolog mutant plants. Root segments of VIP1 homolog single gene mutants and one triple gene mutant were infected with *A. tumefaciens* At849 (transient) or A208 (stable) at the concentration of 10^6 cfu/ml. For the transient assay, the root segments were stained with X-gluc 6 days after infection. For stable transformation, the tumors were scored 30 days after infection. Transient and stable transformation efficiencies of six VIP1 homolog mutants are shown in (A) and (B) respectively. The transformation efficiencies of the triple gene mutant with an inoculum at 10^7 cfu/ml and at 10^6 cfu/ml are shown in C and D, respectively. Numbers represent an average of three biological replicates (each replicate containing >60 root segments) ± SE. Student's t test *P-value < 0.05, **P-value < 0.01, ***P-value < 0.001, ns: not significant

Dominant repression of VIP1 family function by a VIP1-SRDX fusion does not affect transformation susceptibility

To circumvent potential redundant roles among VIP1 family members, we assayed the transformation susceptibility of root segments from three transgenic *Arabidopsis* lines expressing VIP1 fused to the EAR motif repression domain SRDX (Mitsuda et al., 2006; Tsugama et al., 2016). The three independent lines of VIP1-SRDX plants used in this study all showed high expression levels of *VIP1-SRDX* and root waving phenotypes in a previous study (Tsugama et al., 2016), indicating the efficacy of the EAR motif in repressing expression of genes regulated by VIP1 family members. However, they showed transient and stable transformation susceptibility similar to that of wild-type plants (Figures 2.6A and B). Tumor size and morphology also did not change on roots of these lines. We conclude that VIP1 and its homologs are not essential for *Agrobacterium*-mediated transformation.

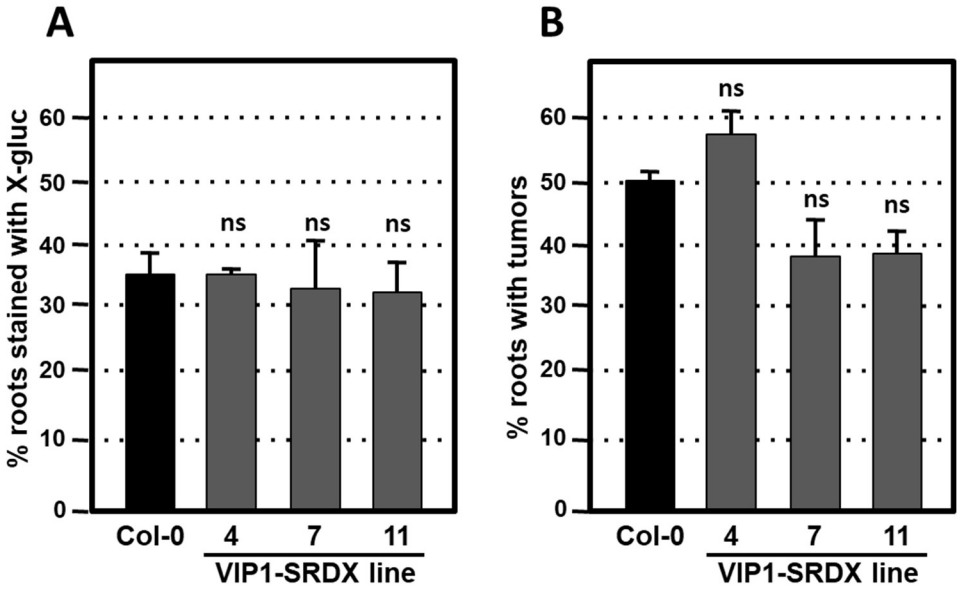

Figure 2.6. Transformation susceptibility of *Arabidopsis* wild-type and VIP1-SRDX mutant roots.

Agrobacterium-mediated transient or stable transformation assays were conducted on wild-type and VIP1-SRDX plants. Root segments were inoculated with the strains *A. tumefaciens* At849 (10^6 cfu/ml for transient) or A208 (10^7 cfu/ml for stable). For transient transformation (A), root segments were stained with X-gluc 6 days after infection; for stable transformation (B), tumors were scored 30 days after infection. Numbers represent an average of three biological replicates (each replicate containing >60 root segments) ± SE. Student's *t* test *P-value < 0.05, **P-value < 0.01, ***P-value < 0.001, ns: not significant

Subcellular localization of VIP1 homologs and their interactions with VirE2

We transfected tobacco BY-2 protoplasts using constructs encoding GFP-tagged VIP1, bZIP52, PosF21, bZIP29, bZIP31, UNE4, and bZIP33 expressed from a Cauliflower Mosaic Virus (CaMV) 35S promoter (Figure 2.7). The subcellular localization of VIP1, bZIP52, bZIP31, and UNE4 is in both the cytoplasm and the nucleus, except that VIP1 localizes predominantly to the nucleoplasm (Figure 2.7A), whereas the other transcription factors also localized to the nucleolus (Figure 2.7B, E, and F). PosF21 and bZIP33 localized predominantly to the cytoplasm (Figure 2.7C and G), with bZIP33 showing perinuclear aggregates (Figure 2.7G). bZIP29 showed exclusively nucleoplasmic localization (Figure 2.7D). Free GFP localized throughout the cytoplasm and nucleus (Figure 2.7H). Thus, although these related transcription factors showed overlapping subcellular localization patterns, none of these patterns is identical to that of VIP1.

We examined the interaction of VirE2 with VIP1, bZIP52, and PosF21 using BiFC. VIP1-VirE2 complexes localized to the perinuclear area and formed aggregates (Figure 8A, Shi et al., 2014). The interaction and co-localization patterns of bZIP52 and PosF21 with VirE2 (Figures 2.8B and C) resemble the pattern of VirE2 localization (Figure 2.8D). These data suggest that through interaction, VirE2 relocalizes these transcription factors in plant cells (compare Figures 2.7 and 8). In our control, we did not detect interaction of VirE2-nYFP with cCFP (Figure 2.8E).

Figure 2.7 Subcellular localization of VIP1 and its homologs in tobacco BY-2 protoplasts. DNA of Venus-tagged VIP1 or its homologs were co-transfected with a nuclear marker mRFP-NLS into tobacco BY-2 protoplasts. Cells were imaged by confocal microscopy 16 hours after transfection. Four images of each cell are presented (clockwise from top left: merged YFP, mRFP, and DIC; YFP; YFP + mRFP; mRFP). Bars indicate 20 μm.

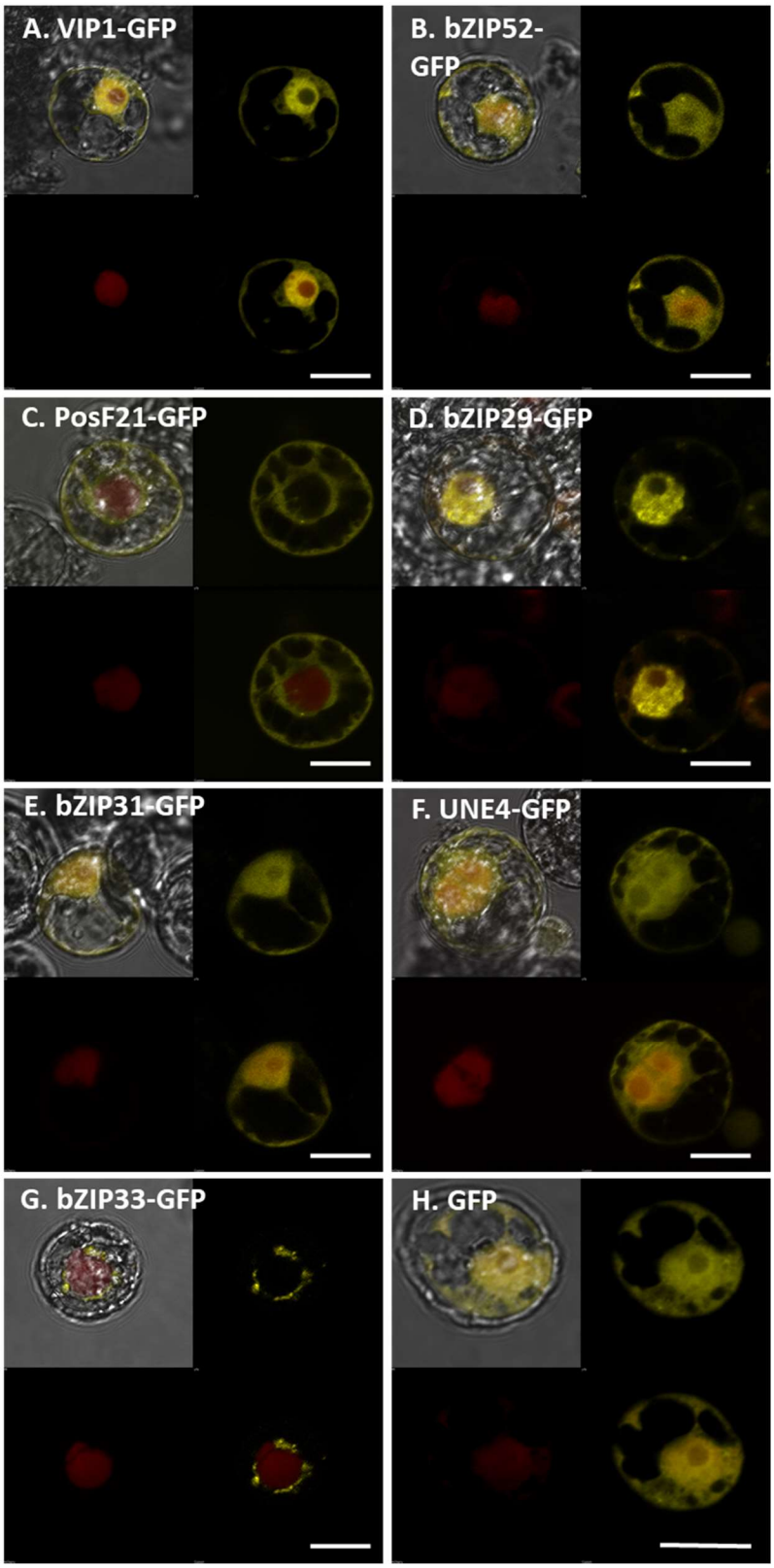
A. VIP1-GFP
B. bZIP52-GFP
C. PosF21-GFP
D. bZIP29-GFP
E. bZIP31-GFP
F. UNE4-GFP
G. bZIP33-GFP
H. GFP

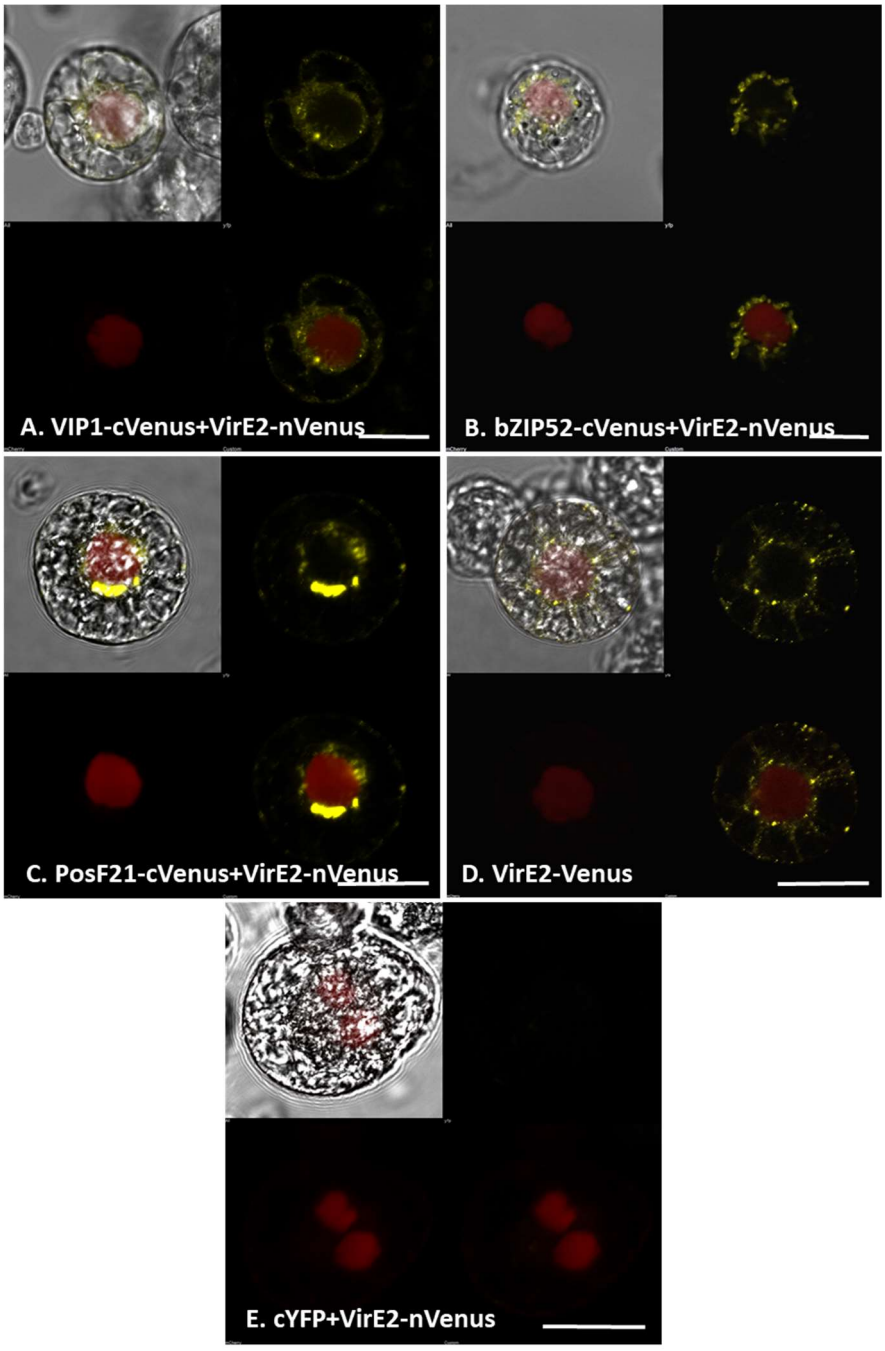

Figure 2.8. Subcellular localization of complexes formed by VirE2 with VIP1 homologs in tobacco BY-2 protoplasts.

Tobacco BY-2 protoplasts were co-transfected with constructs comprised of the indicated cVenus-tagged VIP1 homologs and VirE2-nVenus (A, B, and C); a construct encoding VirE2-Venus (D), or constructs encoding VirE2-nVenus and cCFP (E). A nuclear marker encoding mRFP-NLS was also included in all transfection experiments. The cells were imaged by confocal microscopy after 16 hours. Four images of each cell are presented (clockwise from top left: merged YFP, mRFP, and DIC; YFP; YFP + mRFP; mRFP). Bars indicate 20 μm.

VIP1 target gene expression in the absence and presence of Agrobacterium

To elucidate the expression of VIP1 target genes in the presence of *Agrobacterium*, we generated transgenic *A. thaliana* expressing *VIP1* under the control of an inducible promoter. We incubated roots of these plants in induction or control solutions for 0, 3, or 12 hours in the absence or presence of the avirulent strain *A. tumefaciens* A136 lacking a Ti plasmid. Incubation with bacteria induces plant PAMP (pattern associated molecular pattern) defense responses. After various times, we harvested root tissue and isolated total RNA. We performed quantitative RT-PCR analysis to measure the expression of previously identified VIP1 target genes (Pitzschke et al., 2009; Tsugama et al., 2012, 2014; Andrea Pitzschke, personal communication). These experiments were performed as three technical replicates each of three biological replicates. Representative data are shown in Figure 2.9A-E, and the full analysis is shown in Supplemental Table 2.4. The *VIP1* transgene was strongly expressed in the induced but not the non-induced samples, both in the absence and in the presence of *Agrobacterium* (Figure 2.9A). The VIP1 target gene *MYB44* (*At5g67300*) showed slightly elevated expression to similar levels in all of the induced samples compared to the non-induced samples, both in the presence and in the absence of *Agrobacterium* (Figure 2.9B). The putative VIP1 target gene *PHI-1* (*At1g35140*) showed the highest expression 12 hours after induction in the presence of *Agrobacterium* (Figure 2.9C). Although *CYP707A1* (*At4g19230*) did not respond to induction of *VIP1*, *CYP707A3* (*At5g45340*) did, showing the greatest increase in expression 12 hours after induction in the absence of *Agrobacterium*. However, the expression of *CYP707A3* in the presence of *Agrobacterium* was at a level similar to that found in the 3 hour samples (Figure 2.9E). *CYP707A3* is involved in the inactivation of ABA signaling, suggesting that VIP1 may play a role in modulating ABA responses during stress responses (Tsugama et al., 2012). ABA is a key hormone involved in defense responses against fungal pathogens such as *Botrytis cinerea* (Audenaert et al., 2002; Fan et al., 2009; Sivakumaran et al., 2016). Therefore, we tested the susceptibility of *vip1* mutant plants to *Botrytis cinerea* (Figure 2.10).

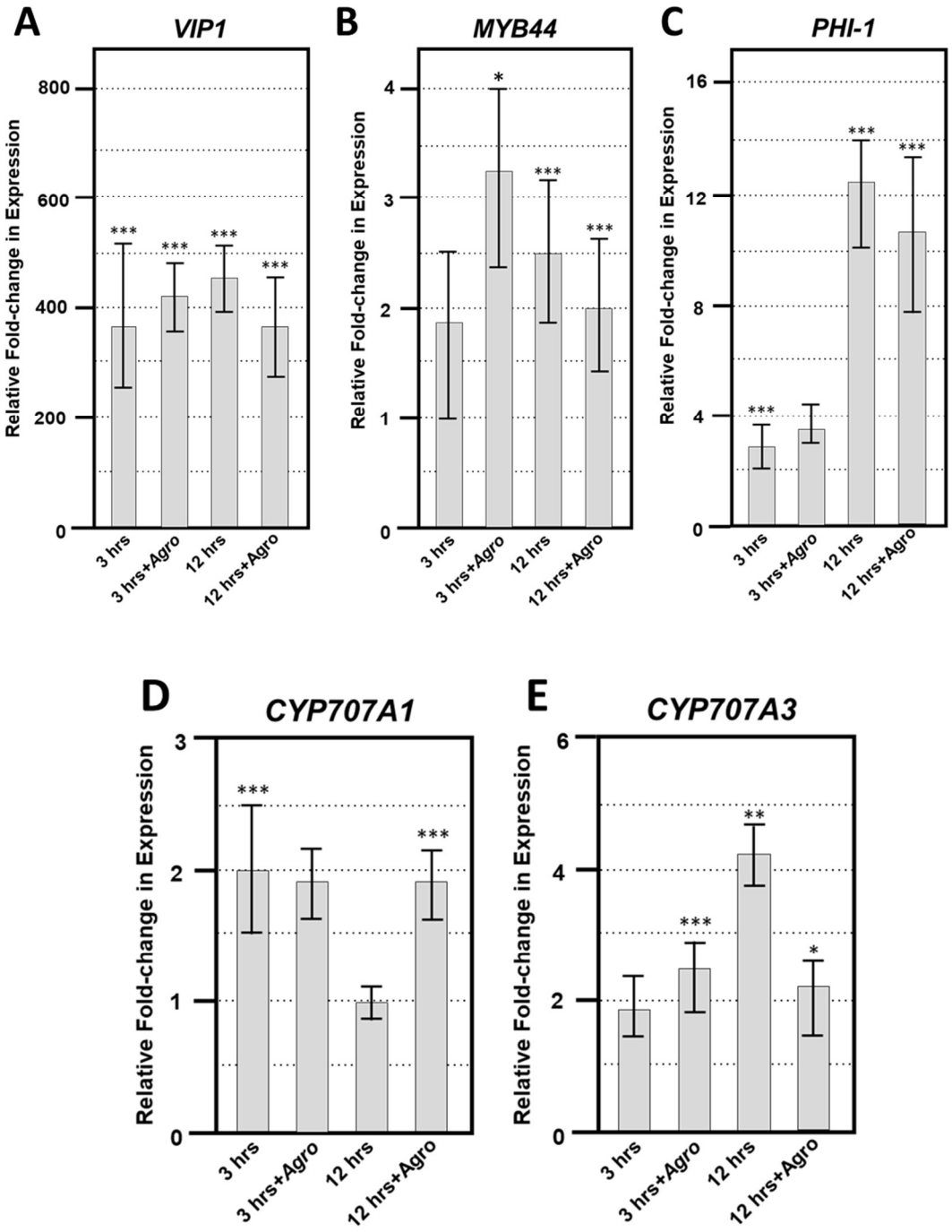

Figure 2.9. Quantitative RT-PCR of VIP1 target and fungal defense genes. Quantitative RT-PCR of (A) *VIP1* transgene, (B) *MYB44*, (C) *PHI-1*, (D) *CYP707A1,* (E) *CYP707A3*, (F) *MES1,* and (G) *LYK3* gene expression in induced relative to that of non-induced roots (y-axis). Results represent an average of three replicates ± SE. Relative expression is shown after 3 and 12 hours of induction in the absence or presence of *Agrobacterium* (+Agro) on the x-axis. Astericks indicate SE according to Student's *t* test: *P-value < 0.05, **P-value < 0.01, ***P-value < 0.001.

Figure 2.9 continued

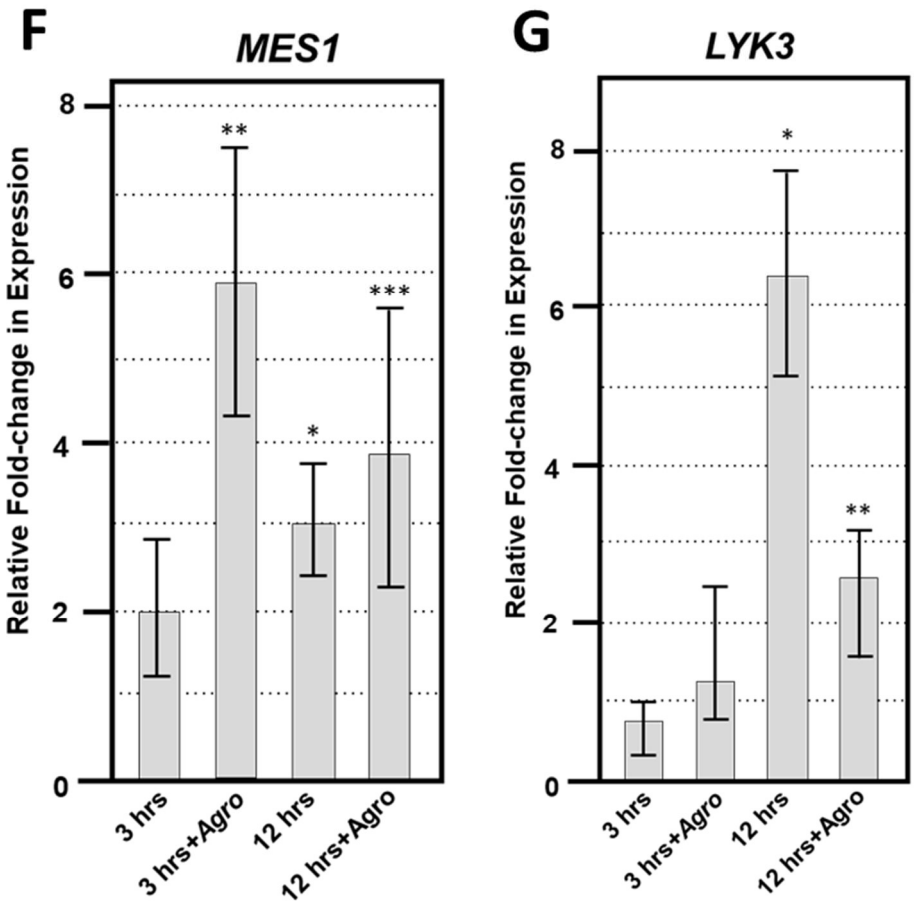

vip1 mutant and VIP1-SRDX lines show increased susceptibility to Botrytis cinerea, but not to Pseudomonas syringae infection

VIP1 is a target of the MAPK cascade and has been proposed to be involved in defense responses (Pitzschke et al., 2009). Although we were unable to find a role for VIP1 and its homologs in defense against *Agrobacterium*, we considered that VIP1 may play a role in defense against other pathogens. We therefore conducted pathogenesis assays, using *Pseudomonas syringae* and *Botrytis cinerea*, on wild-type, *vip1-1, vip1-2*, and *VIP1-SRDX* plants. Leaf lesion size was significantly larger on *B. cinerea* infected *vip1-1*, *vip1-2,* and *VIP1-SRDX* leaves than on wild-type leaves, indicating that VIP1, and perhaps additionally its paralogs, are involved in defense against *Botrytis* infection (Figures 2.10A and B).

vip1 mutants and *VIP1-SRDX* lines responded similarly as did wild-type plants to treatment with both a virulent (*Pst* DC3000) and avirulent (*Pst* DC3000 *hrcC*) *P. syringae* strains (Figures 2.10C and D). These results suggest that *VIP1* plays a role in *B. cinerea*, but not *P. syringae* and *A. tumefaciens*, defense. We also found that expression of the fungal defense genes *MES1* (At2g23620) and *LYK3* (At1g51940) were elevated after induction of *VIP1* transgene expression, suggesting a role for VIP1 in fungal defense (Figures 9F and G; Vlot et al., 2008; Paparella et al., 2014).

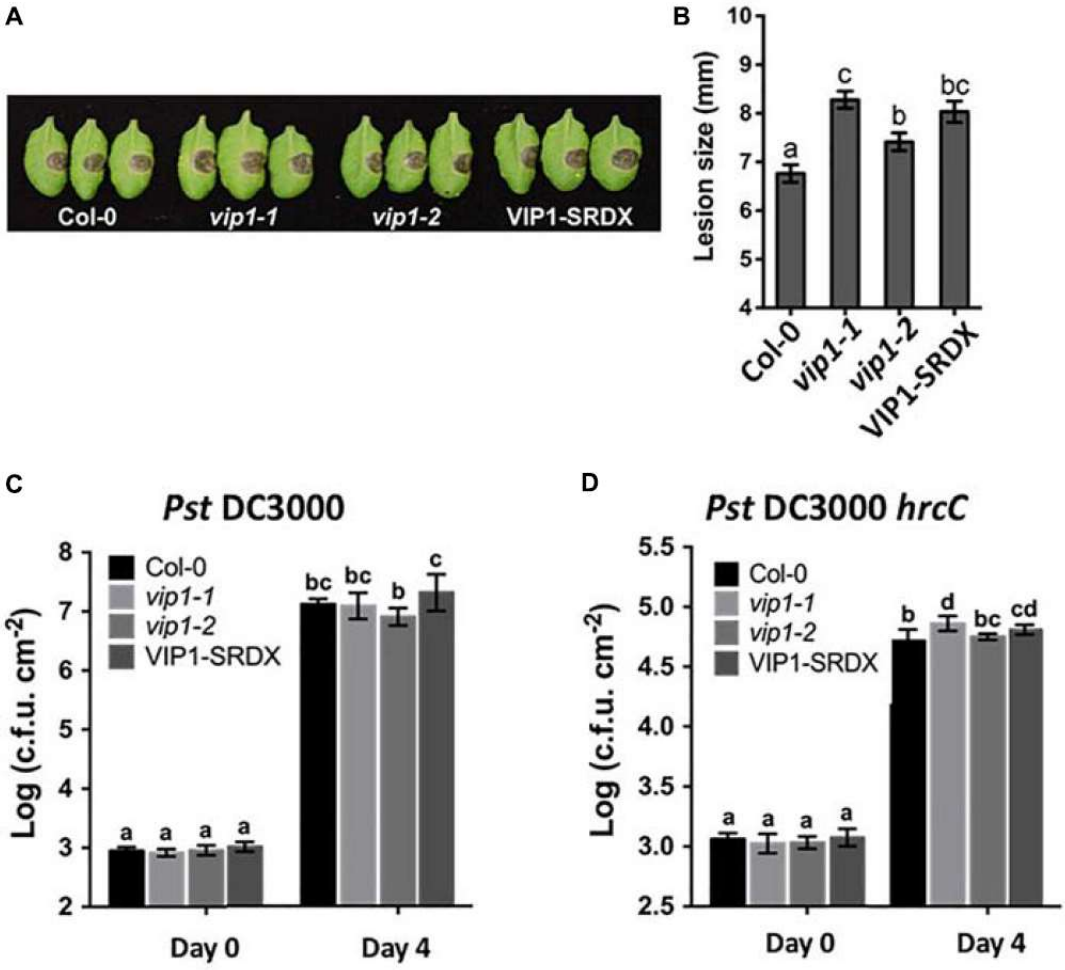

Figure 2.10. VIP1 is important for fungal but not bacterial infection of Arabidopsis. (A) Disease symptoms on leaves of various plants 3 days after inoculated with 5 µl of *B. cinerea* at the concentration of $1.0x10^5$ spores/ml; (B) Averaged lesion size of 18 leaves of each genotype (36 leaves for Col-0) after *B. cinerea* inoculation; (C) Leaves of 5 week old plants were syringe inoculated with *Pseudomonas syringe* c.v. *tomato Pst* DC3000 (A_{600}=0.001) or (D) *Pst* DC3000 *hrcC* (A_{600}=0.005). Growth of *bacteria on leaves* was measured at 0 and 4 dpi. Averaged numbers of bacteria and standard deviations were obtained from three replicates, each consisting of six leaf discs. Different letters indicate significant differences (P<0.05, Student's t test).

vip1 mutant and VIP1-SRDX lines are sensitive to exogenous ABA during, but not after, germination

Botrytis cinerea produces exogenous ABA to suppress plant defense responses (Audenaert et al., 2002; Fan et al., 2009; Sivakumaran et al., 2016). *VIP1* may play a role in abscisic acid (ABA) signaling (Tsugama et al., 2012, 2013, 2014). Under hypo-osmotic conditions, VIP1 re-localizes to the nucleus and activates transcription of *CYP707A1* and *CYP707A3* (Tsugama et al., 2012) which encode proteins that degrade ABA and are therefore involved in osmosensory regulation of plant growth (Supplemental Figure 2.4; Kushiro et al., 2004; Umezawa et al., 2006). In the absence of *VIP1*, plants may be less able to degrade exogenous ABA, which may explain the increased susceptibility of *vip1* mutant plants and *VIP1-SRDX* lines to *B. cinerea* infection. Because ABA is also a negative regulator of germination (Supplemental Figure 2.4; Gimeno-Gilles et al., 2009), we hypothesized that *vip1* mutant and *VIP1-SRDX* lines may display altered germination in the presence of exogenous ABA. We germinated seeds of wild-type, *vip1-1*, *vip1-2*, and *VIP1-SRDX* lines 7-1 and 11 on medium containing either 0, 0.3, or 0.5 µM ABA. In the presence of ABA, almost all the wild-type seeds germinated within eight days after imbibition. Seeds of the *vip1-1* and *vip1-2* mutants, and two *VIP1-SRDX* lines, showed reduced germination in the presence of ABA (Figure 2.11).

Low concentrations of ABA promote root growth, whereas high concentrations inhibit growth (Pilet and Saugy, 1987; Sharp and LeNoble, 2002). To elucidate whether *VIP1* plays a role in ABA signaling during root growth, we first germinated *vip1* mutant and *VIP1-SRDX* plants on MS medium, then transferred the seedlings to plates containing 0, 2, or 20 µM ABA to continue growth. The rate of root growth did not significantly differ from that of wild-type for any of the *vip1* mutant or *VIP1-SRDX* lines (Supplemental Figure 2.5). These results suggest that although *VIP1* appears important for ABA defense signaling and germination, it does not play a role in ABA-dependent regulation of root growth.

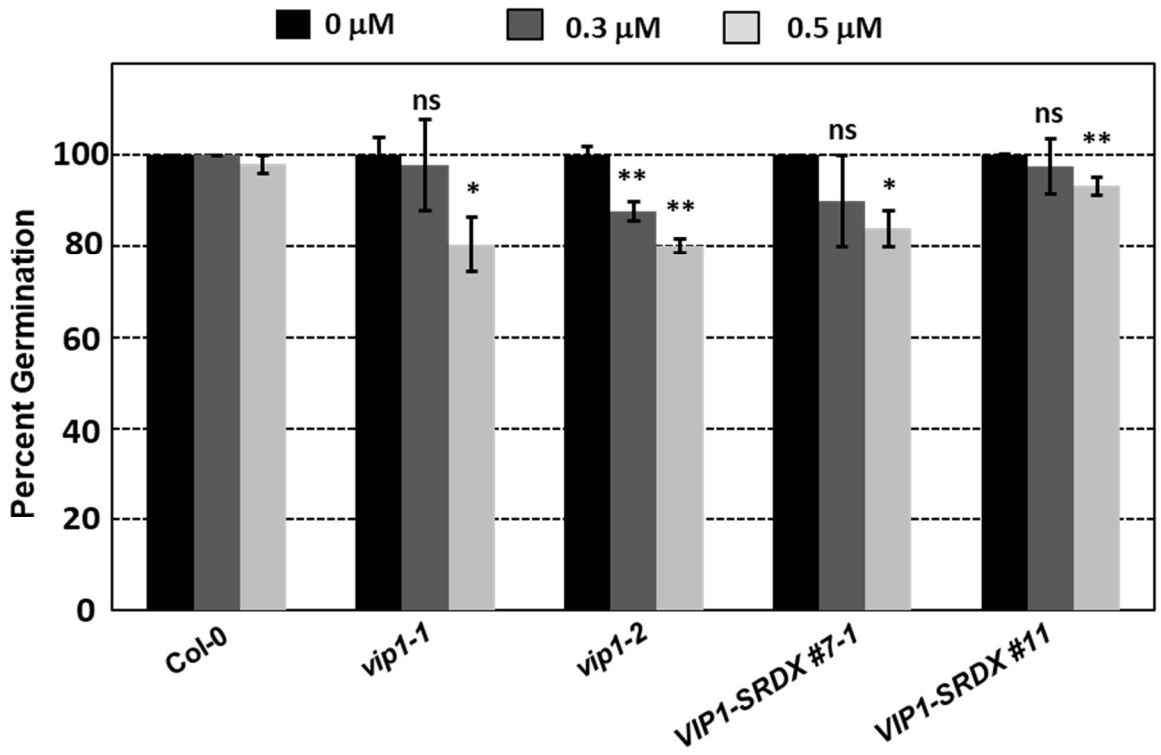

Figure 2.11. Germination of wild-type, *vip1* mutants, and a VIP1-SRDX line on medium containing ABA. Seeds of the indicated lines were germinated on B5 medium containing 0, 0.3, or 0.5 µM ABA. Data represent the average percent germination ± SE. Student's *t* test. *Pvalue < 0.1, **Pvalue < 0.05, ***Pvalue < 0.01, ns: not significant

vip1 mutant and VIP1-SRDX roots are more tolerant to growth in high salt

To determine if VIP1 also plays a role under hyper-osmotic conditions, we performed seed germination and root growth assays on wild-type Col-0, *vip1-2, vip1-1/posf21/bzip29* mutants, and VIP1-SRDX lines. All seeds germinated well on medium containing elevated concentrations of NaCl (Supplemental Figure 2.6). However, roots of all *vip1* mutant lines, and two *VIP1-SRDX* lines, grew better on medium containing salt than did wild-type roots (Figure 2.12). These results indicate that *VIP1* plays a role in root growth under salt stress conditions.

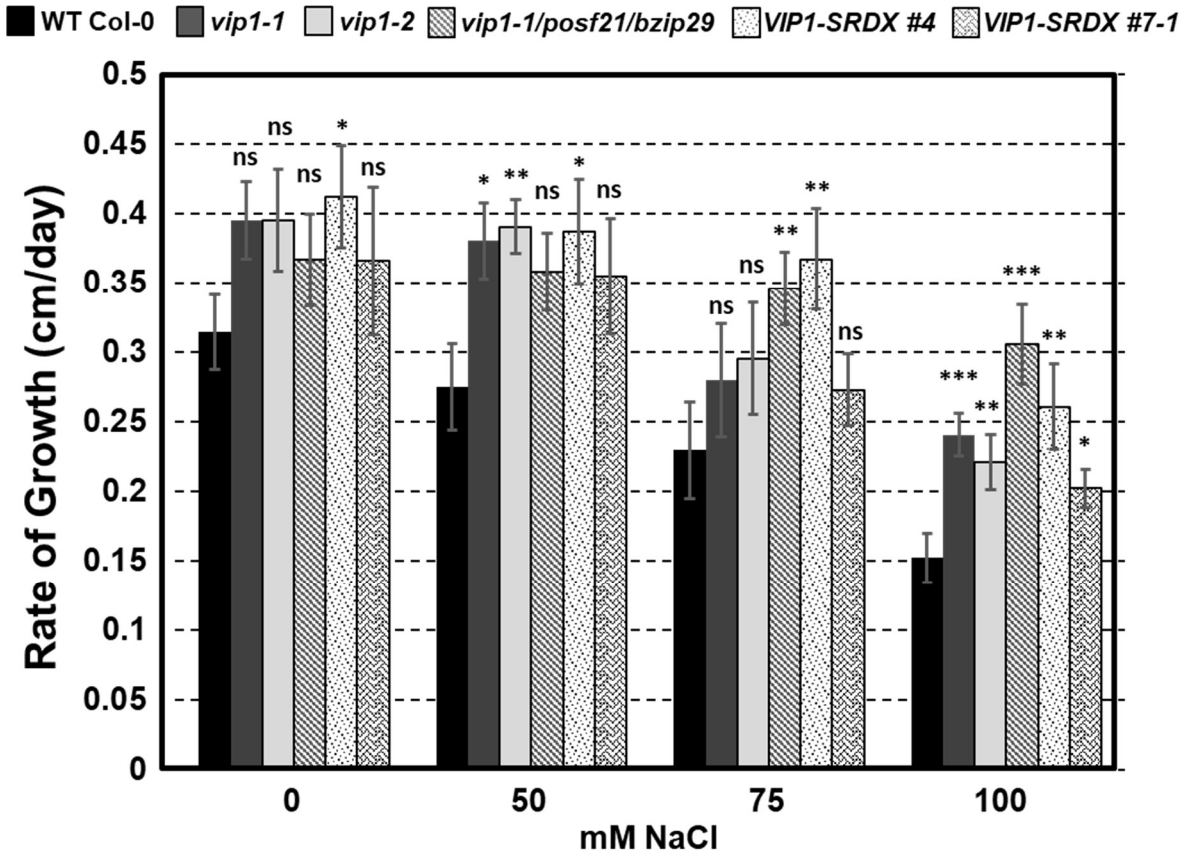

Figure 2.12. Root growth rates of wild-type, *vip1* mutant, and VIP1-SRDX lines on various concentrations of NaCl. Data represent the average rate of root growth ± SE. Student's *t* test *Pvalue < 0.05, **Pvalue < 0.01, ***Pvalue < 0.001, ns: not significant

Discussion

Previous reports indicated that, compared to wild-type plants, *vip1-1 A. thaliana* and *VIP1* antisense tobacco plants showed reduced stable transformation susceptibility, suggesting an important role for *VIP1* in *Agrobacterium*-mediated transformation (Tzfira et al., 2001, 2002; Li et al., 2005). As a consequence of these reports, and observations that plant-generated VirE2 localizes to the nucleus (Zupan et al., 1996) but cannot interact with importin α-1 (AtKapα; Ballas and Citovsky, 1997), VIP1 was proposed to act as an adaptor molecule between importin α-1 and VirE2 for nuclear entry of VirE2-bound T-DNA (the Trojan-horse model; Djamei et al., 2007). However, we have observed that VirE2 can interact with all tested *Arabidopsis* importin α isoforms *in vitro*, in yeast, and in plants (Bhattacharjee et al., 2008). We and others have observed that VirE2 and VIP1-VirE2 complexes synthesized *in planta* localize to the cytoplasm

(Bhattacharjee et al., 2008; Lee et al., 2008; Sakalis et al., 2013; Shi et al., 2014; this study), indicating that VIP1 does not act as an adaptor to localize VirE2 to the nucleus. Recent reports, however, suggest that some VirE2 molecules delivered from *Agrobacterium* may reach the nucleus (Li et al., 2014; Yang et al., 2017). Thus, the role of VirE2 in helping deliver T-strands to the plant nucleus remains controversial. Regardless of the role of VirE2 in nuclear import of T-strands, this current, and a previous, study (Shi et al., 2014) found no significant change in *Agrobacterium*-mediated transformation susceptibility in any *VIP1* mutant background or in *VIP1* overexpressing transgenic lines. Therefore, our data do not support the Trojan-horse model (Djamei et al., 2007).

Although we could not find a role for VIP1 in *Agrobacterium*-mediated plant transformation, we were concerned that other group I bZIP transcription factors related to *Arabidopsis* VIP1 could mask the effect of VIP1 on transformation. *VIP1* is one of a 12-gene family whose members may have redundant functions. Analysis of null mutants of six individual *VIP1* homologs did not reveal any transformation phenotypes, and the *vip1-1/posf21/bzip29* triple mutant showed only a modest reduction in transformation susceptibility, suggesting that some VIP1 family members may slightly potentiate transformation. We therefore analyzed transgenic lines overexpressing VIP1 fused to a SRDX repression domain. The binding of other transcription factors to the promoters of *VIP1* target genes is blocked in these lines (Mitsuda et al., 2006; Tsugama et al., 2016). *VIP1-SRDX* lines also displayed transformation characteristics similar to that of wild-type plants. We therefore conclude that full expression of *VIP1* and its homologs is not required for *Agrobacterium*-mediated transformation. It is possible, however, that residual expression of VIP1 target genes may facilitate transformation.

While testing inducible VIP1 plants in the absence and presence of *Agrobacterium*, we observed differential expression of the VIP1 target genes *MYB44* (At5g67300) and *CYP707A3* (At5g45340) previously identified in the literature (Figures 2.9B and 9E; Pitzschke et al., 2009; Tsugama et al., 2012, 2014). Pitzschke et al. (2009) found that *MYB44* was up-regulated in wild-type plants after treatment with flg22, and that the gene contains multiple copies of a VIP1 responsive element (VRE) in its promoter. We were also able to detect up-regulation of the putative VIP1 target gene *PHI-1* (At1g35140) in response to VIP1 induction (Figure 2.9C; Andrea Pitzschke, personal communication). *CYP707A3* expression also increases upon *VIP1* induction, as well as after tissue rehydration and in the presence of mannitol in *VIP1*

overexpressing plants (Figure 2.9E; Tsugama et al., 2012). Although Tsugama et al. (2012, 2014) showed that *CYP707A1* (At4g19230) is differentially expressed under the same conditions as is *CYP707A3*, we did not detect any significant change in *CYP707A1* expression in our experiments (Figure 2.9D), suggesting that *CYP707A1* up-regulation requires conditions not present in our protocol.

VIP1 is a phosphorylation target of MPK3 and has been proposed to be involved in plant defense responses (Pitzschke et al., 2009). Increased susceptibility of *vip1-1*, *vip1-2*, and *VIP1-SRDX A. thaliana* plants to *Botrytis cinerea*, but not to *P. syringae*, suggests that *VIP1* may play a role in fungal but not bacterial defense responses. Resistance to broad host necrotrophic fungi such as *B. cinerea* is mediated by quantitative resistance mechanisms involving the contributions of many genes (Poland et al., 2009; Lai and Mengiste, 2013). The *VIP1* gene contributes to this resistance, as indicated by the increase in disease lesion size when *VIP1* is debilitated (Figure 2.10A). This model is supported by our observation that the *LYK3* gene, involved in response to chitin, is up-regulated in inducible *VIP1* plants (Figure 2.9G). VIP1 may be phosphorylated by MPK3 in response to *B. cinerea*, leading to the activation of its target genes *CYP707A1* and *CYP707A3*, which are ABA degradation enzymes (Kushiro et al., 2004; Umezawa et al., 2006). CYP707A1 and CYP707A3 may be important for the degradation of exogenous ABA produced by *B. cinerea*, preventing the suppression of defense responses (Audenaert et al., 2002; Fan et al., 2009; Sivakumaran et al., 2016). The role of ABA in fungal infection is consistent with the observation that ABA-deficient tomato plants are highly resistant to *B. cinerea* infection (Asselbergh et al., 2007). The precise role of *VIP1* in defense signaling during *B. cinerea* infection remains unknown. Measuring the expression of *VIP1* target genes throughout infection should provide clues as to how *VIP1* contributes to defense against *B. cinerea* during early and late stages of infection.

The altered growth of *vip1-2* leaves (Fig. 2.3A and B) suggests a role for VIP1 in plant growth and development. This role is supported by the observation of increased touch-induced root waving in *VIP1-SRDX* plants (Tsugama et al., 2016). This and previous studies also suggest a role for VIP1 in the regulation of abiotic stress responses, specifically to hypo- and hyperosmotic conditions (Tsugama et al., 2012; Fig. 2.12). A previous study did not observe any major growth differences of *VIP1-SRDX* compared to wild-type plants in the presence of ABA or under hyperosmotic conditions (mannitol) after three weeks of growth (Tsugama et al., 2016).

Our study, however, measured seed germination and the rate of root growth of plants at earlier times (less than 12 days after plating). This assay allowed us to quantify better the sensitivity of these plants to ABA and hyperosmotic conditions. VIP1 enters the nucleus and binds to the promoters of its target genes, *CYP707A1* and *CYP707A3*, upon rehydration of plant roots, leading to an increase in their expression (Tsugama et al., 2012). It is unknown whether the increase in the expression of *CYP707A1* and *CYP707A3* by VIP1 after rehydration leads to the degradation of ABA or contributes to some other signaling pathway. Whether VIP1 affects plant growth and development under various osmotic conditions via CYP707A1/CYP707A3 degradation of ABA or by other ABA-dependent or -independent signaling mechanisms will require further investigation.

References

Anand, A., Krichevsky, A., Schomack, S., Lahaye, T., Tzfira, T., Tang, Y., Citovsky, V., and Mysore, K.S. (2007) *Arabidopsis* VIRE2 INTERACTING PROTEIN 2 is required for *Agrobacterium* T-DNA integration in plants. *Plant Cell* 19, 1695-1708.

Asselbergh, B., Curvers, K., França, S.C., Audenaert, K., Vuylsteke, M., Van Breusegem, F., and Höfte, M. (2007) Resistance to *Botrytis cinerea* in *sitiens*, an abscisic acid-deficient tomato mutant, involves timely production of hydrogen peroxide and cell wall modifications in the epidermis. *Plant Physiol.* 144, 1863-1877.

Audenaert, K., De Meyer, G.B., and Höfte, M.M. (2002) Abscisic acid determines basal susceptibility of tomato to *Botrytis cinerea* and suppresses salicylic acid-dependent signaling mechanisms. *Plant Physiol.* 128, 491-501.

Babon, J.J., McKenzie, M., and Cotton, R.G.H. (2003) The use of resolvases T4 endonuclease VII and T7 endonuclease I in mutation detection. *Mol Biotech* 23, 73-81.

Ballas, N., and Citovsky, V. (1997) Nuclear localization signal binding protein from *Arabidopsis* mediates nuclear import of *Agrobacterium* VirD2 protein. *Proc. Natl. Acad. Sci. USA* 94, 10723-10728.

Bhattacharjee, S., Lee, L-Y., Oltmanns, H., Cao, H., Veena, Cuperus, J., and Gelvin S.B. (2008) AtImpα-4, an *Arabidopsis* importin α isoform, is preferentially involved in *Agrobacterium*-mediated plant transformation. *Plant Cell* 20, 2661-2680.

Brogna, S., and Wen J. (2009) Nonsense-mediated mRNA decay (NMD) mechanisms. *Nature Struct. Mol. Biol.* 16, 107-113.

Chang, C.-W., Williams, S.J., Cunago, R.M., and Kobe B. (2014) Structural basis of interaction of bipartite nuclear localization signal from *Agrobacterium* VirD2 with rice importin-α. *Mol. Plant* 7, 1061-1064.

Chen, J., Yi, Q., Cao, Y., Wei, B., Zheng, L., Xiao, Q., Xie, Y., Gu, Y., Li, Y., Huang, H., Wang, Y., Hou, X., Long, T., Zhang, J., Liu, H., Liu, Y., Yu, G., and Huang, Y. (2015) ZmbZIP91 regulates expression of starch synthesis-related genes by binding to ACTCAT elements in their promoters. *J. Exp. Bot.* 67, 1327-1338.

Citovsky, V., Zupan, J., Warnick, D., and Zambryski, P. (1992) Nuclear localization of *Agrobacterium* VirE2 protein in plant cells. *Science* 256, 1802-1805.

Citovsky, V., Warnick, D., and Zambryski, P. (1994) Nuclear import of *Agrobacterium* VirD2 and VirE2 proteins in maize and tobacco. *Proc. Natl. Acad. Sci. USA* 91, 3210-3214.

Citovsky, V., Lee, L.-Y., Vyas, S., Glick, E., Chen, M.H., Vainstein, A., Gafni, Y., Gelvin, S.B., and Tzfira, T. (2006) Subcellular localization of interacting proteins by bimolecular fluorescence complementation *in planta*. *J. Mol. Biol.* 362, 1120-1131.

Clough, S.J., and Bent, A.F. (1998) Floral dip: a simplified method for *Agrobacterium*-mediated transformation of *Arabidopsis thaliana*. *Plant J.* 16, 735-743.

Dingwall, C., and Laskey, R.A. (1991) Nuclear targeting sequences—a consensus? *Trends Biochem. Sci.* 16, 478-481.

Djamei, A., Pitzschke, A., Nakagami, H., Rajh, I., and Hirt, H. (2007) Trojan horse strategy in *Agrobacterium* transformation: abusing MAPK defense signaling. *Science* 318, 453-456.

Durfee, T., Nelson, R., Baldwin, S., Plunkett, G., Burland, V., Mau, B., Petrosino, J.F., Qin, X., Muzny, D.M., Ayele, M., Gibbs, R.A., Csörgo, B., Pósfai, G., Weinstock, G.M., and Blattner, F.R. (2008) The complete genome sequence of *Escherichia coli* DH10B: insights into the biology of the laboratory workhorse. *J. Bacteriol.* 190, 2597-2606.

Fan, J., Hill, L., Crooks, C., Doerner, P., Lamb, C. (2009) Abscisic acid has a key role in modulating diverse plant-pathogen interactions. *Plant Physiol.* 150, 1750-1761.

Feng, Z., Zhang, B., Ding, W., Liu, X., Yang, D.-L., Wei, P., Cao, F., Zhu, S., Zhang, F., Mao, Y., Zhu, J.-K. (2013) Efficient genome editing in plants using a CRISPR/Cas system. *Cell Res.* 23, 1229-1232.

Gelvin S.B. (2003) *Agrobacterium*-mediated plant transformation: the biology behind the "gene-jockeying" tool. *Microbiol. Mol. Biol. Rev.* 67, 16-37.

Gelvin S.B. (2012) Traversing the cell: *Agrobacterium* T-DNA's journey to the host genome. *Front. Plant Sci.* 3, 1-11.

Gimeno-Gilles, C., Lelièvre, E., Viau, L., Malik-Ghulam, M., Ricoult, C., Niebel, A., Leduc, N., and Limami, A.M. (2009) ABA-mediated inhibition of germination is related to the inhibition of genes encoding cell-wall biosynthetic and architecture: modifying enzymes and structural proteins in *Medicago truncatula* embryo axis. *Mol. Plant* 2, 108-119.

Grange, W., Duckely, M., Husale, S., Jacob, S., Engel, A., and Hegner, M. (2008) VirE2: A unique ssDNA-compacting molecular machine. *PLoS Biol.* 6, 0343-0351.

Hajdukiewicz, P., Svab, Z., and Maliga, P. (1994) The small, versatile pPZP family of *Agrobacterium* binary vectors for plant transformation. *Plant Mol. Biol.* 25, 989-994.

Hiratsu, K., Ohta, M., Matsui, K., and Ohme-Takagi, M. (2002) The SUPERMAN is an active repressor whose carboxy-terminal repression domain is required for the development of normal flowers. *FEBS Lett.* 514, 351-354.

Jakoby, M., Weisshaar, B., Dröge-Laser, W., Vicente-Carbajosa, J., Tiedemann, J., Kroj, T., Parcy, F., and bZIP Research Group (2002) bZIP transcription factors in *Arabidopsis*. *Trends Plant Sci*. 7, 106-111.

Koncz, C., and Schell, J. (1986) The promoter of TL-DNA gene 5 controls the tissue-specific expression of chimeric genes carried by a novel type of *Agrobacterium* binary vector. *Mol. Gen. Genet.* 204, 383-396.

Kushiro, T., Okamoto, M., Nakabayashi, K., Yamagishi, K., Kitamura, S., Asami, T., Hirai, N., Koshiba, T., Kamiya, Y., and Nambara, E. (2004) The *Arabidopsis* cytochrome P450 CYP707A encodes ABA 8'-hydroxylases: key enzymes in ABA catabolism. *EMBO J* 23, 1647-1656.

Ishida, S., Fukazawa, J., Yuasa, T., and Takahashi, Y. (2004) Involvement of 14-3-3 signaling protein binding in the functional regulation of the transcriptional activator REPRESSION OF SHOOT GROWTH by gibberellins. *Plant Cell* 16, 2641-2651.

Lacroix, B., Loyter, A., and Citovsky, V. (2008) Association of the *Agrobacterium* T-DNA-protein complex with plant nucleosomes. *Proc. Natl. Acad. Sci. USA* 105, 15429-15434.

Lai, Z., and Mengiste, T. (2013) Genetic and cellular mechanisms regulating plant responses to necrotrophic pathogens. *Curr. Opin. Plant Biol.* 16(4), 505-512.

Lee, L.-Y., Fang, M.-J., Kuang, L.-Y., and Gelvin S.B. (2008) Vectors for multi-color bimolecular fluorescence complementation to investigate protein-protein interactions in living plant cells. *Plant Meth.* 4, 24.

Lee, L.-Y., Wu, F.-H., Hsu, C.-T., Shen, S.-C., Yeh, H.-Y., Liao, D.-C., Fang, M.-J., Liu, N.-T., Yen, Y.-C., Dokládal, L., Sýkorová, E., Gelvin, S.B., and Lin C.-S. (2012) Screening a cDNA library for protein-protein interactions directly *in planta*. *Plant Cell* 24, 1746-1759.

Li, J., Krichevsky, A., Vaidya, M., Tzifa, T., and Citovsky, V. (2005) Uncoupling of the functions of the *Arabidopsis* VIP1 protein in transient and stable plant genetic transformation by *Agrobacterium*. *Proc. Natl. Acad. Sci. USA* 102, 5733-5738.

Li, X., Yang, Q., Tu, H., Lim, Z., and Pan, S.Q. (2014) Direct visualization of *Agrobacterium*-delivered VirE2 in recipient cells. *Plant J.* 77, 487-495.

Mitsuda, N., Hiratsu, K., Todaka, D., Nakashima, K., Yamaguchi-Shinozaki, K., and Ohme-Takagi, M. (2006) Efficient production of male and female sterile plants by expression of a chimeric repressor in *Arabidopsis* and rice. *Plant Biotechnol. J.* 4, 325–332.

Nam, J., Matthysse, A.G., and Gelvin, S.B. (1997) Differences in susceptibility of *Arabidopsis* ecotypes to crown gall disease may result from a deficiency in T-DNA integration. *Plant Cell* 9, 317-333.

Nam, J., Mysore, K.S., Zheng, C., Knue, M.K., Matthysse, A.G., and Gelvin S.B. (1999). Identification of T-DNA tagged *Arabidopsis* mutants that are resistant to transformation by *Agrobacterium*. *Mol. Gen. Genet.* 261, 429-438.

Narasimhulu, S.B., Deng, X.-B., Sarria, R., and Gelvin, S.B. (1996). Early transcription of *Agrobacterium* T-DNA genes in tobacco and maize. *Plant Cell* 8, 873-886.

O'Malley, R.C., Huang, S.C., Song, L., Lewsey, M.G., Bartlett, A., Nery, J.R., Galli, M., Gallavotti, A., and Ecker, J.R. (2016) Cistrome and epicistrome features shape the regulatory DNA landscape. *Cell* 165, 1280-1292.

Paparella, C., Savatin, D.V., Marti, L., De Lorenzo, G., and Ferrari, S. (2014) The Arabidopsis LYSIN MOTIF-CONTAINING RECEPTOR-LIKE KINASE3 regulates the cross talk between immunity and abscisic acid responses. *Plant Physiol.* 165(1), 262-276.

Pilet, P-E., and Saugy, M. (1987) Effect of root growth on endogenous and applied IAA and ABA. *Plant Physiol.* 83, 33-38.

Pitzschke, A., Djamei, A., Teige, M., and Hirt, H. (2009) VIP1 response elements mediate mitogen-activated protein kinase 3-induced stress gene expression. *Proc. Natl. Acad. Sci. USA* 106, 18414-18419.

Poland, J.A., Balint-Kurti, P.J., Wisser, R.J., Pratt, R.C., and Nelson, R.J. (2009) Shades of gray: the world of quantitative disease resistance. *Trends Plant Sci.* 14(1), 21-29.

Rossi, L., Hohn, B., and Tinland, B. (1996) Integration of complete transferred DNA is units is dependent on the activity of virulence E2 protein of *Agrobacterium tumefaciens*. *Proc. Natl. Acad. Sci. USA* 93, 126-130.

Sakalis, P.A., van Heusden, G.P.H., and Hooykaas P.J.J. (2013) Visualization of VirE2 protein translocation by the *Agrobacterium* type IV secretion system into host cells. *Microbiol. Open*. 3, 104-117.

Sharp, R.E., and LeNoble, M.E. (2002) ABA, ethylene and the control of shoot and root growth under water stress. *J. Exp. Bot.* 53(366), 33-37.

Sivakumaran, A., Akinyemi, A., Mandon, J., Cristescu, S.M., Hall, M.A., Harren, F.J.M., Mur, L.A.J. (2016) ABA suppresses *Botrytis cinerea* elicited NO production in tomato to influence H_2O_2 generation and increase host susceptibility. *Front. Plant Sci.* 7(709), 1-12.

Sciaky, D.A., Montoya, A.L., and Chilton M.-D. (1978) Fingerprints of *Agrobacterium* Ti plasmids. *Plasmid* 1, 238-253.

Shi, Y., Lee, L.-Y., and Gelvin, S.B. (2014) Is VIP1 important for *Agrobacterium*-mediated plant transformation? *Plant J* 79, 848-860.

Tenea, G.N., Spantzel, J., Lee, L.-Y., Zhu, Y., Lin, K., Johnson, S.J., and Gelvin S.B. (2009) Overexpression of several *Arabidopsis* histone genes increases *Agrobacterium*-mediated transformation and transgene expression in plants. *Plant Cell* 21, 3350-3367.

Tsugama, D., Liu, S., and Takano, T. (2012) A bZIP protein, VIP1, is a regulator of osmosensory signaling in *Arabidopsis*. *Plant Physiol.* 159, 144-155.

Tsugama, D., Liu, S., and Takano, T. (2013) A bZIP protein, VIP1, interacts with *Arabidopsis* heterotrimeric G protein β subunit, AGB1. *Plant Physiol. Biochem.* 71, 240-246.

Tsugama, D., Liu, S., and Takano, T. (2014) Analysis of functions of VIP1 and its close homologs in osmosensory responses of *Arabidopsis thaliana*. *PLoS One* 9(8), e103930.

Tsugama, D., Liu, S., and Takano, T. (2016) The bZIP protein VIP1 is involved in touch responses in *Arabidopsis* roots. *Plant Physiol.* 171, 1355-65.

Tzfira, T., Vaidya, M., and Citovsky, V. (2001) VIP1, an *Arabidopsis* protein that interacts with *Agrobacterium* VirE2, is involved in VirE2 nuclear import and *Agrobacterium* infectivity. *EMBO J.* 20, 3596-3607.

Tzfira, T., and Citovsky, V. (2001) Comparison between nuclear localization of nopaline- and octopine-specific *Agrobacterium* VirE2 proteins in plant, yeast, and mammalian cells. *Mol. Plant Pathol.* 2, 171-176.

Tzfira, T., Vaidya, M., and Citovsky, V. (2002) Increasing plant susceptibility to *Agrobacterium* infection by over-expression of the *Arabidopsis* nuclear protein VIP1. *Proc. Natl. Acad. Sci. USA* 99, 10435-10440.

Umezawa, T., Okamoto, M., Kushiro, T., Nambara, E., Oono, Y., Seki, M., Kobayashi, M., Koshiba, T., Kamiya, Y., and Shinozaki, K. (2006) CYP707A3, a major ABA 8'-hydroxylase involved in dehydration and rehydration response in *Arabidopsis thaliana*. *Plant J.* 4, 171-182.

Van Larebeke, N., Engler, G., Holsters, M., Van Den Elsacker, S., Zaenen, I., Schilperoort, R.A., and Schell, J. (1974) Large plasmid in *Agrobacterium tumefaciens* essential for crown gall-inducing ability. *Nature* 252, 169-170.

Vlot, A.C., Liu, P.P., Cameron, R.K., Park, S.W., Yang, Y., Kumar, D., Zhou ,F., Padukkavidana, T., Gustafsson, C., Pichersky, E., and Klessig D.F. (2008) Identification of likely orthologs of tobacco salicylic acid-binding protein 2 and their role in systemic acquired resistance in *Arabidopsis thaliana*. *Plant Journal* 56(3), 445-456.

Wu, Y., Zhao, Q., Gao, L., Yu, X.-M., Fang, P., Oliver, D.J., and Xiang, C.-B. (2010) Isolation and characterization of low-sulfur-tolerant mutants in *Arabidopsis*. *J Exp Bot* 61, 3407-3422.

Yang, Q., Li, X., Tu, H., and Pan, S.Q. (2017) *Agrobacterium*-delivered virulence protein VirE2 is trafficked inside host cells via a myosin XI-K-powered ER/actin network. *Proc. Natl. Acad. Sci. USA* 114, 2982-298.

Yusibov, V.M., Steck, T.R., Gupta, V., and Gelvin S.B. (1994) Association of single-stranded transferred DNA from *Agrobacterium tumefaciens* with tobacco cells. *Proc. Natl. Acad. Sci. USA* 91, 2994-2998.

Zhu, Y., Nam, J., Humara, J.M., Mysore, K.S., Lee, L.-Y., Cao, H., Valentine, L., Li, J., Kaiser, A.D., Kopecky, A.L., Hwang, H.H., Bhattacharjee, S., Rao, P.K., Tzfira, T., Rajagopal, J., Yi, H., Veena, Yadav, B.S., Crane, Y.M., Lin, K., Larcher, Y., Gelvin, M.J., Knue, M., Ramos, C., Zhao, X., Davis, S.J., Kim, S.I., Ranjith-Kumar, C.T., Choi, Y.J., Hallen, V.K., Chattopadhyay, S., Sui, X., Ziemienowicz, A., Matthysse, A.G., Citovsky, V., Hohn, B., and Gelvin S.B. (2003) Identification of *Arabidopsis* rat mutants. *Plant Physiol.* 132, 494-505.

Zupan, J.R., Citovsky, V., and Zambryski, P. (1996) *Agrobacterium* VirE2 protein mediates nuclear uptake of single-stranded DNA in plant cells. *Proc. Natl. Acad. Sci. USA* 93, 2392-2397.

Zuo, J., Niu, Q.-W., and Chua, N.-H. (2000) An estrogen receptor-based system transactivator XVE mediates highly inducible gene expression in transgenic plants. *Plant J.* 24, 265-273.

CHAPTER 3: NOVEL ROLE OF THE *AGROBACTERIUM* VIRULENCE EFFECTOR PROTEIN VIRE2 IN MODULATING PLANT GENE EXPRESSION

Introduction

Agrobacterium tumefaciens, the causative agent of crown gall disease, transfers virulence effector proteins to infected host plants to facilitate the transfer and trafficking of a piece of its tumor inducing (Ti) plasmid, (T-[transfer] DNA), into and through plant cells. T-DNA may integrate into the host genome where it uses the host's machinery to express transgenes. Scientists have used this process to insert beneficial genes into plants by replacing native T-DNA with engineered T-DNA, making *Agrobacterium*-mediated transformation the preferred method for crop genetic engineering (Gelvin, 2003, 2012).

VirE2 is an *Agrobacterium* effector protein that is important for plant transformation (Gelvin, 2003, 2012). *Agrobacterium* mutant strains lacking *virE2* are severely attenuated in virulence (Stachel and Nester, 1986), and integrated T-DNAs often exhibit large deletions (Rossi et al., 1996). VirE2 can coat single-stranded DNA molecules *in vitro* (Gietl et al., 1987; Christie et al., 1988; Citovsky et al., 1988, 1989; Das, 1988; Sen et al., 1989) and has been proposed to coat the single-stranded T-DNA molecules (T-strands) to protect them from nucleases as they are trafficked through the plant cell (Gietl et al., 1987; Citovsky et al., 1988; Yusibov et al., 1994; Tinland et al., 1994). In addition, expression of VirE2 in the plant can complement a *virE2* mutant *Agrobacterium* strain to full virulence (Citovsky et al., 1992; Simone et al., 2001). These data suggest that VirE2's major function in transformation occurs in the plant and likely involves the maintenance of T-DNA integrity (Citovsky et al., 1988; Gietl et al., 1987).

VirE2 has also been proposed to assist with nuclear import of T-strands (Christie et al., 1988; Tzfira et al., 2001), but conflicting reports of VirE2 subcellular localization have led to controversy in the literature. VirE2 showed nuclear localization when tagged on its N-terminus (Citovsky et al., 1992, 1994, 2004; Tzfira and Citovsky, 2001; Tzfira et al., 2001; Li et al., 2005), whereas C-terminally tagged VirE2 localized to the cytoplasm, often forming perinuclear aggregates (Bhattacharjee et al., 2008; Grange et al., 2008; Lee et al., 2008; Shi et al., 2014; Lapham et al., 2018). In addition, Bhattacharjee et al. (2008) showed that only C-terminally tagged VirE2, but not the N-terminally tagged protein, could complement a *virE2* mutant strain

and restore efficient transformation. Li et al. (2014) showed that VirE2 labeled with a small fragment of GFP retained full virulence. They also demonstrated, using a split GFP approach, that VirE2 delivered into plant cells from bacteria could localize to the nucleus, forming filamentous structures (Li et al., 2014).

VirE2 interacts with the plant transcription factor VIP1 (VirE2-interacting protein 1) which shows both cytoplasmic and nuclear localization (Tzfira et al., 2001; Djamei et al., 2007; Shi et al., 2014; Tsugama et al., 2012, 2013, 2014, 2016a, 2016b; Lapham et al., 2018), and was proposed to assist in VirE2 nuclear import (Tzfira et al., 2001; Djamei et al., 2007). Under stress, VIP1 localizes to the nucleus (Tsugama et al., 2012, 2014, 2016a) where it activates expression of defense response genes (Pitzschke et al., 2009). This observation led to the model that T-DNA-bound VirE2 binds VIP1 and uses VIP1 nuclear localization to deliver T-DNA into the nucleus (the "Trojan Horse" model; Djamei et al., 2007). In contrast to this model, our laboratory has obtained data showing that VirE2 holds at least a portion of the VIP1 pool outside the nucleus (Shi et al., 2014), and that VIP1 and its homologs are not required for transformation (Shi et al., 2014; Lapham et al., 2018).

To determine which subcellular site of localization is required for VirE2 to facilitate transformation, we generated plants expressing C-terminally tagged VirE2-Venus (cytoplasmic localized) or VirE2-Venus plus a nuclear localization signal (NLS; nuclear localized) under the control of a β-estradiol inducible promoter (Zuo et al., 2000). Following induction, these plants were assayed for transformation using a *virE2* mutant *Agrobacterium* strain. Cytoplasmic, but not nuclear, localized VirE2 was able to complement the *virE2* mutant strain back to full virulence, indicating that VirE2's major function in transformation occurs in the cytoplasm.

In addition to its proposed structural role in T-strand binding, we investigated other possible functions of VirE2 in transformation. VirE2 interacts with numerous plant proteins (Lee et al., 2008, 2012) including transcription factors (Tzfira et al., 2001; Anand et al., 2007; Pitzscke et al., 2009). We hypothesized that these interactions could lead to changes in plant gene expression, perhaps facilitating transformation. To investigate this possibility, we performed RNA-seq on transgenic *Arabidopsis thaliana* roots inducibly expressing VirE2. Genes known to be involved in defense response and genes previously shown to be important for transformation were differentially expressed in the presence of VirE2, possibly facilitating transformation. Knockout mutant lines of some of these genes exhibited altered transformation

phenotypes. In addition, we isolated proteins from *A. thaliana* roots expressing VirE2. Proteins known to be important for transformation were more prevalent after VirE2 induction, and transgenic plants overexpressing cDNAs encoding some of these proteins showed enhanced transformation susceptibility. Taken together, our results suggest that VirE2 alters expression of specific plant genes and proteins to facilitate transformation, and that VirE2 must localize to the cytoplasm to promote efficient transformation.

Methods

Plasmid and Strain Constructions

Supplemental Table 3.2 lists the plasmids and strains used in this study. To make the inducible gene constructions, an *Sph*I-*Xho*I fragment containing the *LexA* operator and a minimal Cauliflower Mosaic Virus 35S promoter was excised from the plasmid pER8 (Zuo et al., 2000). The fragment was made blunt using the Klenow fragment of DNA polymerase and was ligated to the blunted plasmid pE3542 previously digested with *Age*I and *Xho*I, to make pE4224. pE4224 is a pSAT1-derived cloning vector (Tzfira et al., 2005) used to make all β-estradiol-inducible gene constructions.

To make the inducible promoter (pI) VirE2-Venus construction, the VirE2-Venus fragment was excised from pE3759 using *Swa*I and *Not*I and ligated into pE4224 digested with *Sma*I and *Not*I to make pE4282. The pI-VirE2-Venus fragment was then excised from pE4282 using *Asc*I and ligated into the *Asc*I site of pE4223 to make pE4292. pE4223 is a binary vector derived from the β-estradiol inducible binary vector pE4215 containing an XVE expression cassette and an *hptII* gene (Lapham et al., 2018). The I-*Sce*I fragment from pE4375, containing P_{nos}-Cerulean-S40NLS, was cloned into the I-*Sce*I site of pE4292 to make pE4376. The P_{nos}-mCherry-ABD2 fragment was removed from pE4376 by digestion with I-*Ceu*I and the resulting fragment was self-ligated to create pE4377. The I-*Ceu*I fragment containing P_{35S}-mCherry-ABD2 from pE4372 was then ligated into the I-*Ceu*I site of pE4377 to create pE4380. The I-*Sce*I fragment containing P_{nos}-Cerulean-SV40NLS was removed from pE4380 and the vector was self-ligated to create pE4386. The I-*Sce*I fragment containing P_{nos}-Cerulean-VirD2NLS from pE4373 was cloned into the I-*Sce*I site of pE4386 to make pE4389. pE4389 was digested with I-

*Ceu*I to remove the P_{35S}-mCherry-ABD2 fragment and self-ligated to make the final pI-VirE2-Venus binary vector, pE4438.

To make the pI-VirE2-Venus-NLS construction, pSAT1-P_{35S}-Venus-VirD2 (pE3561) was digested with *Hin*dIII before self-ligating the backbone fragment to create pSAT1-P_{35S}-Venus-NLS (pE4433). pE4433 was digested with *Pst*I and *Not*I to obtain the C-terminal-Venus (cVenus)-NLS fragment which was cloned into the same sites on pE3759 to make pE4434. A *Swa*I and *Not*I fragment containing VirE2-Venus-NLS from pE4434 was cloned into the *Sma*I and *Not*I sites of pE4224 to make pE4436. pE4436 was digested with *Asc*I to obtain the pI-VirE2-Venus-NLS fragment before cloning it into the *Asc*I site of pE4389 to make pE4435. pE4435 was digested with I-*Ceu*I and self-ligated to make the final pI-VirE2-Venus-NLS binary vector, pE4439. pE4438 and pE4439 were introduced into *A. tumefaciens* GV3101 (Van Larebeke et al., 1974) by electroporation to make *A. tumefaciens* At2155 and At2156, respectively.

To generate the inducible VirE2 overexpression plasmid, a *Swa*I and *Not*I fragment containing the *VirE2* gene from pE4229 was cloned into the *Sma*I and *Not*I sites of pE4224 to create pE4276. The *Asc*I fragment containing pI-VirE2 was cloned into the *Asc*I sites of pE4215 to generate pE4289. pE4289 was electroporated into *A. tumefaciens* GV3101 (Van Larebeke et al., 1974) to make *A. tumefaciens* At2091.

To generate the constitutive overexpression constructs for proteins whose levels are increased in the presence of VirE2, cDNA clones were ordered from the Arabidopsis Biological Resource Center (ABRC: www.arabidopsis.org) for each selected gene (Supplemental Table 3.2). Each gene was amplified from the cDNA clone using PCR and primers with flanking sequences containing restriction enzyme sites (Supplemental Table 3.3). Either Phusion High-Fidelity DNA Polymerase (New England Biolabs) or Platinum SuperFi DNA Polymerase (Invitrogen) was used and the reactions were set up and run according to the manufacturers' protocols. The PCR fragments containing *PIP2A* (AT3G53420), *FLA9* (AT1G03870), *PERX34* (AT3G49120), and *PIP1A* (AT3G61430) were digested with restriction enzymes which recognized their flanking sequences (Supplemental Table 3.3) before cloning those fragments into the same sites on pE4297 to create pE4612, pE4617, pE4622, and pE4624, respectively (Supplemental Table 3.2). After cloning, the plasmid DNAs were submitted for sequencing at the Purdue Genomics Core Facility to ensure that the clones were correct. The blunt-end PCR

fragments containing *AGP31* (AT1G28290), *HDA3* (AT3G44750), *HD2C* (AT5G03740), *ROC2* (AT3G56070), and *ROC3* (AT2G16600) were cloned into pBluescript KS+ cut with *Eco*RV to make pE4626, pE4629, pE4633, pE4637, and pE4640, respectively (Supplemental Table 3.2 and 3). These plasmids were also sequenced. The *Eco*RI-*Bam*HI fragments from pE4629 (*HDA3*), pE4637 (*ROC2*), and pE4640 (*ROC3*) were cloned into the same sites of pE4515 to make pE4630, pE4638, and pE4641, respectively. The *Sal*I-*Bam*HI fragment from pE4626 (*AGP31*) and the *Bgl*II-*Bam*HI fragment from pE4633 (*HD2C*) were cloned into the same sites of pE4297 to make pE4627 and pE4634, respectively. The *Asc*I fragments containing the overexpression cassettes from pE4612 (*PIP2A*), pE4617 (*FLA9*), pE4622 (*PERX34*), pE4624 (*PIP1A*), pE4627 (*AGP31*), pE4630 (*HDA3*), pE4634 (*HD2C*), pE4638 (*ROC2*), and pE4641 (*ROC3*) were cloned into the *Asc*I site of the pE4145 binary vector to make pE4613, pE4618, pE4623, pE4625, pE4628, pE4631, pE4635, pE4639, and pE4642, respectively. Each binary vector was electroporated into *A. tumefaciens* GV3101 (Van Larebeke et al., 1974) to make *A. tumefaciens* strains At2256 (pE4613), At2257 (pE4618), At2259 (pE4623), At2260 (pE4625), At2264 (pE4628), At2265 (pE4631), At2266 (pE4642), At2267 (pE4635), and At2268 (pE4639).

Isolation and Transfection of Tobacco BY-2 Protoplasts

Protoplasts were isolated from tobacco BY-2 protoplasts and transfected as described by Lee et al. (2012). An mRFP-nuclear marker plasmid (pE3170) was co-transfected with the appropriate clones into the protoplasts. Imaging was performed 16 h post-transfection on a Nikon A1R Confocal Laser Microscope System as described in Shi et al. (2014).

Generation and selection of Inducible VirE2, VirE2-Venus, VirE2-Venus-NLS, and transgenic A. thaliana plants constitutively overexpressing selected genes

Wild-type *A. thaliana* plants (ecotype Col-0) were transformed by *A. tumefaciens* At2155, At2156, At2091, At2256, At2257, At2259, At2260, At2264, At2265, At2266, At2267, or At2268 using a flower dip protocol (Clough and Bent, 1998). T0 generation seeds from the transformed plants were surface sterilized for 15-20 min using a 50% commercial bleach and 0.1% sodium dodecylsulfate (SDS) solution before washing five times with sterile water. After overnight incubation at 4^{o}C, the seeds were plated on solidified Gamborg's B5 medium (Caisson

Labs) containing 100 mg mL^{-1} Timentin and 20 mg mL^{-1} hygromycin. The seeds were placed at 23^{o}C under a 16/8-h light/dark cycle. T1 generation hygromycin-resistant seedlings for the inducible lines were transplanted to soil and grown under the same temperature and light conditions. For inducible VirE2 plants, seeds were harvested from each T1 plant and T2 generation plants were grown in soil. T2 generation seeds were harvested and selected on hygromycin. Seeds from homozygous plants (100% progeny surviving on selection) were used for future experiments. T2 plants containing the inducible VirE2-Venus and VirE2-Venus-NLS constructions were selected on hygromycin before each experiment.

T1 generation hygromycin-resistant seedlings for each of the constitutive overexpression lines were transferred to baby food jars containing solidified B5 medium for 10-14 days. The roots of each plant were then cut into 3-5 mm segments and assayed as described in Tenea et al. (2009). Root segments were infected with *A. tumefaciens* At849 (GV3101::pMP90 [Koncz and Schell, 1986] containing pBISN1 [Narasimhulu et al., 1996]) to measure transient transformation at a concentration of 10^6 cfu/mL (Supplemental Table 3.2). After cutting the majority of the root tissue, the plant was returned to the jar for 7 to 10 days to regrow roots before transferring them to soil. The plants were grown at 23^{o}C under a 16/8-h light/dark cycle. One to two technical replicates were assayed for each T1 plant and were compared to two or three replicates of wild-type (ecotype Col-0) root segments pooled from 8 to 10 plants.

Imaging of inducible VirE2-Venus and VirE2-Venus-NLS transgenic A. thaliana roots

Inducible VirE2-Venus and VirE2-Venus-NLS seedlings (T2 generation) were germinated on B5 medium containing 100 mg mL^{-1} Timentin and 20 mg mL^{-1} hygromycin. The seedlings were transferred after two weeks to plates containing B5 medium lacking antibiotics. These plates were placed vertically in racks to promote root growth on the surface of the medium. After 10 days, the plates were placed horizontally and B5 liquid medium containing 10 mM β-estradiol dissolved in DMSO (induction solution) or B5 plus DMSO only (control solution) was pipetted onto the surface until a thin layer covered the root tissue (4-5 mL). The roots were incubated in the solution for 9 h before imaging using a Nikon A1R Confocal Laser Microscope System as described in Shi et al. (2014).

Assaying inducible VirE2-Venus and VirE2-Venus-NLS transgenic A. thaliana roots for complementation of virE2 mutant Agrobacterium

Three transgenic lines of Inducible VirE2-Venus (Lines #4-6) and VirE2-Venus-NLS (Lines #4-6) seedlings (T2 generation) were grown as described above, and were treated with either 10 mM β-estradiol induction or control solution for 24 h. After treatment, the roots were cut into 3-5 mm segments and assayed as described in Tenea et al. (2009). Root segments were either infected with *A. tumefaciens* At1529 (EHA105 [Hood et al., 1993] containing pBISN1 [Narasimhulu et al., 1996]) or the *virE2*- mutant strain At1879 (EHA105 with an in-frame deletion of *virE2* containing pBISN2 [Narasimhulu et al., 1996]) at a concentration of 10^6 or 10^8 cfu/mL, respectively (Supplemental Table 3.2). Three replicates were assayed for each line with root segments of 10-30 plants being pooled for each replicate. A total of 80 or more root segments were scored for each data point and statistical analysis was performed using ANOVA.

VirE2 Induction in the presence of Agrobacterium

Inducible VirE2 T3 generation plants were grown and assayed as described above for the inducible VirE2-Venus and VirE2-Venus-NLS plants, except that cells of *A. tumefaciens* A136 (lacking a Ti plasmid) were added to either the induction (1 mM β-estradiol) or control solution at a concentration of 10^8 cfu/mL before treating the roots. The roots were incubated in the solutions for 0, 3, or 12 h before cutting them from the stems using a razor blade, rinsing with sterile water, dabbing them dry with a paper towel, and freezing them in liquid nitrogen. Root tissue was pooled from 30 individual plants for each treatment before storage at -80^{o}C.

Preparation of Samples for RNA-seq Analysis and Quantitative RT-PCR

For both RNA-seq and quantitative RT-PCR (qRT-PCR) analyses, RNA was isolated from non-induced and induced roots in the presence of *Agrobacterium* after 0, 3, and 12 h of treatment using TriZol reagent (http://www.thermofischer.com). Three biological replicates of inducible VirE2 *A. thaliana* transgenic line #10 were analyzed. RNA from one biological replicate was sequenced for the initial pilot study by the Purdue Genomics Core Facility, whereas RNA from two additional biological replicates was sequenced by the Cornell University Institute of Biotechnology Genomics Facility.

A total of 2 µg of total RNA was treated with Ambion DNase I (Thermo Fisher Scientific) before submitting the RNA for sequencing. For RT-qPCR, cDNA was synthesized from 1.45 µg of total RNA treated with Ambion DNase I using SuperScriptIII reverse transcriptase (Thermo Fisher Scientific) following the manufacturer's protocols. RT-qPCR was performed using FastStart Essential Green Master reagents (Roche) on a Roche LightCycler 96. Primer sequences for gene amplification are listed in Supplemental Table 3.3. RT-qPCR data were analyzed using the LightCycler 96 software and Microsoft Excel.

RNA-seq bioinformatic analysis: Pilot Study

RNA was submitted to the Purdue Genomics Core Facility for sequencing after treatment with DNase I to remove any contaminating genomic DNA. Ribosomal RNA was depleted and cDNA libraries (stranded) were prepared from each of the samples before sequencing. Between 15 to 23 million reads were obtained for each sample (100 nucleotides per read) which were quality trimmed and mapped to the *A. thaliana* genome using TopHat (Trapnell et al., 2010). Differentially expressed genes were determined from the mapped (bam) files using Cuffdiff from the Cufflinks suite of programs (Trapnell et al., 2010). Custom perl scripts were used to extract genes for which fold-changes of 3 or greater occurred between the induced and non-induced control samples at their respective time points. The resulting genes were annotated by hand and separated into categories based on their Gene Ontology (GO) functions. GO enrichment analysis was performed using the PANTHER Classification system and online tools (http://geneontology.org/docs/go-enrichment-analysis/).

RNA-seq bioinformatic analysis by Purdue Bioinformatics Core: Second Study

Sequence quality was assessed using FastQC (v 0.11.7) (https://www.bioinformatics.babraham.ac.uk/projects/fastqc/) for all samples and quality and adapter trimming was done using TrimGalore (0.4.4) (Krueger, 2017) to remove the sequencing adapter sequences and bases with Phred33 scores less than 30. The resulting reads of length $\geq$25 bases were retained (original read length = 50 and lib type = unstranded) respectively. The quality trimmed reads were mapped against the reference genome using STAR (Dobin et al., 2013) (v 2.5.4b). STAR derived mapping results and annotation (GTF/GFF) file for reference

genome were used as input for HTSeq (Anders, Pyl, & Huber, 2015) package (v 0.7.0) to obtain the read counts for each gene feature for each replicate. Counts from all replicates were merged using custom Perl scripts to generate a read count matrix for all samples.

The merged counts matrix was used for downstream differential gene expression analysis. Genes that did not have counts in all samples were removed from the count matrix and genes that had counts in some samples but not in others were changed from 0 to 1 in order to avoid having infinite values calculated for the fold change. Differential gene expression (DEG) analysis between treatment and control was carried out using 'R' (v 3.5.1; http://www.r-project.org/) with two different methods (DESeq2 and edgeR). Basic exploration of the read count data file such as accessing data range, library sizes, etc. was performed to ensure data quality. An edgeR object was created by combining the count's matrix, library sizes, and experimental design using the edgeR (Robinson, McCarthy, & Smyth, 2010) (v 3.24.3) package. Normalization factors were calculated for the count's matrix, followed by estimation of common dispersion of counts. An exact test for differences between the negative binomial distribution of counts for the two experimental conditions resulted in finding differential expression, which was then adjusted for multiple hypothesis testing. DESeq2 (Love, Huber, & Anders, 2014) (v 1.22.2) was also used to find differentially expressed genes. Both use an estimate variance-mean test based on a model using the negative binomial distribution. The significant genes were identified by looking at the adjusted p-value.

Additionally, STAR mapping (bam) files were used for analysis by the Cuffdiff from Cufflinks (v 2.2.1) (Trapnell et al., 2010) suite of programs which perform DE analysis based on FPKM values. Cuffdiff uses bam files to calculate Fragments per Kilobase of exon per Million fragments mapped (FPKM) values, from which differential gene expression between the pairwise comparisons can be ascertained. Differentially expressed gene lists detected by at least two or more methods (DESeq2, edgeR, and Cufflinks) were generated using custom Perl scripts.

Gene annotations were retrieved from BioMart databases using biomartr package in 'R'. The "transcript_biotype", "description" attributes were extracted using mart = "plants_mart" and dataset = "athaliana_eg_gene". GO enrichment analysis was also performed using DEGs from two or more methods while using two replicates. Singular Enrichment Analysis (SEA) from agriGO (Du, Zhou, Ling, Zhang, & Su, 2010) was used to perform GO enrichment analysis (count = 5 with Fisher exact t-test with multiple testing). A GO enrichment analysis was

performed using the PANTHER Classification system and online tools (http://geneontology.org/docs/go-enrichment-analysis/).

Genotyping and Agrobacterium-mediated transient and stable transformation assays of T-DNA insertion lines

A. thaliana T-DNA insertion lines tested in this study are listed in Table 3.1. For genotyping, DNA was isolated from leaves sampled from 10-15 individual plants after freezing the tissue in liquid nitrogen and grinding it into a fine powder using a sterile tube pestle. A total of 0.5 mL of extraction buffer was then added to the ground tissue (contains 100 mM Tris pH 8.0, 50 mM EDTA, 500 mM NaCl) before mixing thoroughly. A total of 26 µL of 20% SDS solution was then added to each sample before mixing them by inverting the tubes. The samples were then incubated in a 65^{o}C water bath for 20 min and the samples were mixed by inverting every 5 min during the incubation. After removing the samples from the water bath, 125 µL of potassium acetate buffer was added to each sample before mixing. The potassium acetate buffer is made by mixing 60 mL of 5 M KOAc from crystals, 11.5 mL glacial acetic acid, and 28.5 mL of filtered H_2O to make 100 mL (3 M of potassium and 5 M of acetate in the final solution). The tubes were placed on ice for up to 20 min before centrifuging them at top speed for 10 min in a microcentrifuge at 4^{o}C. The supernatant solution was transferred to a fresh tube (~600 µL). The samples were centrifuged a second time if cellular debris were still evident within the supernatant solution. A 0.7 volume (420 µL) of isopropanol was added to the supernatant fluid before mixing the samples and placing them at -20^{o}C for at least 1 h to precipitate the DNA. After incubating at -20^{o}C, the samples were centrifuged at top speed for 10 min in a microcentrifuge at 4^{o}C to pellet the DNA. The DNA pellets were then washed with 500 µL of 70% ethanol by flicking the tube until the pellets released from the bottom of the tube. The samples were centrifuged again for 5 min before carefully removing the ethanol. The pellets were then allowed to air-dry for 5 to 10 min to allow the residual ethanol to evaporate before resuspending the pellets in 30 µL of 1 xTE buffer (10 mM Tris-Cl, 1 mM EDTA [pH 8.0]) plus 20 µg mL^{-1} RNase A.

Lines homozygous for the annotated T-DNA insertions were confirmed by PCR (primer sequences are listed in Supplemental Table 3.3). PCR reaction mixes were made using ExTaq

Buffer (TaKaRa), dNTPs (0.2 mM), the appropriate forward and reverse primers (0.2 µM each), homemade Taq polymerase, and water with a tenth volume of sample being added to act as a template. The reactions were incubated at 95^{o}C for 3 min before performing 35 cycles of a 30 sec, 95^{o}C denaturation step, followed by a 30 sec annealing step (temperature was ~5^{o}C lower than the average melting temperature for each primer set), and a 1 min, 72^{o}C extension step (1 min). A final 10 min extension step at 72^{o}C followed the last cycle before PCR products were visualized using gel electrophoresis.

A. thaliana plants homozygous for their annotated T-DNA insertion were grown for 20 days in baby food jars containing sterile Gamborg's B5 medium before cutting their roots into 3-5 mm segments. The segments were assayed as described in Tenea et al. (2009). *A. tumefaciens* At849 (GV3101::pMP90 [Koncz and Schell, 1986] containing pBISN1 [Narasimhulu et al., 1996]) was used to measure transient transformation, whereas *A. tumefaciens* A208 (Sciaky et al., 1978) was used for stable transformation (Supplemental Table 3.2). Three replicates were assayed for each experiment with root segments from 10 plants pooled for each replicate. A minimum of 80 root segments were scored for each data point and statistical analysis was performed using ANOVA.

Protein Isolation and Proteomics Analysis

Roots were homogenized in 8 M urea using a Percellys®24 homogenizer (Bertin) and incubated at room temperature for 1 h with continuous vortexing before centrifugation at 14,000 rpm for 15 min at 4^{o}C. The supernatant solution was transferred to a new tube and the protein concentration was determined using a Pierce™ BCA assay (Thermo Fisher Scientific). A total of 100 µg protein from each sample (equivalent volume) was taken for digestion. Proteins were first precipitated using 4 volumes of cold acetone (-20^{o}C) overnight before centrifugation at 14,000 rpm for 15 min at 4^{o}C to collect the precipitated proteins. Protein pellets were washed twice with 80% cold (-20^{o}C) acetone, dried in the speed vacuum for 5 min, and then solubilized in 8 M urea. Samples were reduced using 10 mM dithiotreitol and cysteine alkylated using 20 mM iodoacetamide. This was followed by digestion using sequence grade Lyc-C/Trypsin (Promega) mix at a 1:25 (enzyme : substrate) ratio to enzymatically digest the proteins. All digestions were

carried out at 37^{o}C overnight. The samples were then cleaned over C18 MicroSpin columns (Nest Group), dried and resuspended in 97% purified H_2O/3% acetonitrile (ACN)/0.1% formic acid (FA). After BCA at the peptide level, 1 µg of each sample was loaded onto the column.

Digested samples were analyzed using a Dionex UltiMate 3000 RSLC Nano System coupled with a Q Exactive™ HF Hybrid Quadrupole-Orbitrap Mass Spectrometer (Thermo Scientific, Waltham, MA). Peptides were first loaded onto a 300 µm x 5 mm C18 PepMap™ 100 trap column and washed with 98% purified water/2% acetonitrile (ACN)/0.01% formic acid (FA) using a flow rate of 5 µL min^{-1}. After 5 min, the trap column was switched in-line with a 75 µm x 50 cm reverse phase Acclaim™ PepMap™ RSLC C18 analytical column heated to 50^{o}C. Peptides were separated over the analytical column using a 120 min method at a flow rate of 300 nL min^{-1}. Mobile phase A contained 0.01% FA in purified water while mobile phase B consisted of 0.01 % FA/80% ACN in purified water. The linear gradient began at 2% B and reached 10% B in 5 min, 30% B in 80 min, 45% B in 91 min, and 100% B in 93 min. The column was held at 100% B for the next 5 min before returning to 5% B where it was equilibrated for 20 min. Samples were injected into the QE HF through the Nanospray Flex™ Ion Source fitted with an emitter tip from New Objective. MS spectra were collected from 400 to 1600 m/z at 120,000 resolution, a maximum injection time of 100 ms, and a dynamic exclusion of 15 s. The top 20 precursors were fragmented using higher-energy C-trap dissociation (HCD) at a normalized collision energy of 27%. MS/MS spectra were acquired in the Orbitrap at a resolution of 15,000 with a maximum injection time of 20 ms.

The raw data were analyzed using MaxQuant software (v. 1.5.3.28) against a TAIR 10 protein database combined with VirE2 proteins (Cox et al., 2008; 2011; 2014). The search was performed with the precursor mass tolerance set to 10 ppm and MS/MS fragment ions tolerance was set to 20 ppm. The enzyme was set to trypsin and LysC, allowing up to two missed cleavages. Oxidation of methionine was defined as a variable modification, and carbamidomethylation of cysteine was defined as a fixed modification. The "unique plus razor peptides" (razor peptides are the non-unique peptides assigned to the protein group with the most other peptides) were used for peptide quantitation. The false discovery rate (FDR) of peptides and proteins identification was set at 0.01. iBAQ scores and MS/MS counts for each identified protein were compared between the non-induced and induced samples. Proteins which showed a 0.2-fold (20%) increase or decrease in abundance in the induced versus non-induced samples for

at least two biological replicates by comparing both iBAQ scores and MS/MS counts were considered to have levels which changed in response to VirE2 induction.

Results

Cytoplasmic but not nuclear localized VirE2 can support transformation

The location of VirE2 within the plant cell remains controversial. N-terminally tagged VirE2 was initially shown to localize to nuclei (Citovsky et al., 1992, 1994, 2004; Tzfira and Citovsky, 2001; Tzfira et al., 2004; Li et al., 2005). However, subsequent studies showed that C-terminally tagged VirE2 localized to the cytoplasm, commonly forming perinuclear aggregates (Bhattacharjee et al., 2008; Grange et al., 2008; Lee et al., 2008; Shi et al., 2014; Lapham et al., 2018).

Plant-expressed VirE2 can complement a *virE2* mutant *Agrobacterium* strain, restoring efficient transformation (Citovsky et al., 1992; Simone et al., 2001). However, Bhattacharjee et al. (2008) demonstrated that only C-terminally tagged VirE2, but not the N-terminally tagged protein, could complement a *virE2* mutant strain back to full virulence. To determine if cytoplasmic localization is required for VirE2 to facilitate transformation, plasmids were constructed to create the recombinant proteins VirE2-Venus or VirE2-Venus-NLS (containing a nuclear localization signal [NLS]). Tobacco BY-2 protoplasts were individually co-transfected with DNA from each of these constructs and a plasmid containing an RFP nuclear marker. The protoplasts were imaged 16 hr later using confocal microscopy (Figure 3.1). Consistent with observations in previous studies (Bhattacharjee et al., 2008; Grange et al., 2008; Lee et al., 2008; Li et al., 2014; Shi et al., 2014; Li and Pan, 2017; Lapham et al., 2018; Roushan et al., 2018), VirE2-Venus localized to the cytoplasm (Figure 3.1A-D); however, VirE2-Venus-NLS localized to the nucleus (Figure 3.1E-H).

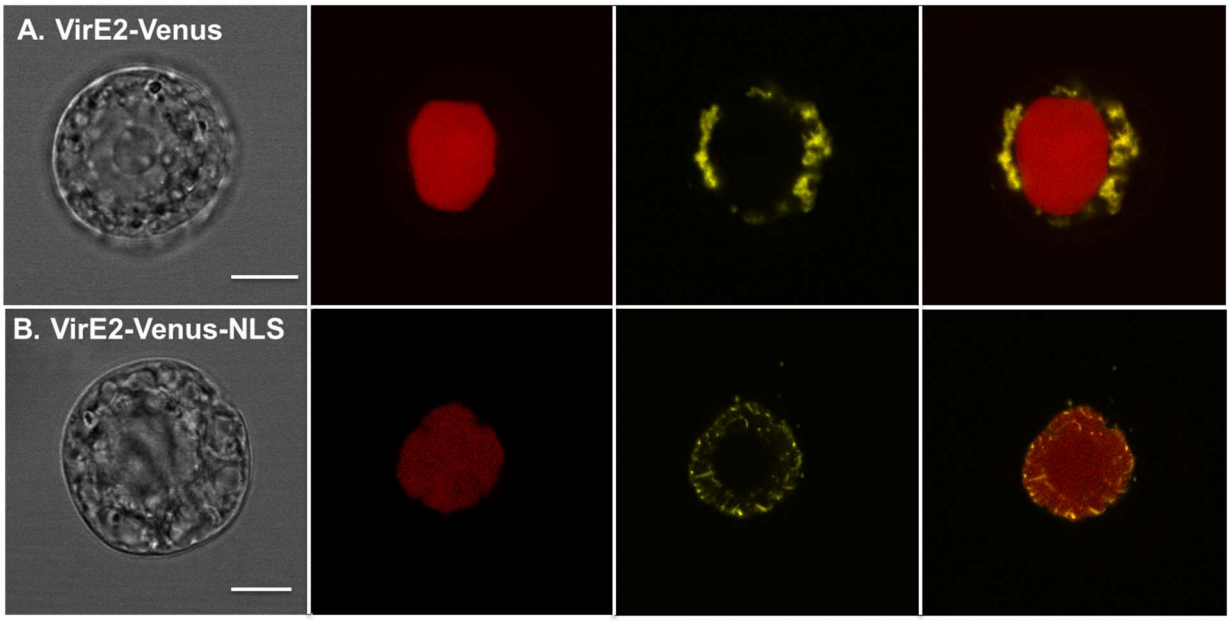

Figure 3.1. Subcellular localization of VirE2-Venus (A) and VirE2-Venus-NLS (B) in tobacco BY-2 protoplasts. A total of 10 µg of DNA encoding VirE2-Venus or VirE2-Venus-NLS was co-transfected with 10 µg of DNA encoding a nuclear marker mRFP-NLS into tobacco BY-2 protoplasts. Cells were imaged by confocal microscopy 16 hr after transfection and representative images are shown. Four images of each cell are presented (left to right: DIC; mRFP; YFP; merged YFP + mRFP). Bars indicate 10 µm.

Transgenic *A. thaliana* plant lines were generated expressing VirE2-Venus or VirE2-Venus-NLS under the control of a β-estradiol inducible promoter (Zuo et al., 2000). The plants also expressed a Cerulean-NLS nuclear marker under the control of a constitutive Cauliflower Mosaic Virus (CaMV) double 35S promoter. After incubating the roots in either control (non-induced) or β-estradiol (induced) solution, the tissue was imaged using confocal microscopy (Figure 3.2). Only induced roots showed a yellow fluorescence signal (Figure 3.2A-D; I-L), whereas the Cerulean marked nuclei were evident in both non-induced and induced roots. VirE2-Venus localized outside of the nucleus and throughout the cytoplasm (Figure 3.2A-D), whereas VirE2-Venus-NLS co-localized with the Cerulean nuclear marker (Figure 3.2I-L) in transgenic *Arabidopsis* roots. Western blots using anti-GFP antibodies showed that the VirE2-Venus-NLS protein was expressed at equal or greater amounts than was VirE2-Venus protein after induction for the respective lines (Fang-Yu Hsu, unpublished data).

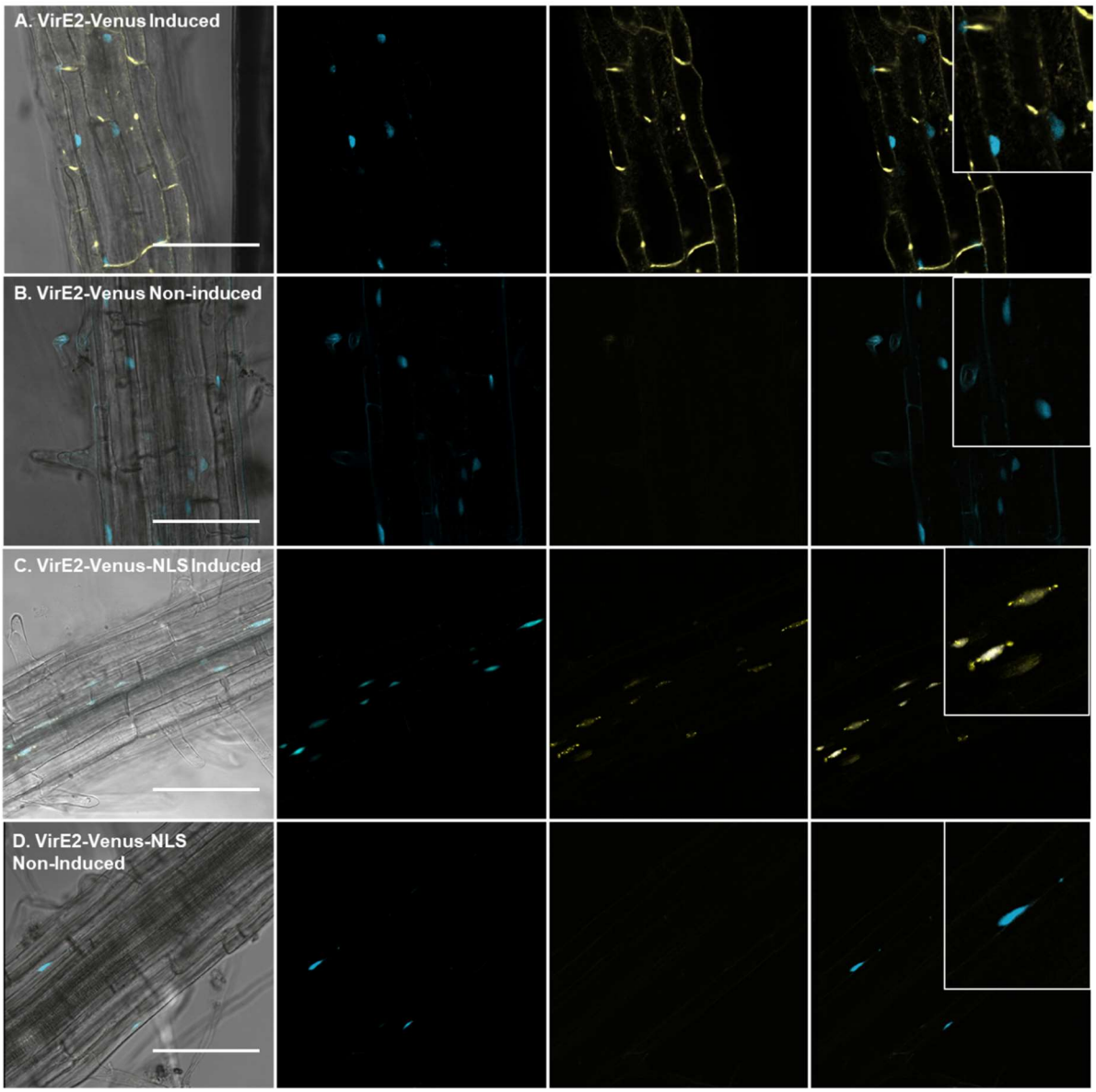

Figure 3.2. Subcellular localization of VirE2-Venus (A-B) and VirE2-Venus-NLS (C-D) in A. thaliana roots. Transgenic *A. thaliana* plants expressing inducible VirE2-Venus, VirE2-Venus-NLS, VirE2-Venus-sNLS were treated with β-estradiol (induced; A, C) or control solution (B, D). Cerulean-NLS under the control of a CaMV 2x35S promoter was used to mark the nuclei. Root cells were imaged by confocal microscopy 9 h after treatment and representative images are shown. Four images of each cell are presented (left to right: Merged YFP + Cerulean + Bright-field (DIC); Cerulean; Venus; merged Venus + Cerulean). Bars indicate 100 µm.

Transformation assays were performed on wild-type (Col-0) non-transgenic, inducible VirE2-Venus, and inducible VirE2-Venus-NLS transgenic plants. Plant roots were treated with either control or induction solution for 24 hours before cutting the roots into small segments and infecting them with a *virE2* mutant *Agrobacterium* strain (Figure 3.3A) containing the T-DNA binary vector pBISN1 as well as a *virE2*+ control strain (Figure 3.3B). The T-DNA of pBISN1 contains a plant-active *gusA*-intron gene (Narasimhulu et al., 1996). A low level of transformation was observed in all the samples infected with the *virE2* mutant *Agrobacterium* strain. Such low-level *virE2*-independent transformation has been observed previously (Stachel and Nester, 1986; Rossi et al., 1996; Dombek and Ream, 1997). However, only induction of transgenic plants encoding cytoplasmic-localized VirE2-Venus, but not nuclear-localized VirE2-Venus-NLS, increased transient transformation efficiency above that of non-induced levels. The nuclear-localized VirE2-Venus-NLS inability to complement the *virE2* mutant strain to full virulence is likely not due to some toxic effect of the protein because both inducible VirE2-Venus and inducible VirE2-Venus-NLS plants showed comparable transformation rates when infected with a *virE2*+ strain (Figure 3.3B). Thus, in order for VirE2 to promote transformation, it must be localized in the cytoplasm.

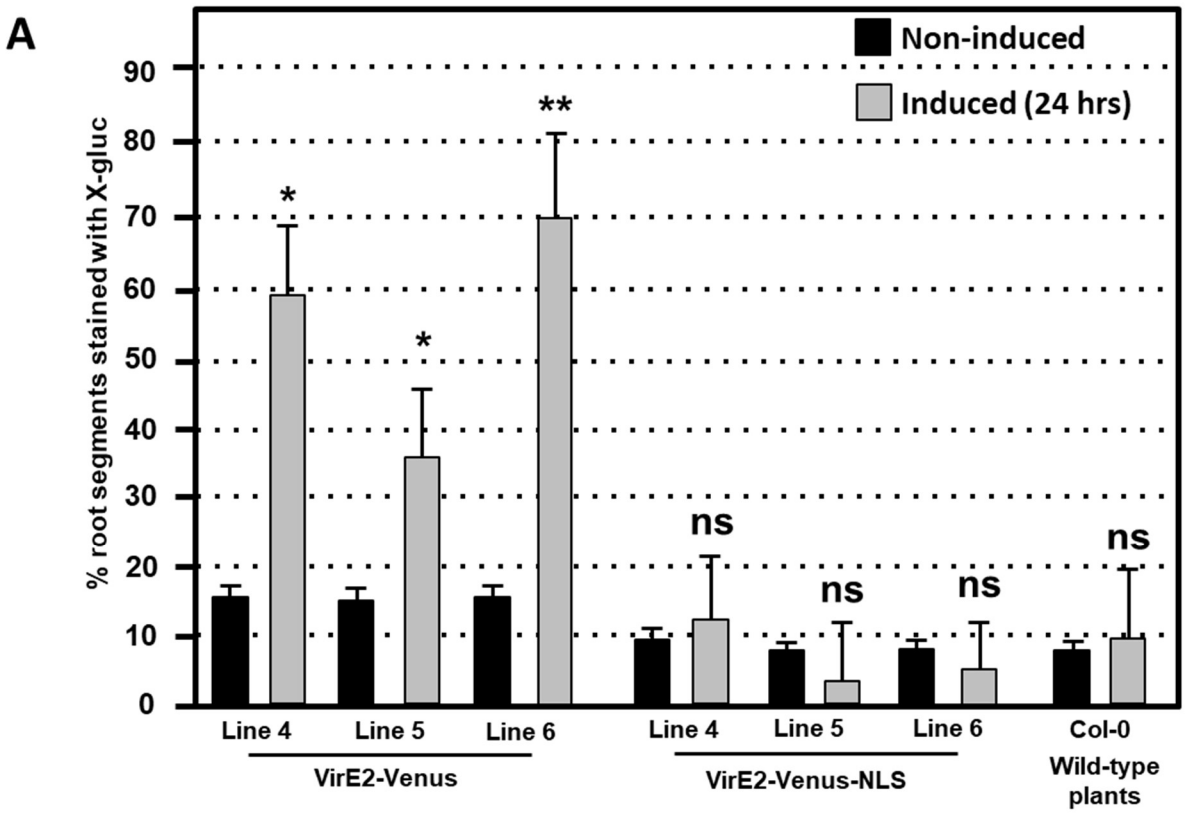

Figure 3.3. Transformation susceptibility of *Arabidopsis* wild-type (Col-0) and β-estradiol inducible transgenic VirE2-Venus and VirE2-Venus-NLS plants

Agrobacterium-mediated transient transformation assays were conducted on Col-0 (right side), three transgenic lines of inducible VirE2-Venus (left side), and three lines of inducible VirE2-Venus-NLS (middle). Root segments were inoculated with 10^8 cfu/ml of the *virE2* mutant strain *A. tumefaciens* At1879 containing the T-DNA binary vector pBISN2 (A) and with 10^6 cfu/mL (B) and 10^5 cfu/mL (C) of the EHA105::pBISN1 (*virE2*+) At1529 strain. The root segments were stained with X-gluc 6 days after infection. Bars represent an average of three biological replicates (each replicate containing > 60 root segments) $\pm$ SE. ANOVA test *Pvalue < 0.05, **Pvalue < 0.01, ns: not significant.

Figure 3.3 continued

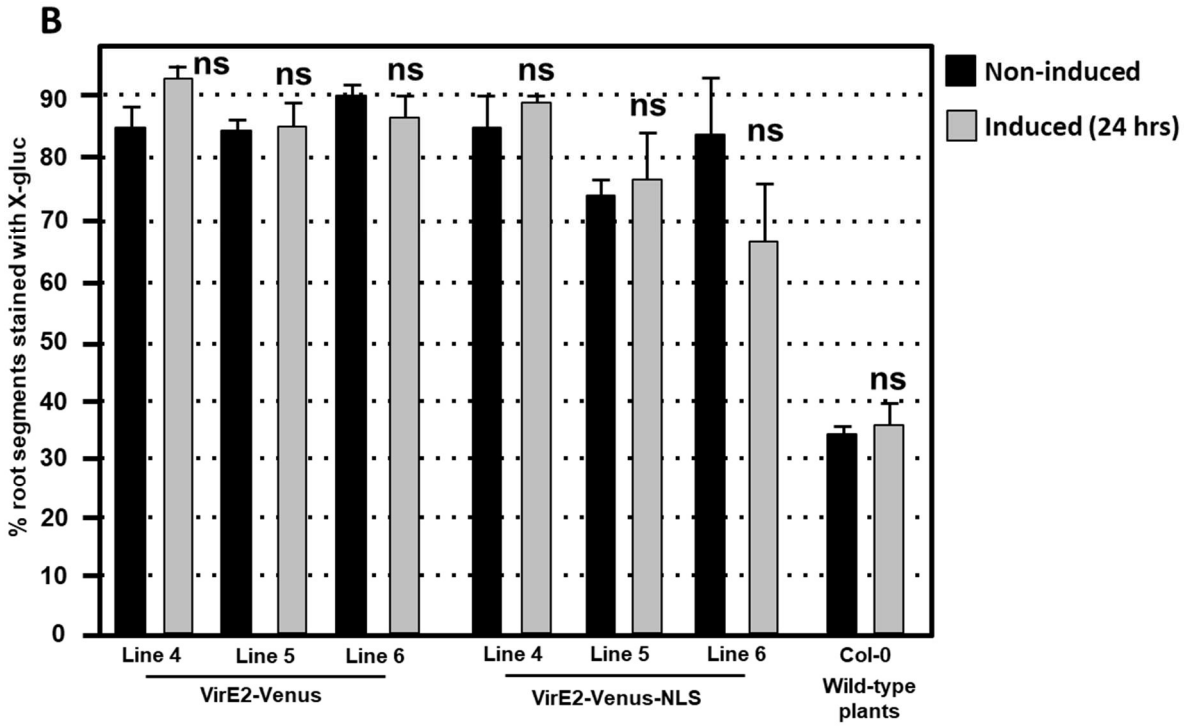

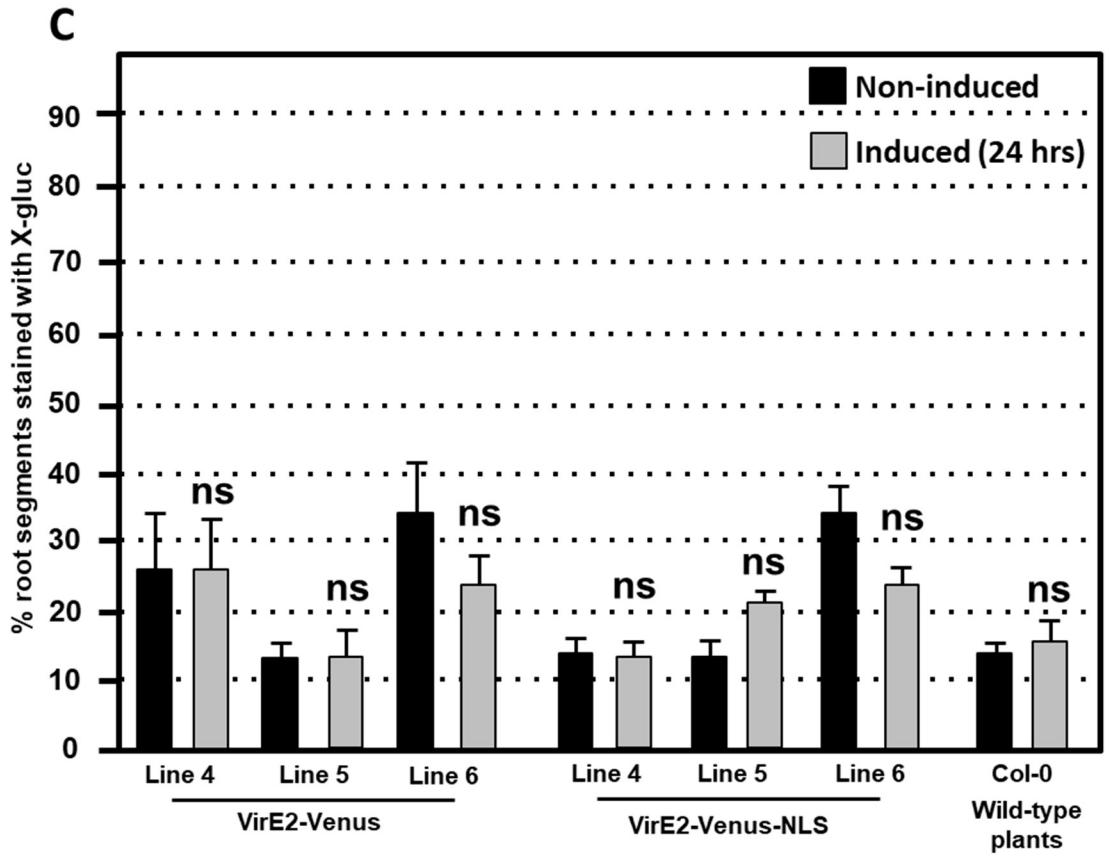

Cytoplasmic-localized VirE2 alters expression of numerous Arabidopsis genes, including those involved in defense response and transformation susceptibility

We generated multiple transgenic *A. thaliana* lines expressing *VirE2* under the control of a β-estradiol inducible promoter (Zuo et al., 2000) and tested them for *VirE2* induction by RT-PCR. VirE2 transcripts were detectable within 1 hour of induction (Supplemental Figure 3.1A). Root tissue pooled from ~30 plants was harvested after treating either with inducer or control (non-induced) solution for 3 or 12 hr. Both the control and induction solutions contained the avirulent strain *A. tumefaciens* A136 that lacks a Ti-plasmid (Sciaky et al., 1978) at a concentration of 10^8 cfu/mL. The inclusion of this bacterial strain was done to mimic more closely natural infection conditions because a plant cell will only be exposed to VirE2 in the presence of *Agrobacterium*. RNA was extracted from each sample and induction of *VirE2* was confirmed using quantitative RT-PCR (RT-qPCR; Supplemental Figure 3.1B) before submitting the RNA sample for RNA-seq analysis. This analysis was initially performed on one biological replicate as a pilot study to identify potential target genes to test for transformation phenotypes. Differentially expressed genes were determined using Cufflinks (Trapnell et al., 2012) for this initial study; however, two additional biological replicates were analyzed at a later date. For the pilot study, considering all time points a total of 443 *A. thaliana* genes (~1.5% of the genome) were differentially expressed in VirE2-induced versus non-induced samples (Supplemental Data Sheet 3.1). Differentially expressed genes were displayed according to their annotated Gene Ontology (GO) biological process (Figure 3.4; Ashburner et al., 2000). These differentially expressed genes are involved in processes such as defense response, growth and differentiation, ion and nitrate transport, oxidative stress response, protein translation, protein turnover and modification, transcription, RNA silencing, RNA modification and processing, and DNA/chromatin modification (Figure 3.4). Most expression changes occurred 12 hr after induction and not at 3 hours A GO enrichment analysis showed that genes involved in ribosome biogenesis, detoxification, cytoplasmic translation, triterpenoid metabolic process, cellular response to hypoxia, and cellular response to sulfur starvation were enriched among genes up-regulated in the presence of VirE2 whereas genes involved in protein modification processes were under-represented (Figure 3.5A).

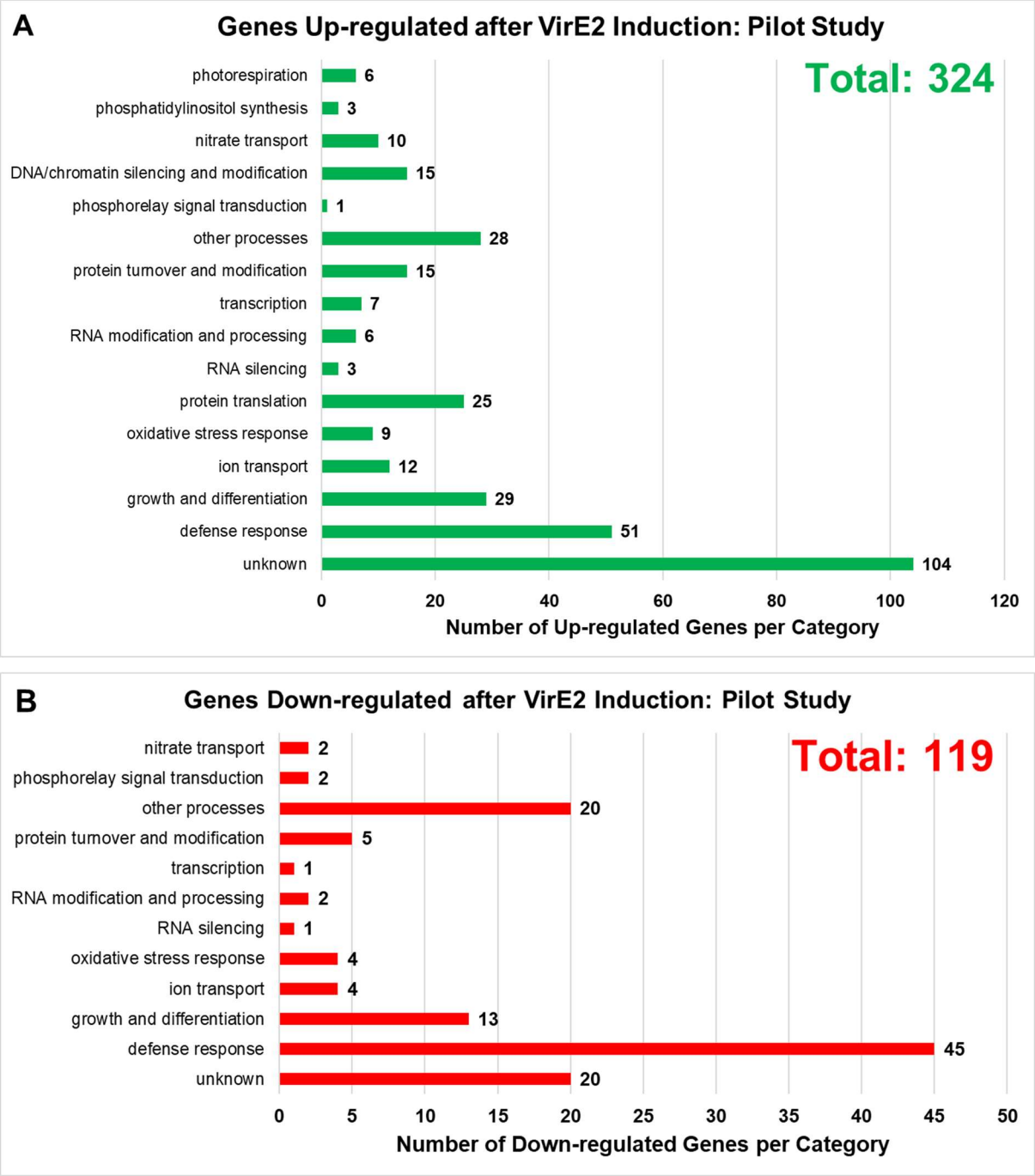

Figure 3.4. Gene Ontology (GO) Biological Process Categories of up- (A) and down-regulated (B) genes in the presence of VirE2: Pilot Study. Displayed are genes with 3-fold or more changes in expression at all time points.

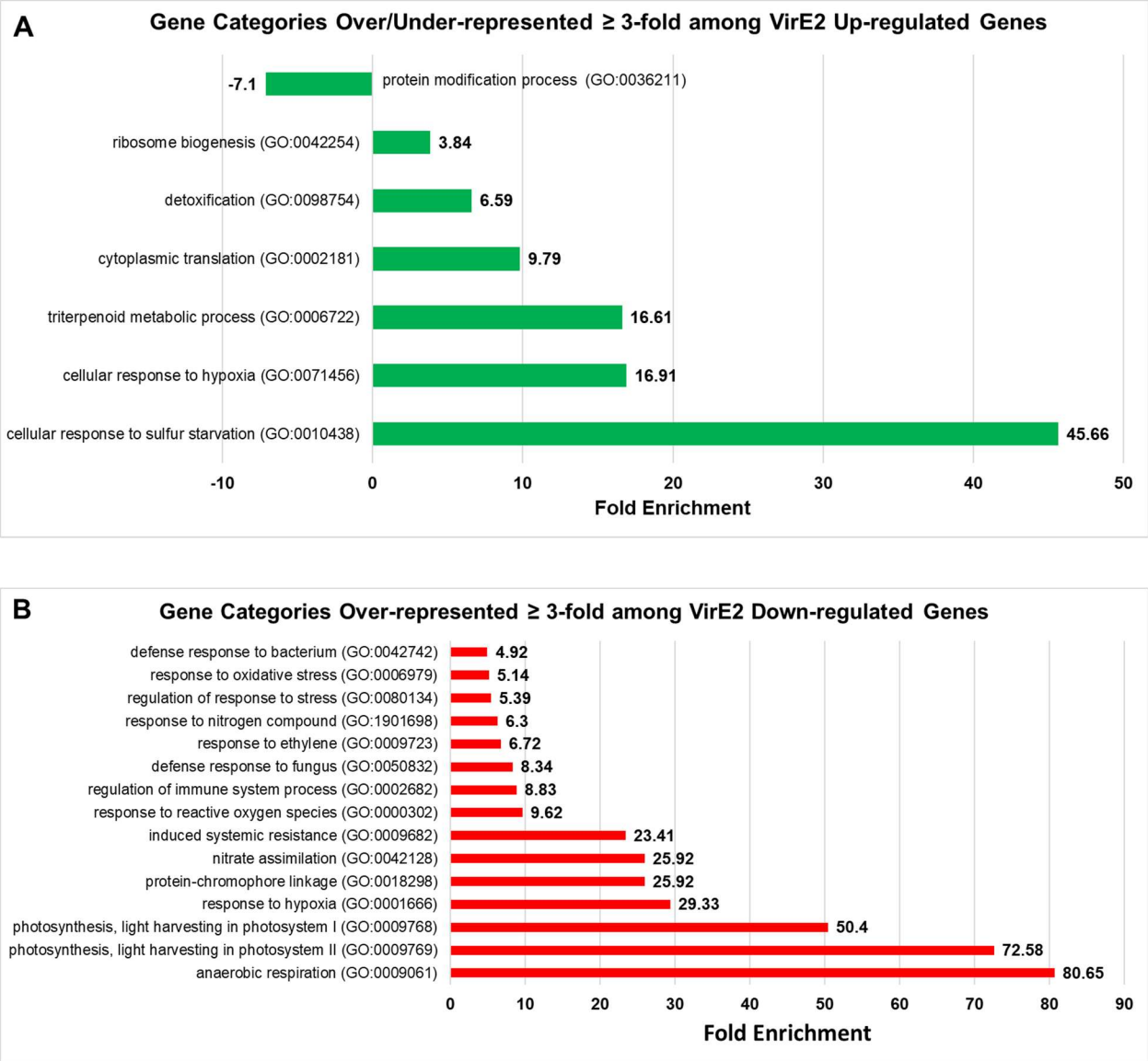

Figure 3.5. Gene Ontology (GO) Enrichment Analysis of VirE2 differentially expressed genes: Pilot Study. GO biological processes of over-/under-represented gene categories for up-regulated (A) and down-regulated (B) genes at all time points. Displayed only are results with a false discovery rate (FDR) < 0.05.

A subset of genes differentially expressed following VirE2 induction (VirE2 differentially expressed genes; DEGs) are involved in defense responses (Figure 3.6). Genes involved in MAPK cascade signaling and salicylic acid-mediated bacterial defense responses (Seyfferth and Tsuda, 2014; Bi and Zhou, 2017) were down-regulated in VirE2-induced plants (Figure 6B), and many genes associated with various defense responses were enriched among genes down-regulated in the presence of VirE2 (Figure 3.5B). These results suggest that VirE2

could function to suppress plant defense responses, and consequently help facilitate transformation. Genes previously shown to be important for transformation, such as protein phosphatase 2C and arabinogalactan proteins (Nam et al., 1999; Gaspar et al., 2004; Tao et al., 2004), also showed changes in expression (Supplemental Data Sheet 3.1). These VirE2-induced changes could also facilitate transformation.

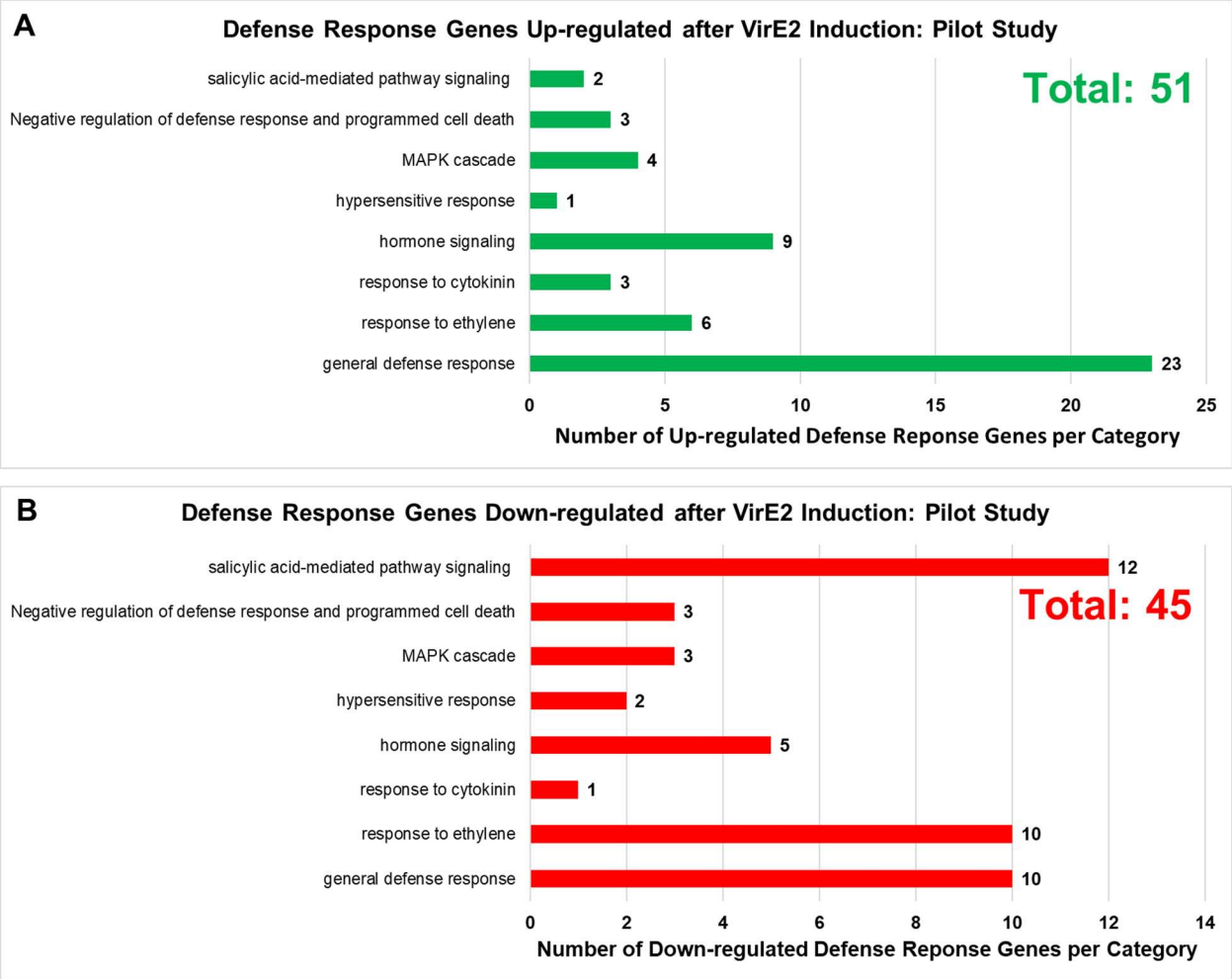

Figure 3.6. Gene Ontology (GO) Biological Process Categories of up- (A) and down-regulated (B) defense response genes in the presence of VirE2: Pilot Study. Displayed are genes with 3-fold or more changes in expression at all time points.

A subset of genes which showed significant changes in expression were tested using RT-qPCR to confirm the RNA-seq results (Supplemental Table 3.1 and Supplemental Figure 3.2). All genes tested by RT-qPCR showed changes in expression consistent with the RNA-seq data.

At a later date, we submitted RNA for sequencing from two additional biological replicates of the same inducible *VirE2* line. In total, 145 up-regulated genes and 25 down-regulated genes in induced versus non-induced samples were identified by at least two computational methods with an adjusted P-value cut-off of 0.1 across all analyses (Supplemental Data Sheet 3.2). Of the 160 differentially expressed genes, 61 were identified in the pilot study. The newly identified DEGs are involved in the same categories of biological processes identified in the pilot study (Figure 3.7). Most expression changes again occurred 12 hours after induction, and the identified up-regulated (Figure 3.7A) and down-regulated (Figure 3.7B) genes are displayed according to their annotated GO biological processes (Ashburner et al., 2000). A GO enrichment analysis was performed (http://geneontology.org/docs/go-enrichment-analysis/; Mi et al., 2013) to determine which categories of genes were over-represented 3-fold or more in the RNA-seq dataset. Genes involved in response to hypoxia, heat, and protein unfolding were enriched in genes up-regulated in the presence of VirE2 (Figure 3.8A). Many genes involved in defense responses and innate immunity were also enriched; these results are consistent with those observed for our pilot study (Figure 3.8A; Figure 3.6). Interestingly, genes whose molecular function involves binding misfolded proteins, and heat shock proteins were strongly enriched among VirE2 up-regulated genes (Figure 3.8B). Specifically, *HEAT SHOCK PROTEIN 90.1 (HSP90)* was up-regulated ~6-fold in VirE2 induced versus non-induced plants (Supplemental Data Sheet 3.2). Park et al. (2014) demonstrated that plants over-expressing *HSP90* showed increased susceptibility to *Agrobacterium*-mediated transformation. VirE2-induced up-regulation of *HSP90* and other heat shock proteins could therefore facilitate transformation.

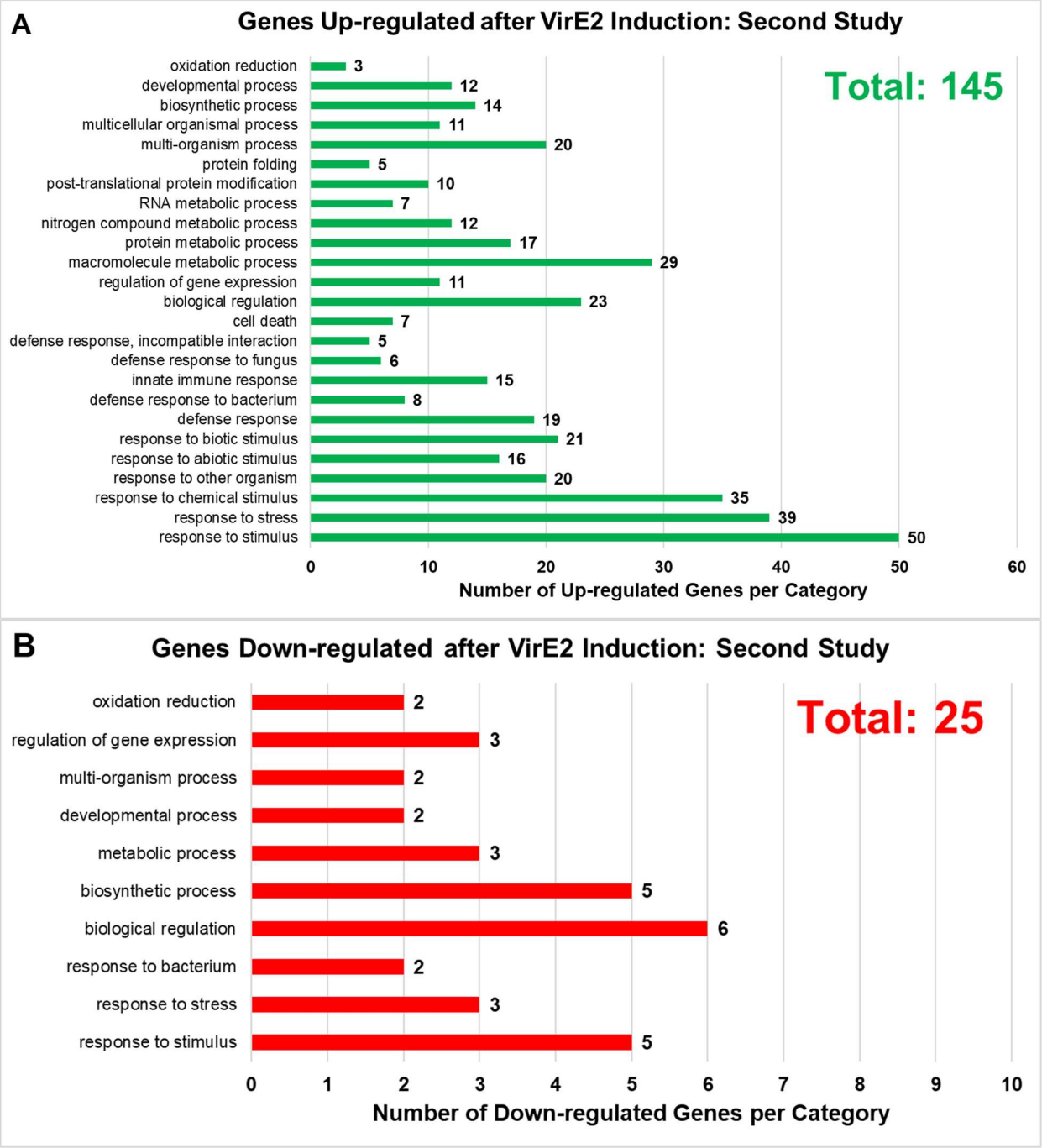

Figure 3.7. Gene Ontology (GO) Biological Process Categories of up- (A) and down-regulated (B) genes in the presence of VirE2: Second study. Displayed only are results with an adjusted P-value of < 0.1 calculated across two or three computational analyses at all time points.

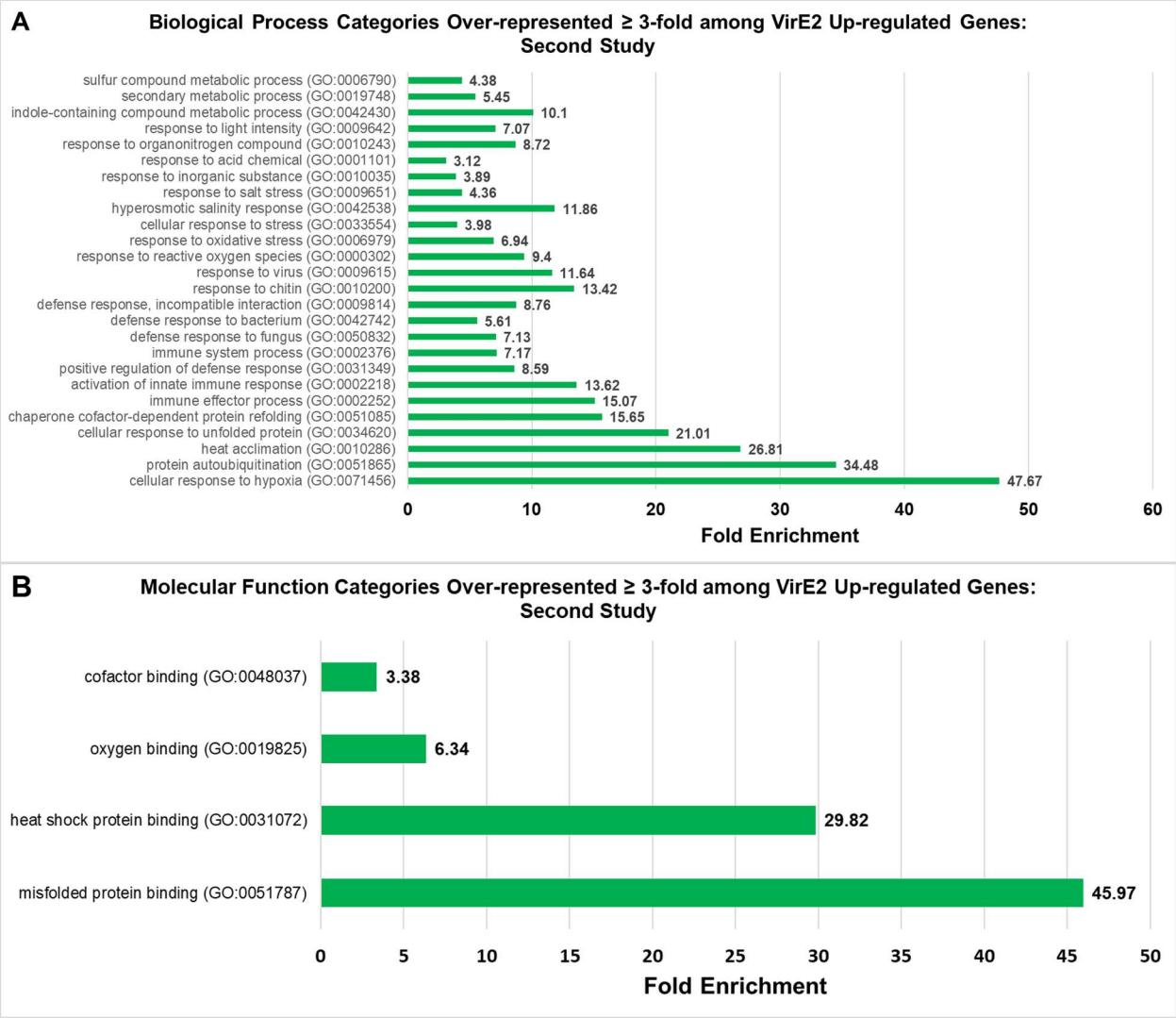

Figure 3.8. Gene Ontology (GO) Enrichment Analysis of VirE2 up-regulated genes: Second Study. GO biological processes (A) and molecular functions (B) of over-/under-represented gene categories for VirE2 up-regulated genes at all time points. Displayed only are results with a false discovery rate (FDR) < 0.05.

Arabidopsis lines harboring mutations in some of the VirE2-induced differentially expressed genes exhibit altered transformation phenotypes

T-DNA insertion mutant lines of a subset of the VirE2 differentially expressed genes identified by the pilot study were obtained from the Arabidopsis Biological Resource Center (ABRC, www.arabidopsis.org), genotyped for homozygosity, and tested for transformation susceptibility (Table 3.1). Transformation results for mutants of VirE2 up-regulated genes are shown in Figure 3.9, whereas transformation results of mutants of down-regulated genes are

shown in Figure 3.10. If a mutant showed no statistically significant difference in transformation efficiency at any of the tested bacterial concentrations, the results are reported as “No change”. However, some of these mutations may still have a minor impact on transformation.

The *atpsk3, tst18*, and *miR163* mutant lines (Table 3.1; Figure 3.9B, C, G) showed decreased transformation compared to that of wild-type plants. All three of these genes are up-regulated in the presence of VirE2 and may therefore facilitate transformation. The *pr5* mutant showed an increase in transient transformation (Table 3.1; Figure 3.10D). *PR5* is important for activating defense responses in *Prunus domestica* (El-kereamy et al., 2011), and over-expression of PR5 protein enhances disease resistance in several crop species (Liu et al., 1994; Chen et al., 1999; Datta et al., 1999; Mackintosh et al., 2007). *PR5* is up-regulated in the presence of VirE2, and because of its role in defense response and effector-triggered immunity (ETI; Wu et al., 2014) one would predict that the *pr5* mutant would be more susceptible to *Agrobacterium*-mediated infection. This prediction is consistent with our results (Figure 3.10D).

Several of the mutants for genes down-regulated in the presence of VirE2 showed increased transient or stable transformation efficiency compared to that of wild-type plants (Figure 3.10B-F). These genes may act to inhibit transformation, and their VirE2-dependent down-regulation may facilitate transformation, as reflected by the increased susceptibility of their respective knockout mutant lines to *Agrobacterium*-mediated transformation. A *PROTEIN PHOSPHATASE 2C* (Figure 3.10F) was previously identified as a transformation inhibitor (Tao et al., 2004). Conversely, the *exl1*, *oep6*, and *rld17* mutants showed decreased transformation (Table 3.1; Figure 3.10A, D, E) even though they are down-regulated in the presence of VirE2. These genes may be important for transformation, but their mechanism of action and regulation during transformation remain unknown.

Table 3.1 T-DNA insertion mutant lines of VirE2 differentially expressed genes tested for transformation phenotypes

Gene Name	Gene_ID	Encoded Protein	Up/Down-regulated (Fold-change)	ABRC Stock_ID	Transformation Result
lncRNA	At3g12965	Long non-coding RNA	Up (5.8)	SALK_086573	No change
atpsk3	At3g44735	phytosulfokine 3 precursor	Up (5)	SALK_044781	*Decreased transient
acs6	At4g11280	1-aminocyclopropane-1-carboxylate synthase 6	Up (3)	SALK_054467	No change
tst18	At5g66170	thiosulfate sulfurtransferase 18	Up (3.7)	CS867285	*Decreased transient and stable
pr5	At1g75040	pathogenesis-related protein 5	Up (14)	SALK_055063C	*Increased transient
agp14	At5g56540	arabinogalactan protein 14	Up (4.9)	SALK_096806	No change
tasi4	At3g25795	Trans-acting siRNA 4	Up (15.1)	SALK_066997	No change
miR163	At1g66725	microRNA 163	Up (3.3)	CS879797	**Decreased stable
samp	At2g41380	S-adenosyl-L-methionine-dependent methyltransferases superfamily protein	Up (10.1)	SALK_209995C	No change
tasi3	At3g17185	Trans-acting siRNA 3	Up (3)	GABI-Kat Stock N432182 (N2051875)	No change
exl1	At1g23720	Proline-rich extensin-like family protein 1	Down (3.3)	SALK_010243C	**Decreased stable
mee39	At3g46330	maternal effect embryo arrest 39 (putative LRR receptor-like serine/threonine-protein kinase)	Down (4.7)	SALK_065070C	No change
rbc3b	At5g38410	ribulose bisphosphate carboxylase small chain 3B	Down (7.4)	SALK_117835	No change
abah3	At5g45340	abscisic acid 8'-hydroxylase 3	Down (3.4)	SALK_078170	*Increased transient
ntr2.6	At3g45060	high affinity nitrate transporter 2.6	Down (28)	SALK_204101C	*Increased transient
cup	At3g60270	cupredoxin superfamily protein	Down (31.3)	SALK_201444C	**Increased transient
ntr2:1	At1g08090	Nitrate transporter 2:1	Down (35.7)	SALK_035429C	*Increased transient
oep6	At3g63160	outer envelope protein 6 (chloroplast)	Down (5.6)	CS862774	*Decreased stable
esm1	At3g14210	epithiospecifier modifier 1	Down (10)	SALK_150833C	**Increased stable
rld17	At2g17850	rhodanese-like domain-containing protein 17	Down (4.7)	SALK_115776C	***Decreased transient and stable
pp2c25	At2g30020	putative protein phosphatase 2C 25	Down (3.5)	SALK_104445	**Increased transient
adh1	At1g77120	alcohol dehydrogenase 1	Down (23.2)	SALK_052699	***Increased transient

ANOVA test *Pvalue < 0.05, **Pvalue < 0.01, ***Pvalue < 0.001.

Figure 3.9. Transformation susceptibility of *Arabidopsis* wild-type (Col-0) and T-DNA insertion mutant plants of VirE2 up-regulated genes

Agrobacterium-mediated transient (left) or stable (right) transformation assays were conducted on Col-0, *lncRNA* (A), *atpsk3*, *acs6* (B), *tst18* (C), *pr5* (D), *agp14* (E), *tasi4* (F), *miR163*, *samp* (G), and *tasi3* (H) mutant plants. Root segments were inoculated with 10^7, 10^6, or 10^5 cfu/ml of *A. tumefaciens* At849 (transient) or A208 (stable). For the transient assay, the root segments were stained with X-gluc 6 days after infection. For stable transformation, tumors were scored 30 days after infection. Numbers represent an average of three biological replicates (each replicate containing >60 root segments) + SE. ANOVA test *Pvalue < 0.05, **Pvalue < 0.01, ns: not significant. The data are shown only if the transformation efficiency was ≥ 5%.

Figure 3.9 continued

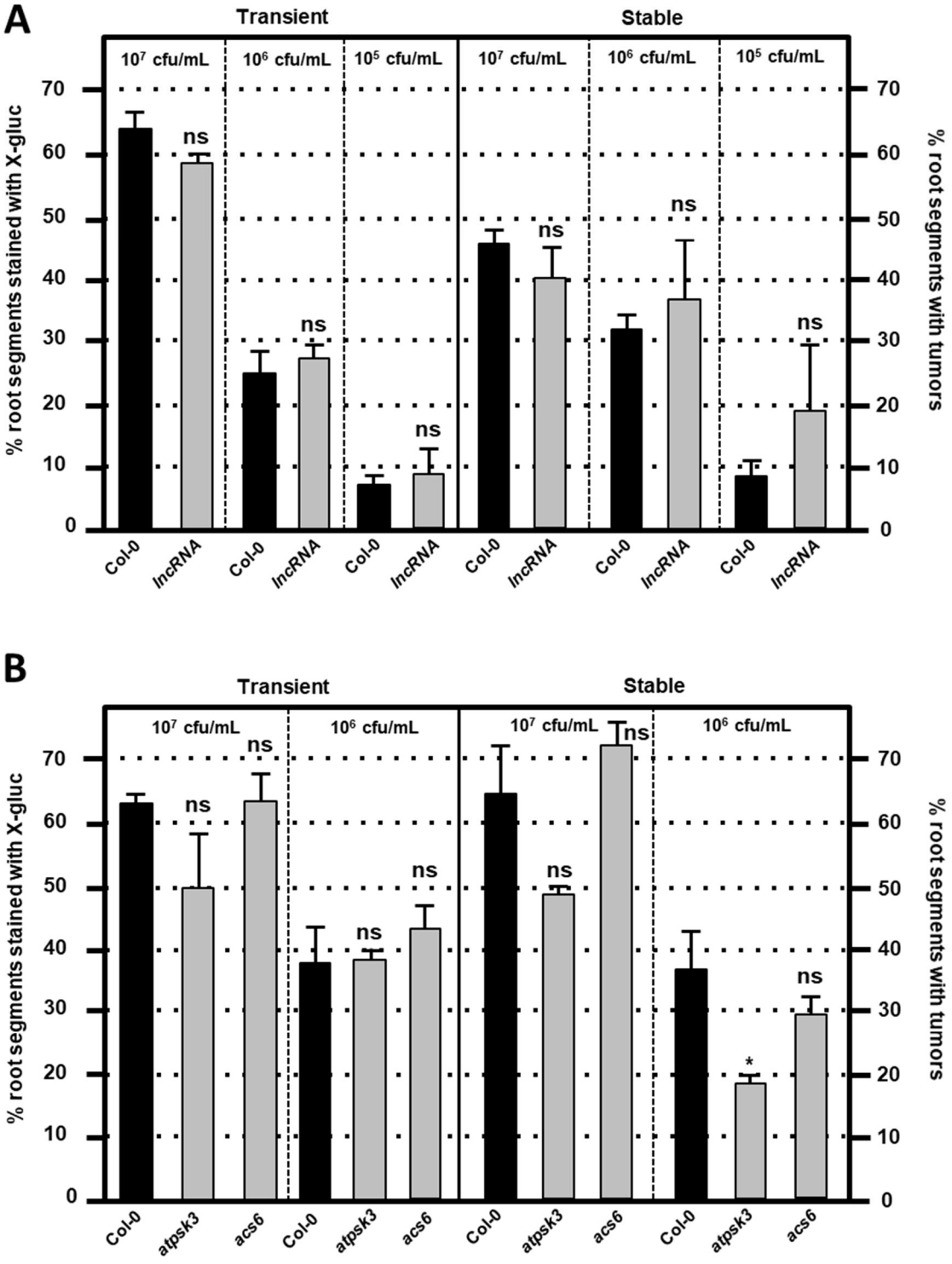

Figure 3.9 continued

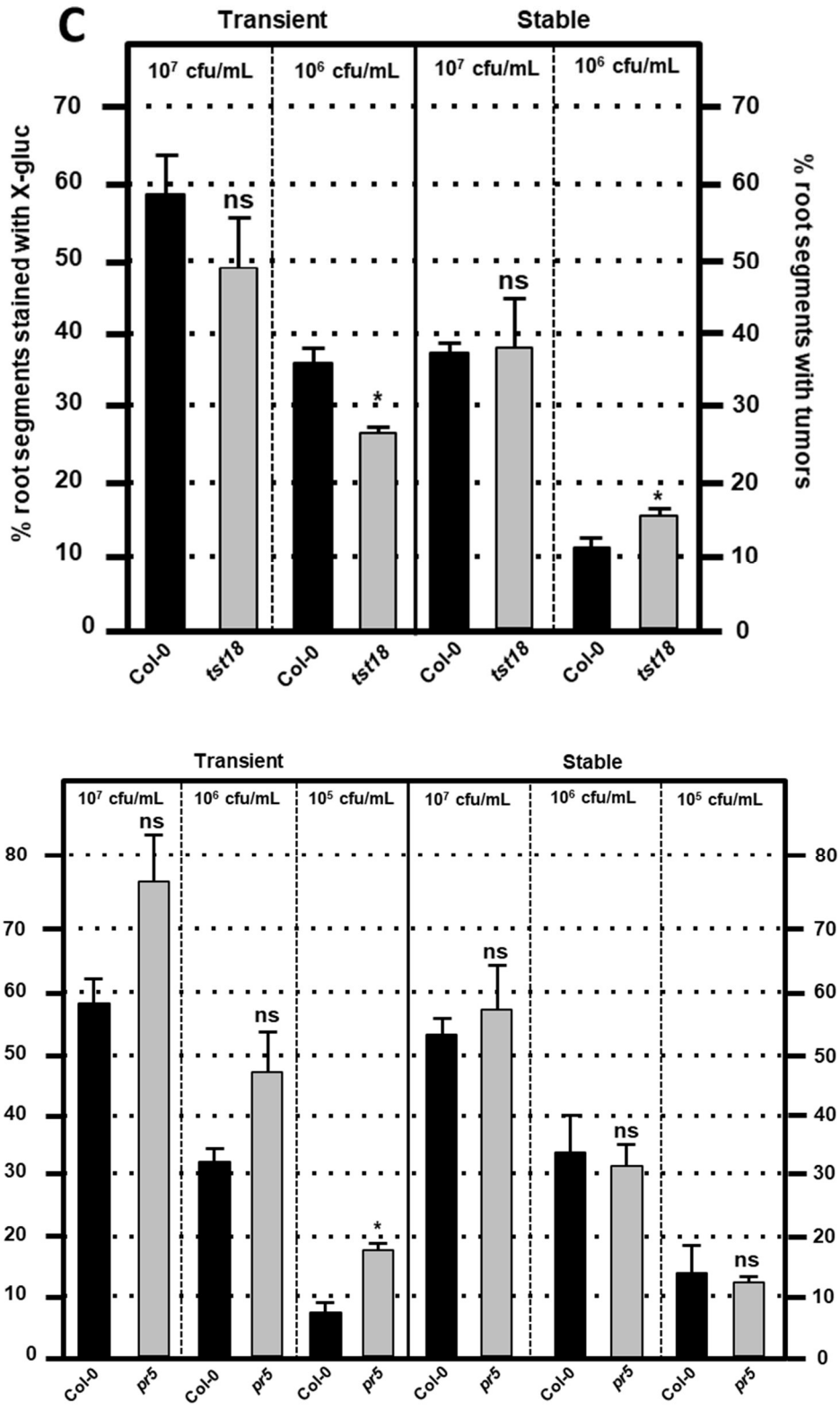

Figure 3.9 continued

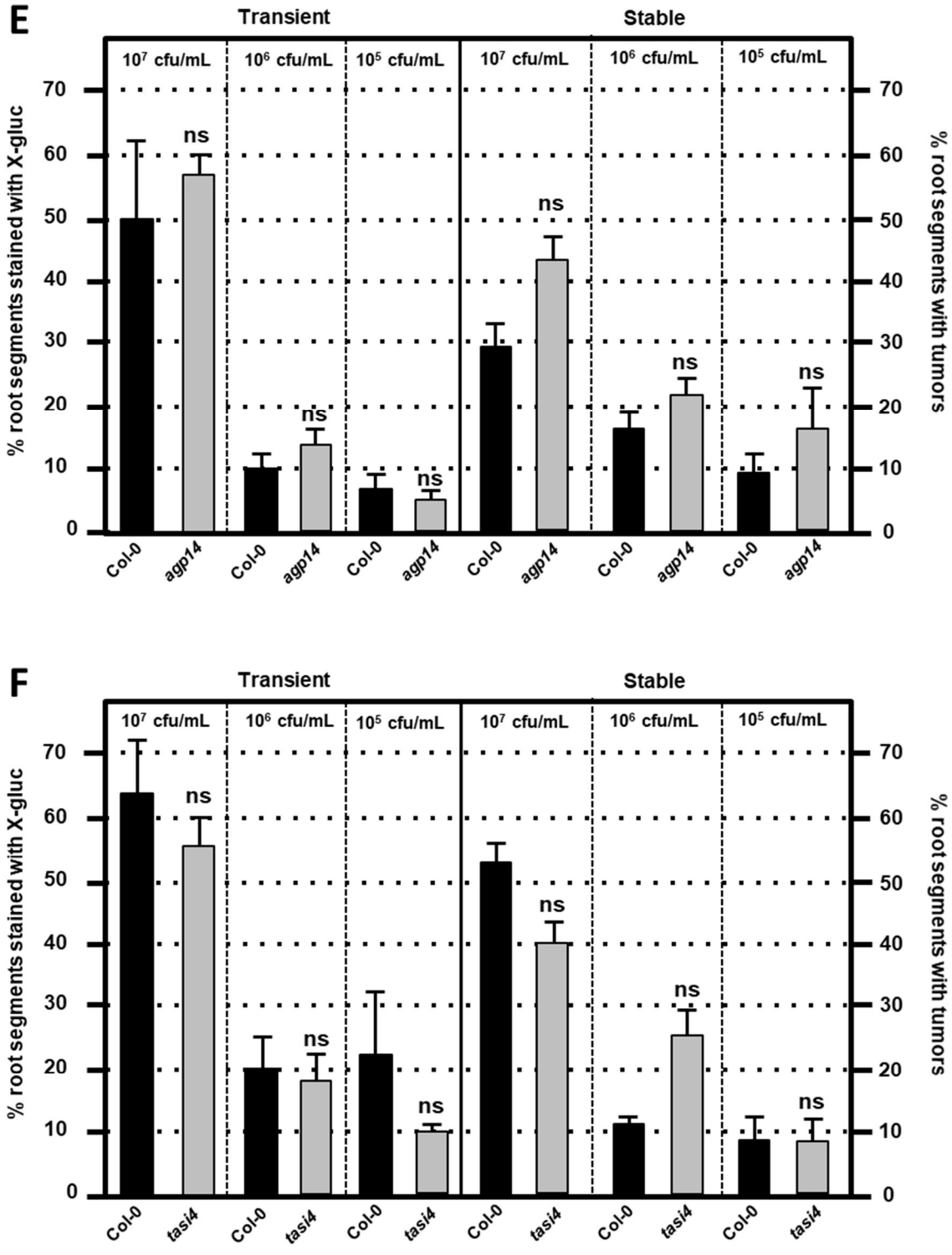

Figure 3.9 continued

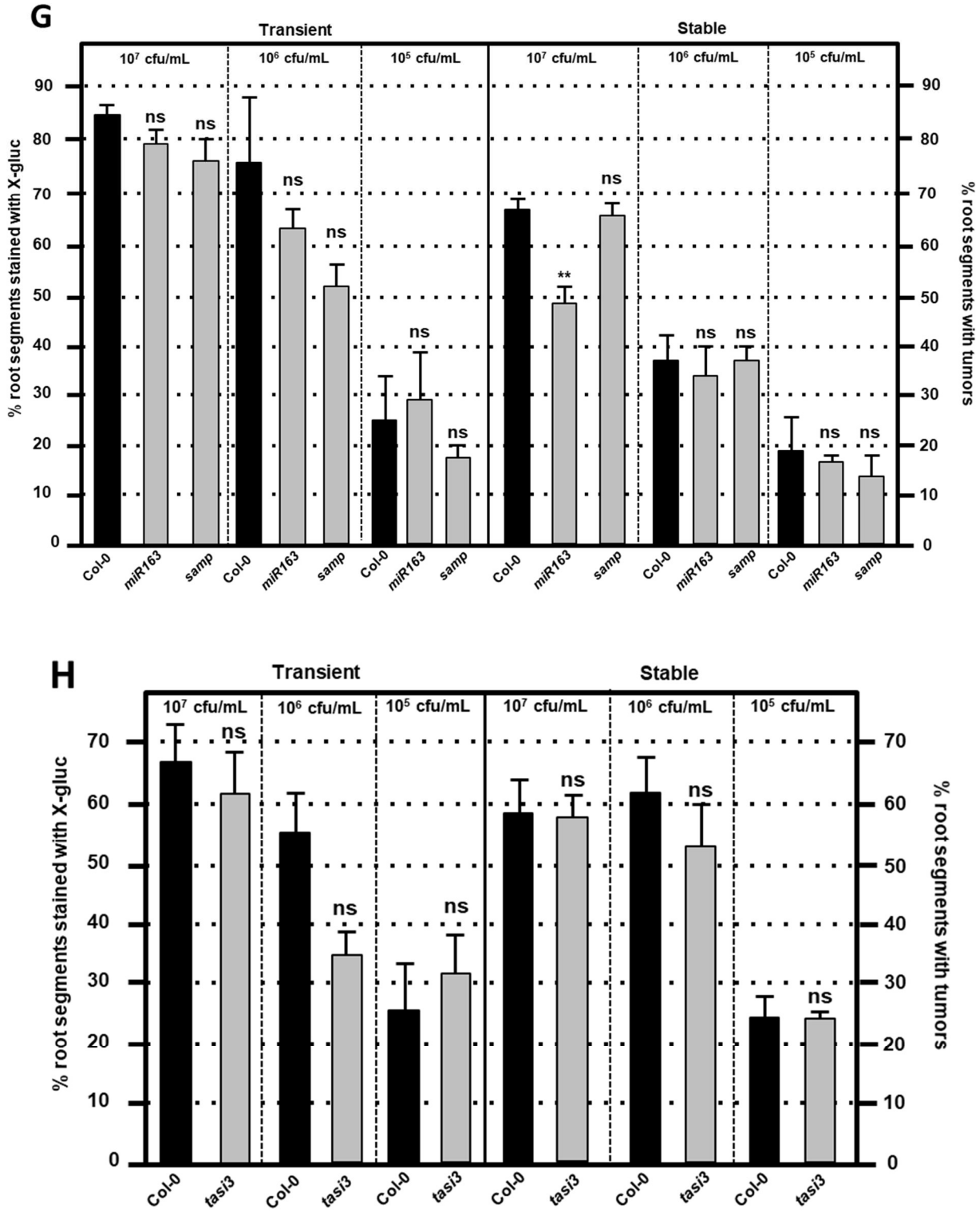

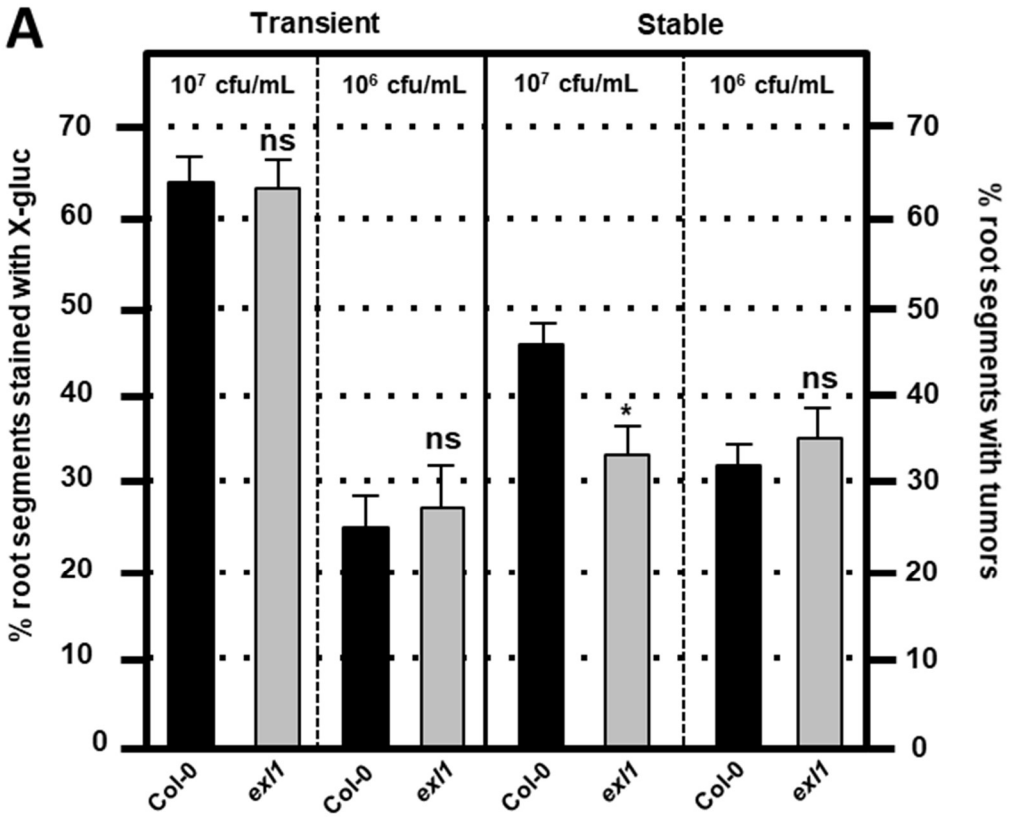

Figure 3.10. Transformation susceptibility of *Arabidopsis* wild-type (Col-0) and T-DNA insertion mutant plants of VirE2 down-regulated genes.
Agrobacterium-mediated transient (left) or stable (right) transformation assays were conducted on Col-0, *exl1* (A), *mee39*, *rbc3b*, *abah3* (B), *ntr2.6*, *cup* (C), *ntr2.1*, *oep6* (D), *esm1*, *rld17* (E), *pp2c25*, and *adh1* (F) mutant plants. Root segments were inoculated with 10^7 or 10^6 cfu/ml of *A. tumefaciens* At849 (transient) or A208 (stable). For the transient assay, the root segments were stained with X-gluc 6 days after infection. For stable transformation, tumors were scored 30 days after infection. Numbers represent an average of two or three biological replicates (each replicate containing > 60 root segments) $\pm$ SE. ANOVA test *Pvalue < 0.05, **Pvalue < 0.01, ***Pvalue < 0.001, ns: not significant.

Figure 3.10 continued

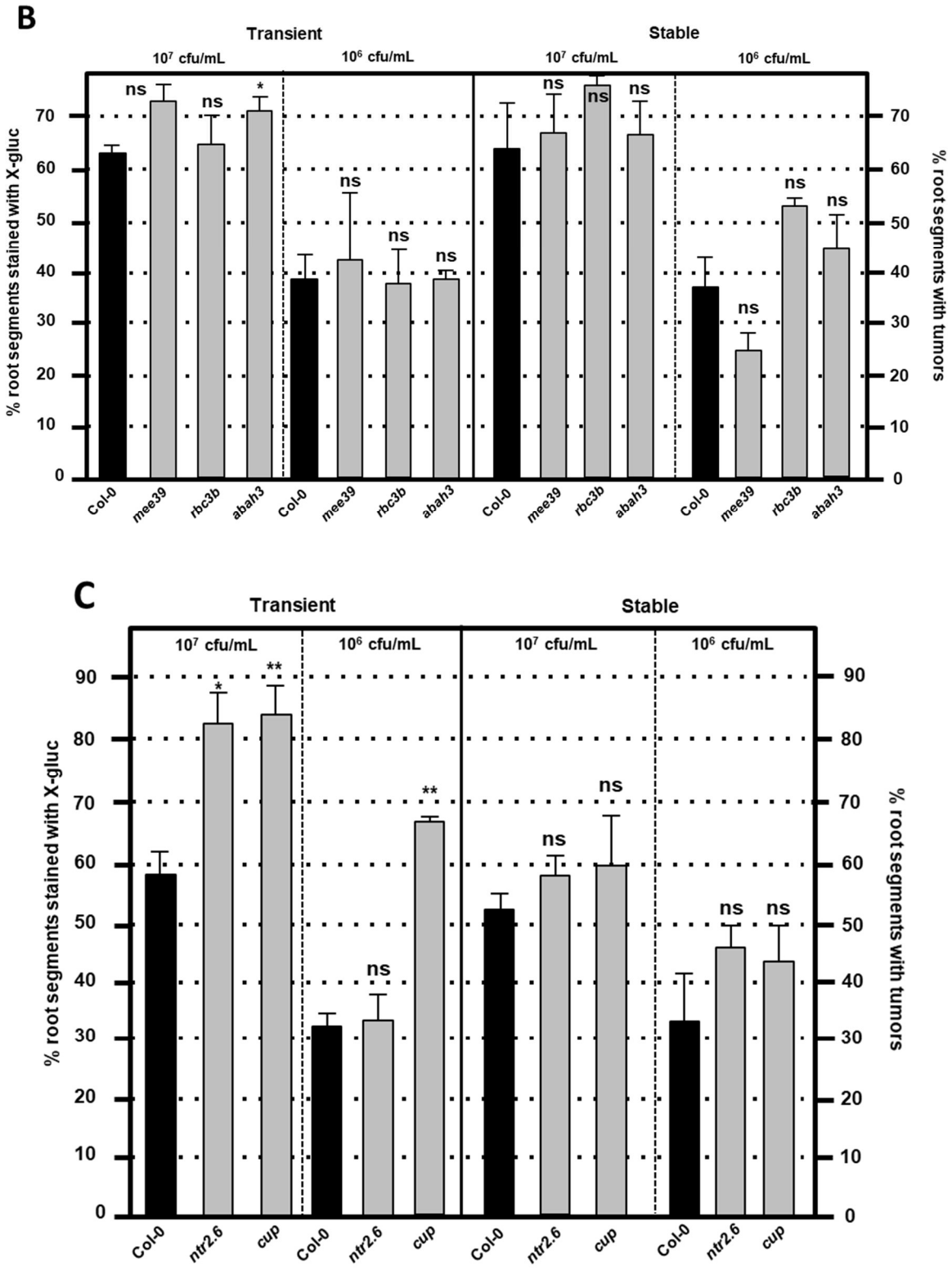

Figure 3.10 continued

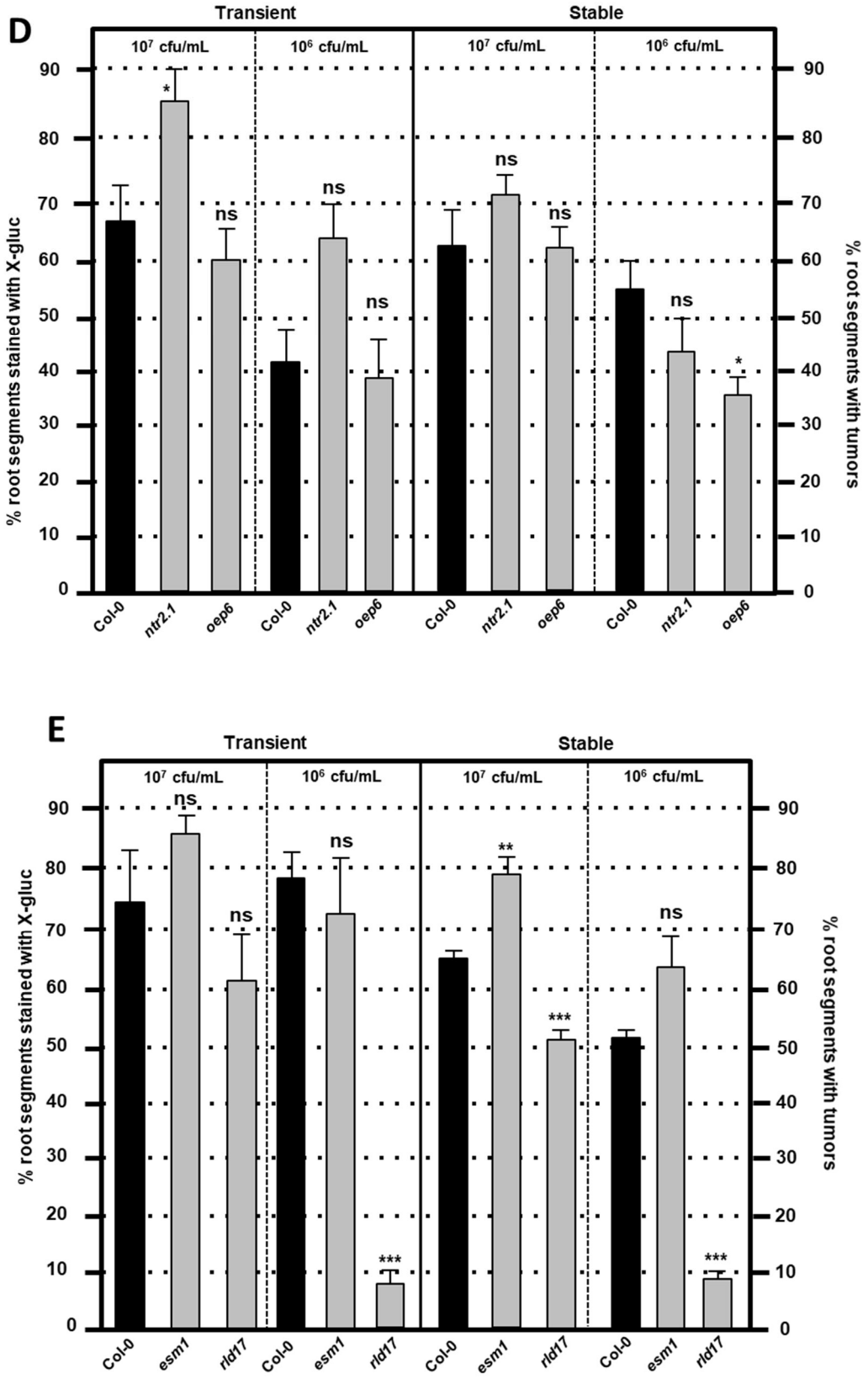

Figure 3.10 continued

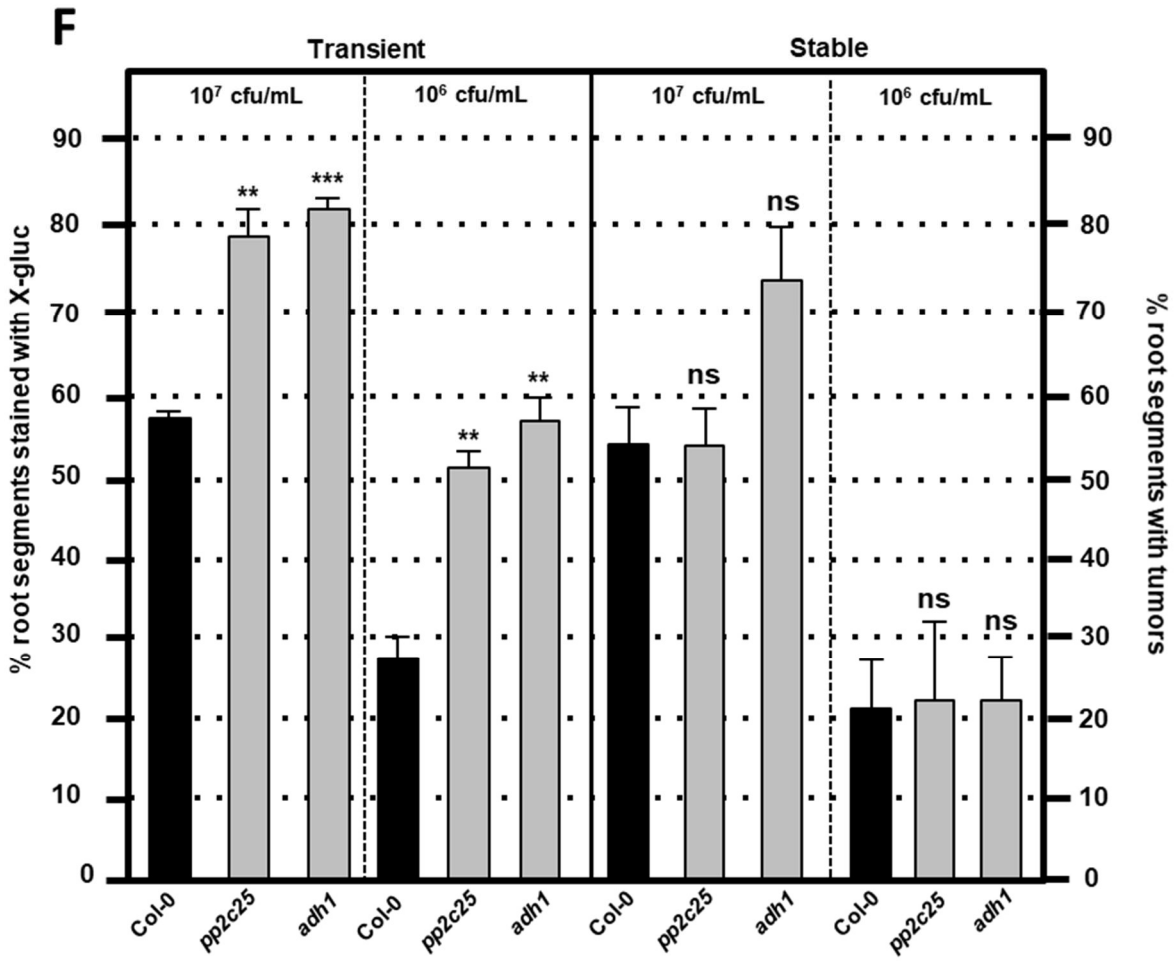

VirE2 alters the Arabidopsis proteome early during infection to facilitate transformation.

Using the same transgenic inducible *VirE2 Arabidopsis* line that we employed for transcriptome analysis, we investigated the effect of VirE2 on the *Arabidopsis* root proteome. A total of 135 *A. thaliana* proteins (~0.6% of the detectable proteins) showed a minimum 20% statistically significant change in abundance in all three biological replicates of VirE2-induced samples (Supplemental Dataset 3.3) with the VirE2 protein only being detected in the induced samples. These proteins were graphed according to their annotated Gene Ontology (GO) biological process (Figure 3.11; Ashburner et al., 2000). Proteins previously shown to be important for transformation (histones and histone modifying proteins, arabinogalactan proteins, and cyclophilins) showed increased abundance in the presence of VirE2 (Table 3.2;

Supplemental Dataset 3.3; Deng et al., 1998; Nam et al., 1999; Gaspar et al., 2004; Crane and Gelvin, 2007; Tenea et al., 2009). These VirE2-induced changes to protein levels likely facilitate transformation. Proteins whose levels changed in the presence of VirE2 did not show changes in their RNA levels, suggesting that VirE2-induced changes to RNA and protein levels are occurring post-transcriptionally.

Transgenic lines of *A. thaliana* were generated that constitutively overexpress selected genes whose proteins showed increased abundance in response to VirE2-induction (Table 3.3). Roots from individual T1 generation transgenic plants were assayed for transient transformation susceptibility (Figure 3.12). Some plants overexpressing cDNAs encoding *PEROXIDASE 34* (*PERX34*: Figure 3.12G) showed decreased transient transformation when compared to wild-type plants whereas most of the *ROTAMASE CYCLOPHILIN 2* (*ROC2*) overexpressing plants showed increased transformation (Figure 3.12I and J). *PERX34* is involved in producing reactive oxygen species (ROS) during defense response (Arnaud et al., 2017) and may show increased protein levels in response to VirE2 induction due to defense response signaling. Our results are consistent with a role for PERX34 in defense response because T1 plants overexpressing *PERX34* showed decreased transformation. VirD2 interacts with various cyclophilin proteins, including ROC2, and these interactions are necessary for efficient transformation (Deng et al., 1998; Bako et al., 2003) which is consistent with our results showing that the majority of plants overexpressing *ROC2* have enhanced transformation.

Plants overexpressing *PLASMA MEMBRANE INTRINSIC PROTEIN 2A* (*PIP2A*: Figure 3.12A and B), *PIP1A* (Figure 12C), *FASCICLIN-LIKE ARABINOGALACTAN 9* (*FLA9*: Figure 3.12D and E), *HISTONE DEACTYLASE 3* (*HDA3*: Figure 3.12F), or *ROTAMASE CYCLOPHILIN 3* (Figure 3.12H) showed comparable transient transformation efficiency when compared to wild-type plants. It is possible that these proteins may play a role in T-DNA integration or expression and will need to be assayed for stable transformation phenotypes. Other host or bacterial proteins may be required to interact with these proteins and overexpression of one protein may not be sufficient to promote transformation. However, these data suggest that VirE2-induced changes to specific protein levels may help to facilitate transformation. Taken together, our results suggest that VirE2 impacts the plant cell on both the RNA and protein levels to facilitate transformation.

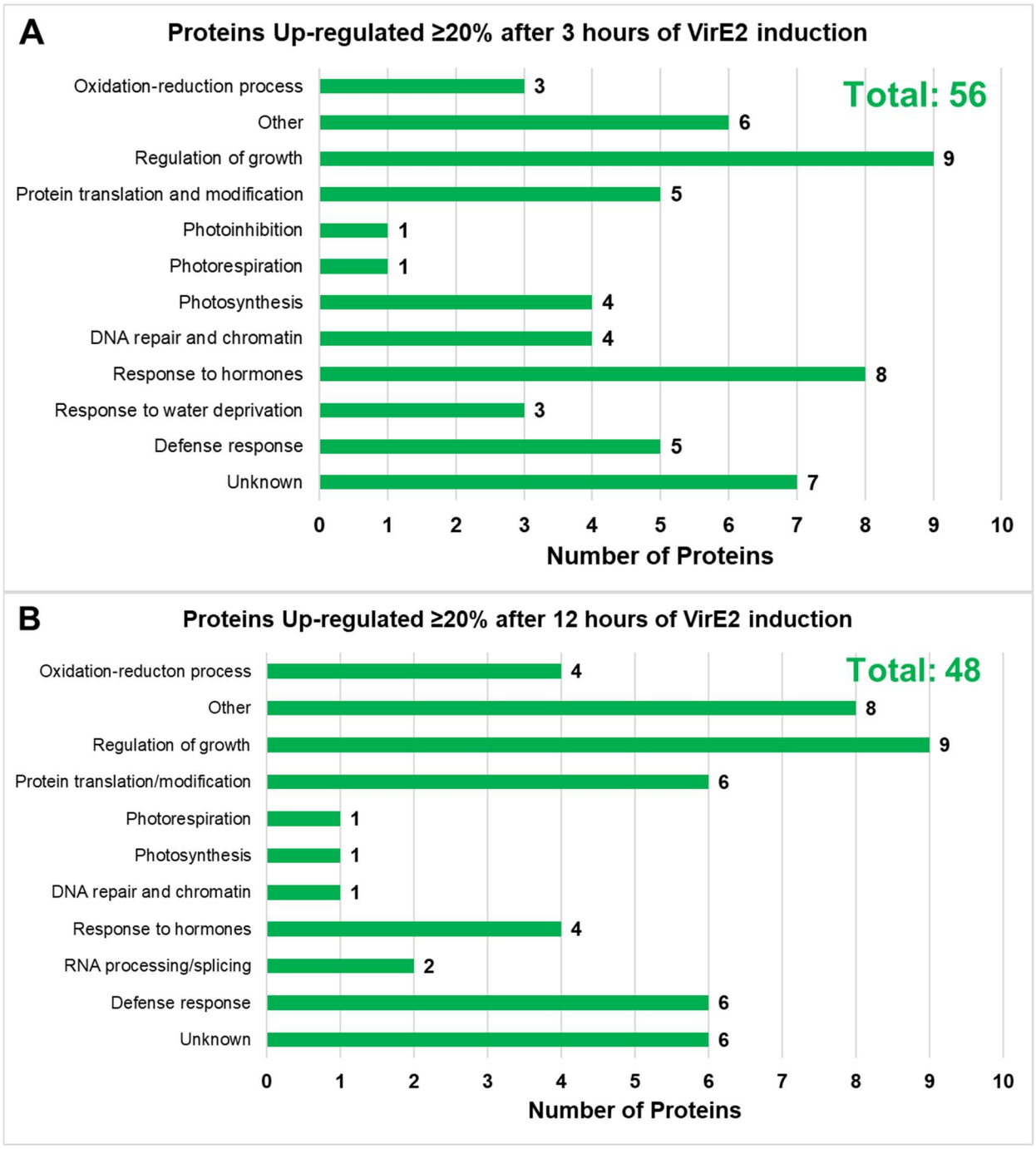

Figure 3.11. Gene Ontology (GO) Biological Process Categories of VirE2 differentially expressed proteins.

Proteins are grouped according to Gene Ontology (GO) process terms. Up-regulated proteins after 3 (A) or 12 (B) hours of VirE2 induction are shown along with down-regulated proteins after 3 (C) or 12 (D) hours of VirE2 induction. Only proteins which showed at least a 20% change in abundance for all three biological replicates determined by two different computational methods are shown. Total protein number is shown in the upper right corner of each graph and is highlighted in green (up-regulated) or in red (down-regulated).

Figure 3.11 continued

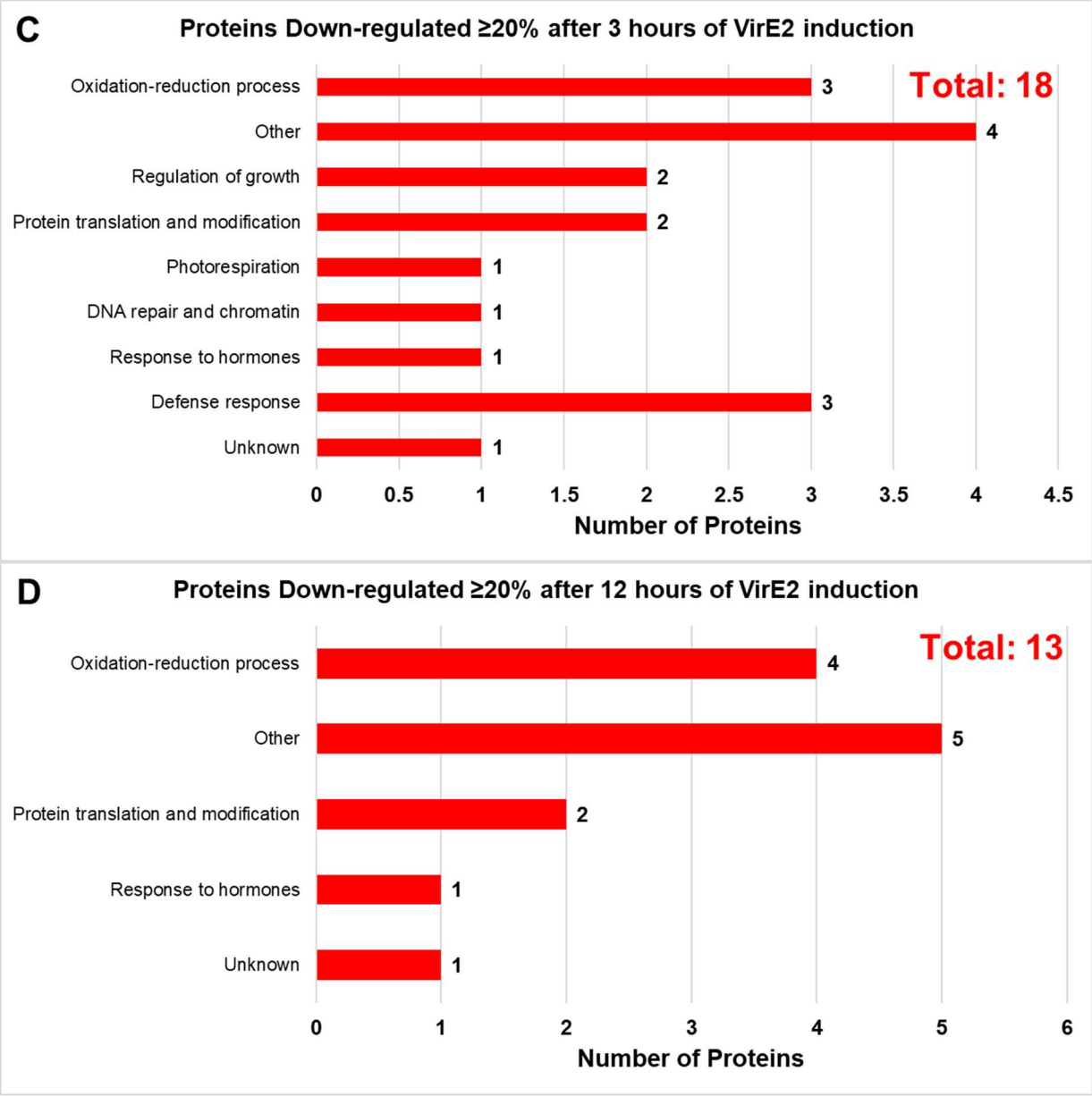

Table 3.2 Proteins previously identified to be important for transformation show increased abundance in the presence of VirE2.

Gene ID	**Gene Name**	**Encoded Protein**	**Minimum Protein % Level Change** **(Time Post-VirE2 Induction)**
AT2G28740	*HIS4* (formerly *HFO4*)	Histone H4	+37% (3 hours)
AT4G27230	*HTA2*	Histone H2A2	+140% (3 hours)
AT5G03740	*HD2C* (formerly *HDT3*)	Histone deacetylase 2C	+35% (3 hours)
AT3G44750	*HDA3* (formerly *HDT1*)	Histone deacetylase 3	+50% (12 hours)
AT2G16600	*ROC3*	Rotamase cyclophilin 3	+20% (12 hours)
AT3G56070	*ROC2*	Rotamase cyclophilin 2	+85% (12 hours)
AT1G03870	*FLA9*	FASCICLIN-like arabinogalactan 9	+25% (3 hours)
AT1G28290	*AGP31*	Arabinogalactan protein 31	+50% (3 hours)

Table 3.3 Constitutive overexpression *A. thaliana* lines of genes whose proteins show increased abundance post-VirE2 induction

Gene ID	**Gene Name**	**Encoded Protein**	**Minimum Protein % Level Change (Time Post-VirE2 Induction)**	**Transformation Phenotype relative to wild-type**
AT3G49120	*PERX34*	Peroxidase 34	+38% (3 hours)	Decreased (5/15 T1 plants tested)
AT3G53420	*PIP2A*	Plasma membrane intrinsic protein 2A	+36% (3 hours)	Comparable to wild-type (20/25 T1 plants tested)
AT3G61430	*PIP1A*	Plasma membrane intrinsic protein 1A	+49% (3 hours)	Comparable to wild-type (12/15 T1 plants)
AT5G03740	*HD2C* (formerly *HDT3*)	Histone deacetylase 2C	+35% (3 hours)	Still testing
AT3G44750	*HDA3* (formerly *HDT1*)	Histone deacetylase 3	+50% (12 hours)	Comparable to wild-type (5/5 T1 plants tested)
AT2G16600	*ROC3*	Rotamase cyclophilin 3	+20% (12 hours)	Comparable to wild-type (9/10 T1 plants tested)
AT3G56070	*ROC2*	Rotamase cyclophilin 2	+85% (12 hours)	Increased (19/25 T1 plants tested)
AT1G03870	*FLA9*	FASCICLIN-like arabinogalactan 9	+25% (3 hours)	Comparable to wild-type (13/20 T1 plants tested)
AT1G28290	*AGP31*	Arabinogalactan protein 31	+50% (3 hours)	Still testing

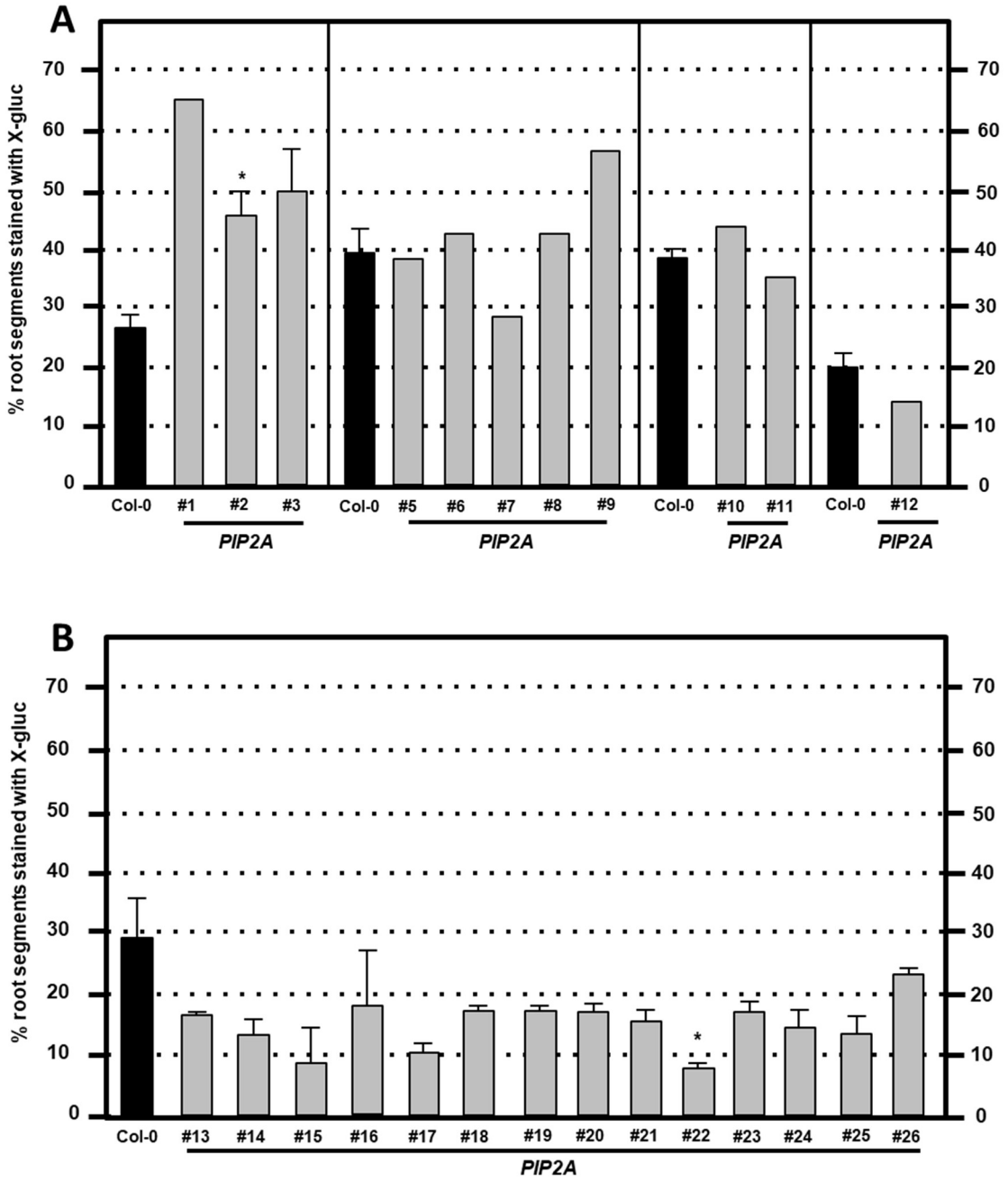

Figure 3.12. Transformation susceptibility of *Arabidopsis* wild-type (Col-0) and overexpression plants of genes whose protein levels are increased in response to VirE2.
Agrobacterium-mediated transient transformation assays were conducted on Col-0, *PIP2A* (A + B), *PIP1A* (C), *FLA9* (D + E), *HDA3* (F), *PERX34* (G), *ROC3* (H), and *ROC2* (I + J) overexpression plants. Root segments were inoculated with 10^6 cfu/ml of *A. tumefaciens* At849 (transient). For the transient assay, the root segments were stained with X-gluc 6 days after infection. Numbers represent one or an average of two technical replicates (each replicate containing > 60 root segments) + SE for each independent transgenic plant (T1 generation). ANOVA test *Pvalue < 0.05, **Pvalue < 0.01

Figure 3.12 continued

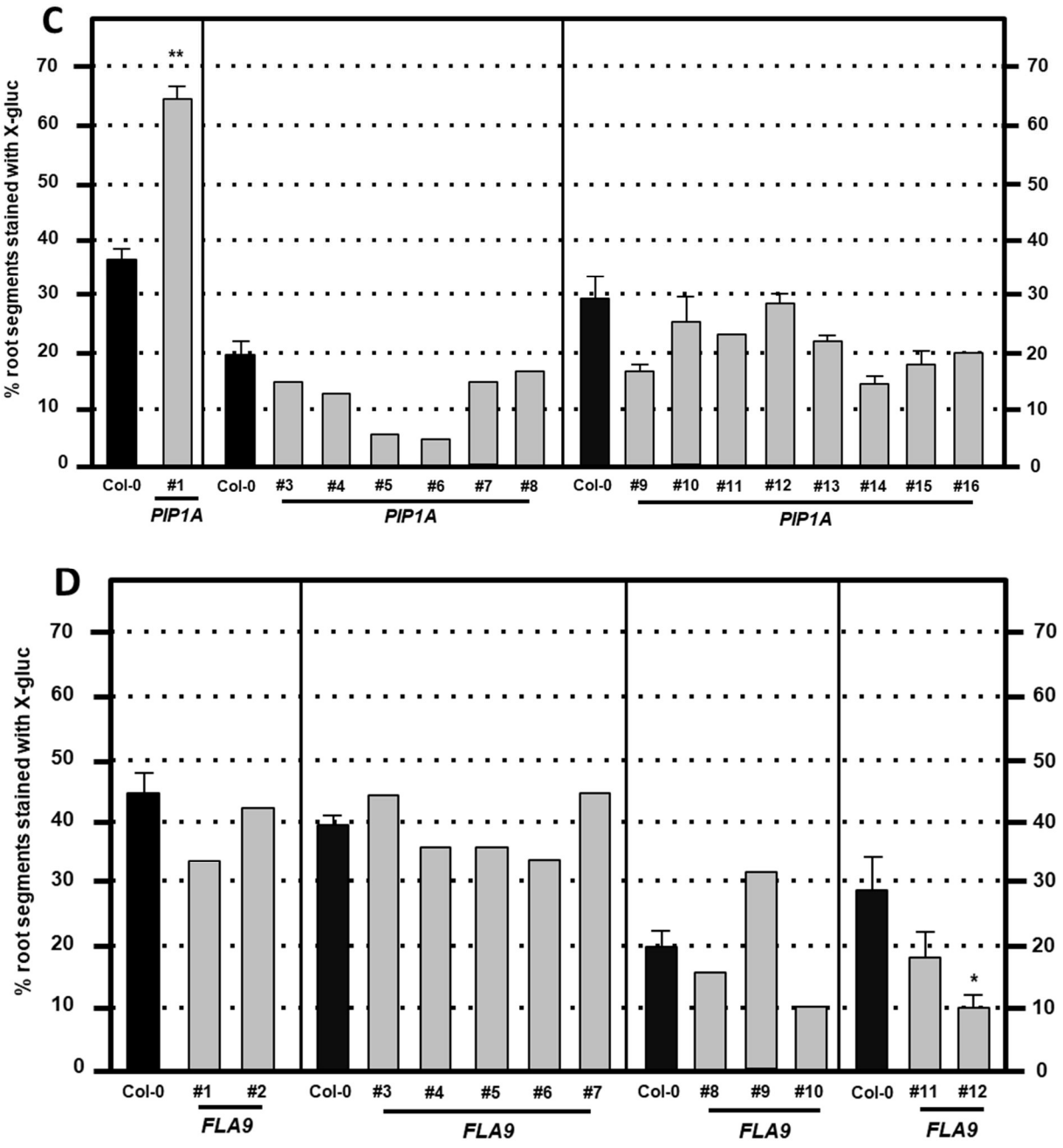

Figure 3.12 continued

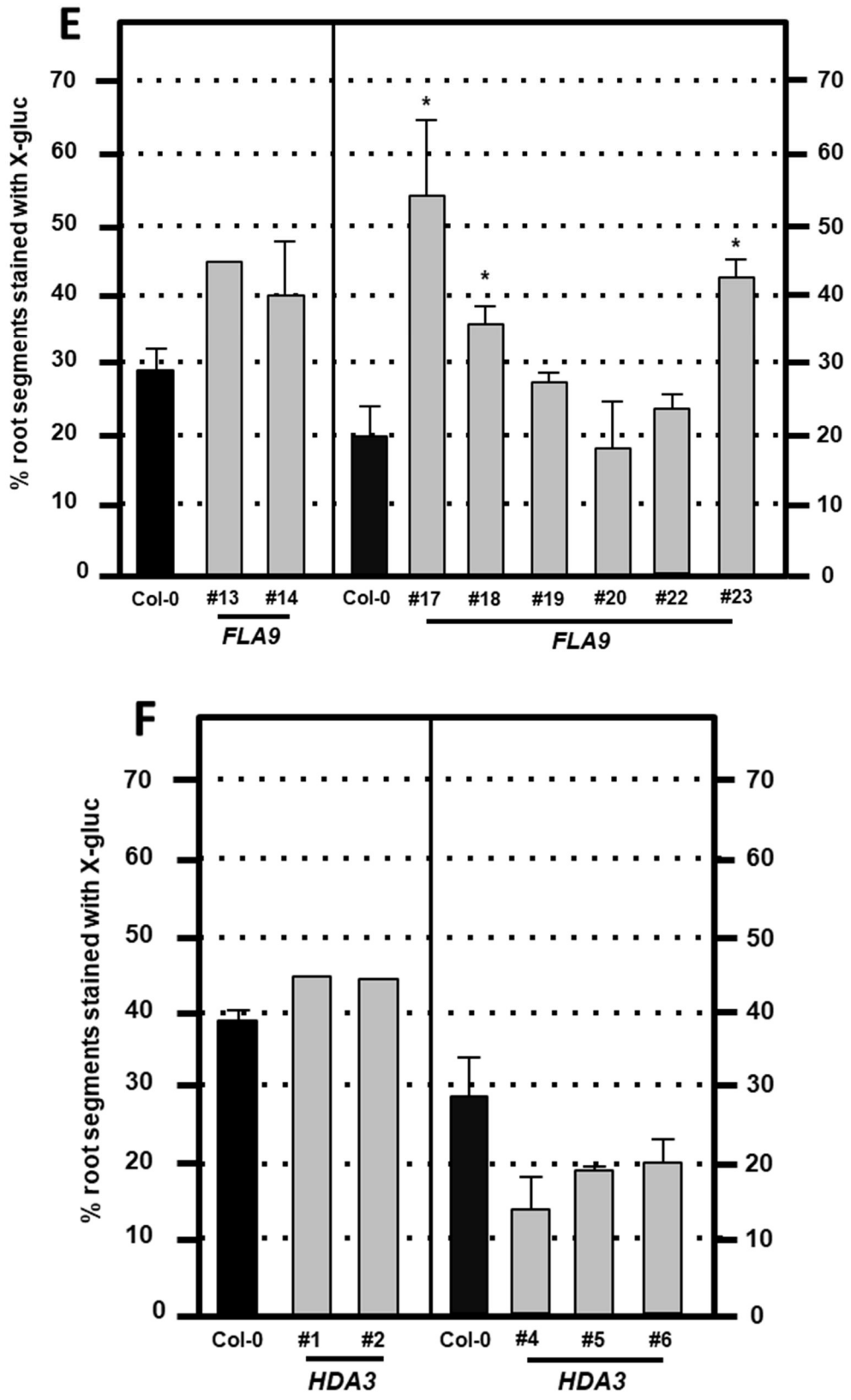

Figure 3.12 continued

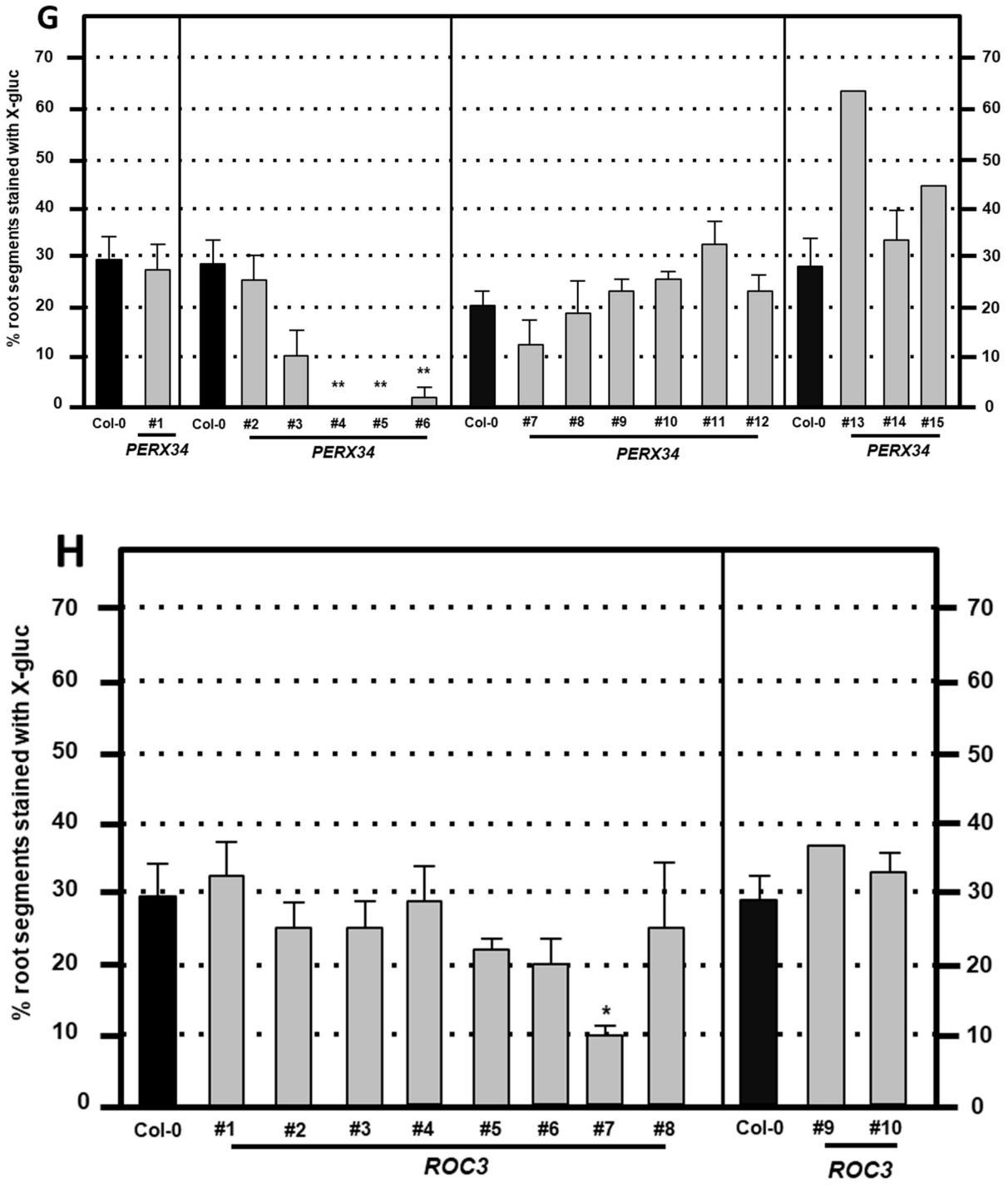

Figure 3.12 continued

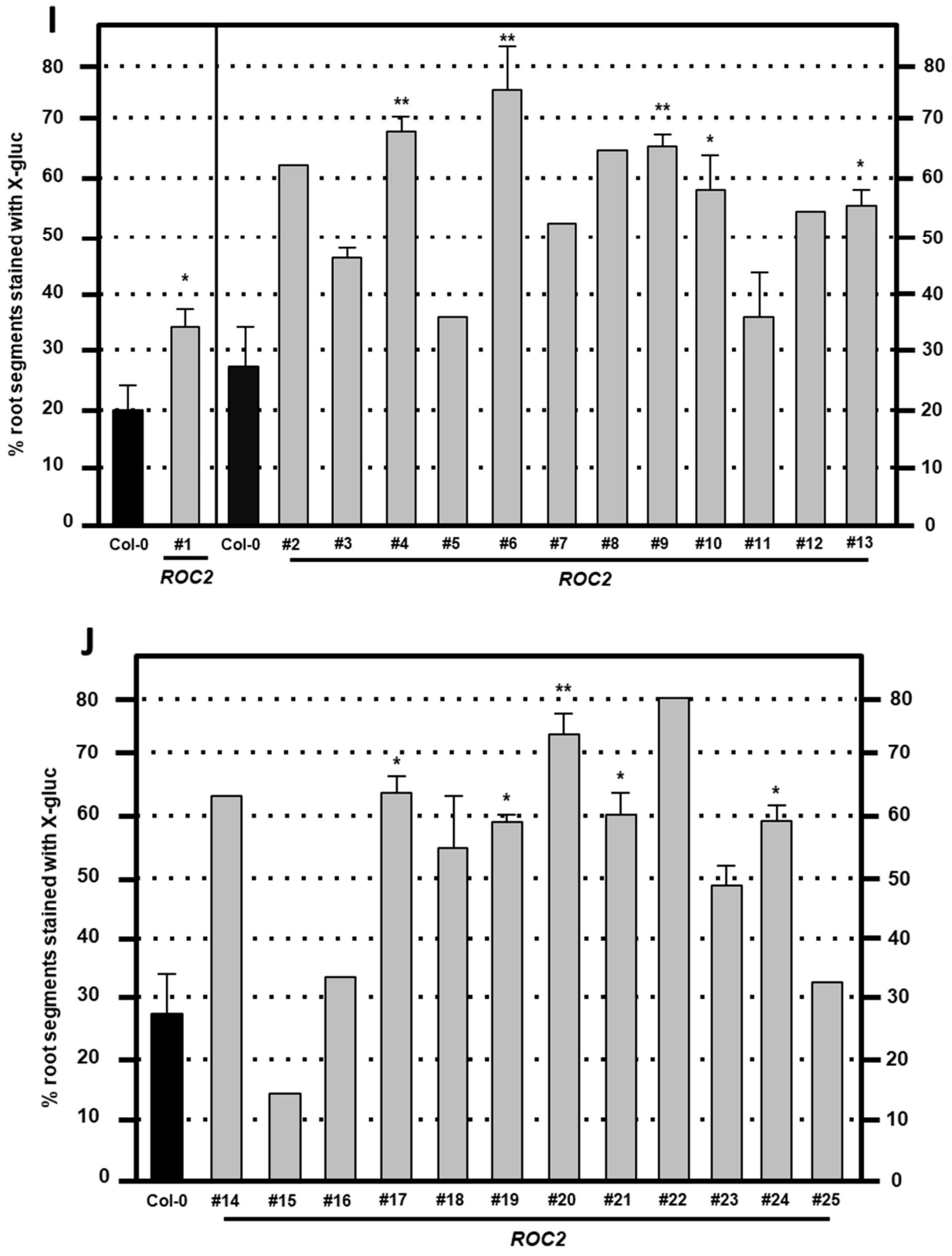

Discussion

We have shown that VirE2 must localize to the plant cytoplasm to complement a *virE2* mutant *Agrobacterium* strain to full virulence. Although cytoplasmically localized VirE2-Venus could restore virulence to such a strain, nuclear localized VirE2-Venus-NLS could not. These results suggest that the major role of VirE2 in transformation occurs in the cytoplasm.

The reported subcellular localization of VirE2 is controversial. When tagged on its N-terminus, VirE2 was shown to localize to the nucleus (Citovsky et al., 1992, 1994, 2004; Tzfira and Citovsky, 2001; Tzfira et al., 2001; Li et al., 2005). However, other studies showed that both N- and C-terminally tagged VirE2 localized to the cytoplasm (Bhattacharjee et al., 2008; Grange et al., 2008; Lee et al., 2008; Shi et al., 2014; Lapham et al., 2018). However, only the C-terminally tagged fusion protein could complement a *virE2* mutant strain and restore efficient transformation (Bhattacharjee et al., 2008). These studies utilized plant-expressed VirE2 proteins.

More recently, Li et al. (2014) internally tagged VirE2 with a small GFP fragment (VirE2-GFP11). They showed that an *Agrobacterium* strain expressing VirE2-GFP11 retained full virulence (Li et al., 2014). Using this strain and a split-GFP approach, they observed delivery of VirE2 from *Agrobacterium* into a plant expressing GFP1-10 (Li et al., 2014). Within the plant, VirE2 molecules formed filamentous structures, a few of which could be detected within the nucleus. However, the majority of these structures were observed in the cytoplasm (Li et al., 2014). Roushan et al. (2018) used phiLOV2.1 to tag VirE2 internally and showed that, when transferred from *Agrobacterium*, the protein localized to the cytoplasm of *Arabidopsis* roots and *N. tabacum* leaves. It is possible that VirE2 molecules originating from *Agrobacterium* may localize differently from plant-expressed VirE2. Nevertheless, our current results indicate that an inducible plant-expressed VirE2-Venus protein, localized to the cytoplasm, can complement a *virE2* mutant *Agrobacterium* strain. These results confirm our previous observations (Bhattacharjee et al., 2008). Furthermore, an inducible nuclear-localized VirE2-Venus-NLS protein could not complement the *virE2* mutant strain. Our results therefore indicate that VirE2 must localize to the cytoplasm to perform its major functions in facilitating transformation.

We cannot rule out that VirE2 has no function within the nucleus. VirE2 can interact in plant cells with several *Arabidopsis* importin α (Impα) protein isoforms when both VirE2 and Impα are constitutively overexpressed (Bhattacharjee et al., 2008, Lee et al., 2008). The native VirE2

protein contains two bipartite NLS sequences (Citovsky et al., 1992, 1994). However, structural analyses (Chang et al., 2017) indicated that the interactions between Impα and the VirE2 NLS sequences were weak. The interactions observed by Bhattacharjee et al. (2008), and nuclear localization of VirE2-Impa-4 (but not VirE2-Impa-1) complexes (Lee et al., 2008), may have resulted from high levels of protein expression. Overexpression of a truncated VirE2 protein (lacking the ability to bind ssDNA, but retaining both NLS sequences) in both tobacco and grape vines inhibited transformation by a virulent *Agrobacterium* strain (Citovsky et al., 1994; Krastanova et al., 2010). These authors suggested that this interference resulted from decreased nuclear import of the bound T-strand. Ziemienowicz et al. (2001) observed that VirE2 bound to ssDNA could not be imported into isolated tobacco nuclei, but they did observe the import of free VirE2 molecules into the nucleus. VirE2, in addition to the effector protein VirD2, was required for nuclear import of large ssDNA molecules in this *in vitro* system (Ziemienowicz et al., 2001). It is possible that a small amount of VirE2 localizes to the nucleus during transformation. However, based on our results, exclusive nuclear localization of VirE2 does not support transformation.

We investigated possible functions of VirE2 in transformation other than its proposed structural roles in protecting T-strands (Howard and Citovsky, 1990) and/or shaping T-strands to traverse the nuclear pores (Ziemienowicz et al., 2001). VirE2 interacts with the *Arabidopsis* transcription factors VIP1 and VIP2 (Tzfira et al., 2001; Anand et al., 2007; Pitzschke et al., 2009) and various other plant proteins (Lee et al., 2008, 2012). Although VIP1 and its orthologs do not play a role in *Agrobacterium*-mediated transformation (Shi et al., 2014; Lapham et al., 2018), interactions with VIP2 or other proteins could lead to changes in plant gene expression, perhaps facilitating transformation. RNA-seq analysis of transgenic *Arabidopsis thaliana* roots inducibly expressing VirE2 revealed that most transcript abundance changes occurred 12 hours post-VirE2 induction (Supplemental Data Sheet 3.1 and 3.2). Conversely, proteomics analysis indicated that numerous proteins changed abundance 3 hr after VirE2 induction, but none of the transcripts for these proteins changed abundance at that early time (Supplemental Data Sheet 3.3). These results suggest that alterations in mRNA and protein abundance in response to VirE2 expression occur post-transcriptionally. This hypothesis is consistent with cytoplasmic- rather than nuclear-localized VirE2. It is also supported by our data showing that genes involved in translation are differentially expressed and enriched among those genes up-regulated in response

to VirE2 (Figure 3.4A and 3.5A). Proteins involved in translation also exhibited changes in their steady-state amounts in response to VirE2 induction (Figure 3.11).

Genes involved in plant defense were differentially expressed in response to VirE2 induction (Figure 3.4, 3.6, and 3.7; Supplemental Data Sheets 3.1 and 3.2) and were over-represented as determined by GO enrichment analysis of both RNA-seq datasets (Figures 3.5 and 3.8). A subset of these genes is involved in defense against bacteria and in innate immune responses (Figure 3.5B, 3.6, 3.7A, and 3.8A; Supplemental Data Sheet 3.1 and 3.2). Duan et al. (2018) tested the expression of several defense genes and observed that some of these genes were up-regulated in *A. thaliana* constitutively expressing VirE2 24 hr after the plants were treated with the avirulent *Agrobacterium* strain A136. They also found that plants constitutively expressing VirE2 had reduced transformation efficiency compared to wild-type plants. They proposed that this inhibition was caused by enhanced defense responses in the VirE2 expressing plants. We also observed up-regulation of genes involved in innate immune responses 12 hr after VirE2 induction in the presence of the avirulent *Agrobacterium* strain A136 (Figure 3.4A, 3.6A, 3.7A, and 3.8A), but the genes we identified differed from those identified previously by Duan et al. (2018; Supplemental Data Sheet 3.1 and 3.2). Ditt et al. (2006) found that genes involved in response to biotic stimulus, abiotic stimulus, and stress were enriched for transcripts up-regulated 48 hr after infection of *Arabidopsis* cell cultures (ecotype Ler) by the tumorigenic *Agrobacterium* strain A348. We also observed up-regulation of these same gene categories 12 hr after VirE2 induction in the presence of the avirulent *Agrobacterium* strain A136 (Figure 3.7A). In addition, we observed down-regulation of other defense genes involved in responding to bacteria, salicylic-acid, oxidative stress, and genes involved in the regulation of immune responses (Figure 3.4B, 3.5B, 3.6B, and 3.7B). Veena et al. (2003) observed the induction of defense response genes early (3-6 hours) after *Agrobacterium* infection of *N. tabacum* BY-2 suspension cells, but expression of these genes was suppressed at later infection times (30-36 hr) in the presence of *Agrobacterium* strains that could transfer virulence proteins. However, suppression of this delayed defense response did not occur when the plants were infected with a transfer-deficient *Agrobacterium* strain (Veena et al., 2003). Similarly, we observed down-regulation of defense response genes only after 12 hours of VirE2-induction (Supplemental Data Sheet 3.1 and 3.2). Therefore, VirE2 may modulate the expression of some defense response genes to help facilitate transformation.

The stress-response associated *ALCOHOL DEHYDROGENASE 1* (*ADH1*) gene was strongly down-regulated in the presence of VirE2 (Table 3.1; Supplemental Data Sheet 3.1) and a knockout mutant line of this gene showed increased transformation (Figure 3.10F). Veena et al. (2003) also found that a tobacco alcohol dehydrogenase gene was down-regulated in the presence of a virulent *Agrobacterium* strain at later infection time points. In addition, our RNA-seq experiments revealed that the transcription factor *WRKY33* was up-regulated 12 hr after VirE2 induction (Supplemental Data Sheet 3.2). Zheng et al. (2006) showed that ectopic over-expression of *WRKY33* resulted in increased susceptibility to the bacterial pathogen *Pseudomonas syringae*, and that *WRKY33* could act as a negative regulator of bacterial defense responses. Taken together, our data suggest that VirE2 modulates the expression of several defense response genes to facilitate transformation.

Genes known to be important for transformation, including those encoding a protein phosphatase 2C (Tao et al., 2004), arabinogalactan proteins (Nam et al., 1999; Gaspar et al., 2004), and heat shock proteins (Park et al., 2014), showed changes in expression in response to VirE2 (Supplemental Data Sheet 3.1 and 3.2). *PROTEIN PHOSPHATASE 2C 25* (*PP2C25*) was down-regulated by VirE2 (Table 3.1) and its knockout mutant line exhibited increased transformation (Figure 3.10F). A tomato protein phosphatase 2C (*DIG3*) was previously shown to act as a negative regulator of transformation by dephosphorylating a serine residue in VirD2 that is critical for VirD2 nuclear import (Tao et al., 2004). VirE2-mediated down-regulation of *PP2C25* may therefore facilitate more efficient nuclear import of VirD2/T-strand complexes.

Induction of VirE2 increased transcript and protein levels of some arabinogalactan protein (AGP) genes (Supplemental Data Sheets 3.1 and 3.3). *ARABINOGALACTAN PROTEIN 17* (*AGP17*) was previously shown to be important for transformation by mediating attachment of *Agrobacterium* to plant cells (Nam et al., 1999; Gaspar et al., 2004). VirE2 may therefore modulate the levels of these AGPs to facilitate transformation. We assayed a knockout mutant of the *AGP14* gene for transformation susceptibility but did not observe any significant difference in transformation compared to wild-type plants (Figure 3.9F). Schlutz et al. (2002) identified 50 *Arabidopsis* genes encoding AGPs, and it is plausible that many have redundant functions in the plant cell. Overexpression of the *FASCICLIN-LIKE ARABINOGALACTAN 9* (*FLA9*) did not result in any significant change in transient transformation susceptibility (Figure 3.12B). Overexpression of this protein alone may be insufficient to promote transformation.

Some heat shock protein transcript and protein levels increased in response to VirE2 induction (Supplemental Data Sheet 3.2), including the transcript encoding *HEAT SHOCK PROTEIN 90* (*HSP90*). Park et al. (2014) demonstrated that over-expression of *HSP90* increased *Arabidopsis* root transformation susceptibility and proposed that HSP90 could act as a molecular chaperone to stabilize VirE2 and other proteins important for transformation. Up-regulation of *HSP90* by VirE2 could also facilitate transformation.

Histones, histone modifying enzymes, and cyclophilins showed increased protein levels in response to VirE2 (Table 3.1; Supplemental Data Sheet 3.3) and have previously been shown, or proposed, to play important roles in transformation (Deng et al., 1998; Nam et al., 1999; Bako et al., 2003; Crane and Gelvin, 2007; Tenea et al., 2009). Histone H2A2 (HTA2) and histone H4 (HIS4: formerly HFO4) protein levels increased in the presence of VirE2 (Table 3.1; Supplemental Data Sheet 3.3). Over-expression of *HIS4*, *HTA2*, and other histone H2A variants increased transformation susceptibility of *Arabidopsis* (Tenea et al., 2009). The histone deacetylases *HD2C* (formerly *HDT3*) and *HDA3* (formerly *HDT1*) also showed increased protein levels in response to VirE2 (Table 3.1; Supplemental Table 3.3). Crane and Gelvin (2007) showed that RNAi-mediated silencing of *HDA3* and other chromatin-related genes resulted in reduced transformation and T-DNA integration. Increased levels of these histones and histone modifying proteins in response to VirE2 may also facilitate transformation. Preliminary results showed that plants overexpressing *HDA3* did not have significantly different transient transformation susceptibility (Figure 3.12B), but these (and more) plants will need to be tested for stable transformation.

Two cyclophilin proteins, *ROC2* and *ROC3*, showed increased protein levels post-VirE2 induction (Table 3.1; Supplemental Data Sheet 3.3). VirD2 interacts with various cyclophilin proteins, and this interaction is important for efficient transformation (Deng et al., 1998). Our data suggest that VirE2 increases the levels of some cyclophilin proteins, facilitating transformation. This is confirmed by our results showing that plants overexpressing *ROC2* have increased transformation susceptibility (Figures 3.12I and J).

VirE2 thus alters the steady-state levels of specific plant RNAs and proteins which are known to be important for transformation. VirE2 likely mediates these changes post-transcriptionally. This model is supported by the rapid changes in levels of certain proteins and more delayed changes in levels of specific RNAs we observed in response to VirE2 induction.

We also observed that cytoplasmic localization of VirE2 is required for it to function in transformation, which is consistent with a post-transcriptional role in modulating mRNA and protein levels. We therefore conclude that cytoplasmic localization of VirE2 modulates specific plant steady-state RNA and protein levels post-transcriptionally to facilitate transformation.

References

Anand, A., Krichevsky, A., Schornack, S., Lahaye, T., Tzfira, T., Tang, Y., Citovsky, V., and Mysore K.S. (2007) *Arabidopsis* VirE2 INTERACTING PROTEIN 2 is required for *Agrobacterium* T-DNA integration in plants. *Plant Cell* 19, 1695-1708.

Anders, S., Pyl, P.T., and Huber, W. (2015) HTSeq—a Python framework to work with high-throughput sequencing data. *Bioinformatics* 31, 166-169.

Arnaud, D., Lee, S., Takebayashi, Y., Choi, D., Choi, J., Sakakibara, H., and Hwang, I. (2017) Cytokinin-mediated regulation of reactive oxygen species homeostasis modulates stomatal immunity in Arabidopsis. *Plant Cell*. 29, 543-559.

Ashburner, M., Ball, C.A., Blake, J.A., Botstein, D., Butler, H., Cherry, J.M., Davis, A.P., Dolinski, K., Dwight, S.S., Eppig, J.T., Harris, M.A., Hill, D.P., Issel-Tarver, L., Kasarkis, A., Lewis, S., Matese, J.C., Richardson, J.E., Ringwald, M., Rubin, G.M., and Sherlock, G. (2000) Gene ontology: Tool for the unification of biology. *Nat. Genet.* 25, 25-29.

Bakó, L., Umeda, M., Tiburcio, A.F., Schell, J., and Koncz, C. (2003) The VirD2 pilot protein of *Agrobacterium*-transferred DNA interacts with the TATA box-binding protein and a nuclear protein kinase in plants. *Proc. Natl. Acad. Sci. USA* 100, 10108-10113.

Bhattacharjee, S., Lee, L.-Y., Oltmanns, H., Cao, H., Veena, Cuperus, J., and Gelvin, S.B. (2008) AtImpa-4, an *Arabidopsis* importin α isoform, is preferentially involved in *Agrobacterium*-mediated plant transformation. *Plant Cell* 20, 2661–2680.

Bi, G., and Zhou J.-M. (2017) MAP kinase signaling pathways: A hub of plant-microbe interactions. *Cell Host Microbe* 21, 270-273.

Chang, C.W., Counago, R.L., Williams, S.J., Boden, M., and Kobe, B. (2012) Crystal structure of rice importin-alpha and structural basis of its interaction with plant-specific nuclear localization signals. *Plant Cell* 24, 5074-5088.

Chen, W.P., Chen, P.D., Liu, D.J., Kynast, R., Friebe, B., Velazhahan, R., Muthukrishnan, S., and Gill, B.S. (1999) Development of wheat scab symptoms is delayed in transgenic wheat plants that constitutively express a rice thaumatin-like protein gene. *Theor. Appl. Genet.* 99, 755–760.

Christie, P.J., Ward, J.E., Winans, S.C., and Nester, E.W. (1988) The *Agrobacterium tumefaciens* virE2 gene product is a single-stranded-DNA-binding protein that associates with T-DNA. *J. Bacteriol.* 170, 2659–2667.

Citovsky, V., De Vos, G., and Zambryski, P. (1988) Single-stranded DNA binding protein encoded by the virE locus of *Agrobacterium tumefaciens*. *Science* 240, 501–504.

Citovsky, V., Wong, M.L., and Zambryski, P. (1989) Cooperative interaction of *Agrobacterium* VirE2 protein with single-stranded DNA: implications for the T-DNA transfer process. *Proc. Natl. Acad. Sci. U.S.A.* 86, 1193–1197.

Citovsky, V., Zupan, J., Warnick, D., and Zambryski, P. (1992) Nuclear localization of *Agrobacterium* VirE2 protein in plant cells. *Science* 256, 1802–1805.

Citovsky, V., Warnick, D., and Zambryski, P. (1994) Nuclear import of *Agrobacterium* VirD2 and VirE2 proteins in maize and tobacco. *Proc. Natl. Acad. Sci. USA* 91, 3210–3214.

Citovsky, V., Kapelnikov, A., Oliel, S., Zakai, N., Rojas, M.R., Gilbertson, R.L., Tzfira, T., and Loyter, A. (2004) Protein interactions involved in nuclear import of the *Agrobacterim* VirE2 protein in vivo and in vitro. *J. Biol. Chem.* 279, 29528–29533.

Clough, S.J., and Bent, A.F. (1998) Floral dip: A simplified method for *Agrobacterium*-mediated transformation of *Arabidopsis thaliana*. *Plant J.* 16, 735-743.

Cox, J., and Mann, M. (2008) MaxQuant enables high peptide identification rates, individualized p.p.b.range mass accuracies and proteome-wide protein quantification. *Nat. Biotechnol.* 26, 1367-1372.

Cox, J., Neuhauser, N., Michalski, A., Scheltema, R. A., Olsen, J. V., and Mann, M. (2011) Andromeda: a peptide search engine integrated into the MaxQuant environment. *J. Proteome Res.* 10, 1794-1805.

Cox, J., Hein, M. Y., Luber, C. A., Paron, I., Nagaraj, N., and Mann, M. (2014) Accurate proteome-wide label-free quantification by delayed normalization and maximal peptide ratio extraction, termed MaxLFQ. *Mol. Cell Proteomics* 13, 2513-2526.

Crane, Y.M., and Gelvin, S.B. (2007) RNAi-mediated gene silencing reveals involvement of *Arabidopsis* chromatin-related genes in *Agrobacterium* -mediated root transformation. *Proc. Natl. Acad. Sci. USA* 104, 15156-15161.

Das, A. (1988) *Agrobacterium tumefaciens* virE operon encodes a single-stranded DNA-binding protein. *Proc. Natl. Acad. Sci. U.S.A.* 85, 2909–2913.

Datta, K., Velazhahan, R., Oliva, N., Ona, I., Mew, T., Khush, G.S., Muthukrishnan, S., and Datta, S.K. 1999) Over-expression of the cloned rice thaumatin-like protein (PR-5) gene in transgenic rice plants enhances environmental friendly resistance to *Rhizoctonia solani* causing sheath blight disease. *Theor. Appl. Genet*. 98, 1138–1145.

Deng, W., Chen, L., Wood, D.W., Metcalfe, T., Liang, X., Gordon, M.P., Comai, L, and Nester, E.W. (1998) *Agrobacterium* VirD2 protein interacts with plant host cyclophilins. *Proc. Natl. Acad. Sci. USA* 95, 7040-7045.

Djamei, A., Pitzschke, A., Nakagami, H., Rajh, I., and Hirt, H. (2007) Trojan horse strategy in *Agrobacterium* transformation: abusing MAPK defense signaling. *Science* 318, 453–456.

Dobin, A., Davis, C.A., Schlesinger, F., Drenkow, J., Zaleski, C., Jha, S., Batut, P., Chaisson, M., and Gingeras, T.R. (2013) STAR: Ultrafast universal RNA-seq aligner. *Bioinformatics* 29, 15-21.

Dombek, P., and Ream, W. (1997) Functional domains of *Agrobacterium tumefaciens* single-stranded DNA-binding protein VirE2. *J. Bacteriol*. 179, 1165-1173.

Duan, K., Willig, C.J., De Tar, J.R., Spollen, W.G., and Zhang, Z.J. (2018) Transcriptomic analysis of *Arabidopsis* seedlings in response to *Agrobacterium*-mediated transformation process. *MPMI* 31, 445-459.

Du, Z., Zhou, X., Ling, Y., Zhang, Z., and Su, Z. (2010) agriGO: A GO analysis toolkit for the agricultural community. *Nucl. Acids Res*. https://doi.org/10.1093/nar/gkq310

El-kereamy, A., El-sharkawy, I., Ramamoorthy, R., Taheri, A., Errampalli, D., Kumar, P., and Jayasankar, S. (2011) *Prunus domestica* pathogenesis-related protein-5 activates the defense reponse pathway and enhances the resistance to fungal infection. *PloS ONE* 6, e17973.

García-Cano, E., Magori, S., Sun, Q., Ding, Z., Lazarowitz, S.G., and Citovsky, V. (2015) Interaction of *Arabidopsis* trihelix-domain transcription factors VFP3 and VFP5 with *Agrobacterium* virulence protein VirF. *PLOS ONE* DOI:10.1371/journal.pone.0142128, 1-23

García-Rodríguez, F.M., Schrammeijer, B., and Hooykaas, P.J. (2006) The *Agrobacterium* effector VirE3 effector protein: a potential plant transcriptional activator. *Nucleic Acid Res.* 34: 6496-6504.

Gaspar, Y.M., Nam, J., Schultz, C.J., Lee, L.-Y., Gilson, P.R., Gelvin, S.B., and Bacic, A. (2004) Characterization of the *Arabidopsis* lysine-rich arabinogalactan-protein *AtAGP17* mutant (*rat1*) that results in a decreased efficiency of *Agrobacterium* transformation. *Plant Physiol*. 135, 2162-2171.

Gelvin, S.B. (2003) *Agrobacterium*-mediated plant transformation: the biology behind the "gene-jockeying" tool. *Microbiol. Mol. Biol. Rev.* 67, 16-37.

Gelvin, S.B. (2012) Traversing the cell: *Agrobacterium* T-DNA's journey to the host genome. *Front. Plant Sci.* 3, 1-11.

Gietl, C., Koukolikova-Nicola, Z., and Hohn, B. (1987) Mobilization of T-DNA from *Agrobacterium* to plant cells involves a protein that binds single-stranded DNA. *Proc. Natl. Acad. Sci. U.S.A.* 84, 9006–9010.

Grange, W., Duckely, M., Husale, S., Jacob, S., Engel, A., and Hegner, M. (2008) VirE2: a unique ssDNA-compacting molecular machine. *PLoS Biol.* 6, e44. doi:10.1371/journal.pbio.0060044

Hood, E.E., Gelvin, S.B., Melchers, L.S., and Hoekema, A. (1993) New *Agrobacterium* helper plasmids for gene transfer to plants. *Trans. Res.* 2, 208-218.

Howard, E., and Citovsky, V. (1990) The emerging structure of the *Agrobacterium* T-DNA transfer complex. *BioEssays* 12, 103-108.

Koncz, C. and Schell, J. (1986) The promoter of T_L-DNA gene *5* controls the tissue-specific expression of chimaeric genes carried by a novel type of *Agrobacterium* binary vector. *Mol. Gen. Genet.* 204, 383-396.

Krastanova, S.V., Balaji, V., Holden, M.R., Sekiya, M., Xue, B., Momol, E.A., and Burr, T.J. (2010) Resistance to crown gall disease in transgenic grapevine rootstocks containing truncated *virE2* of *Agrobacterium*. *Transgenic Res.*, 19, 949-958

Krueger, F. (2017) Babraham Bioinformatics - Trim Galore! https://doi.org/10.1007/s10439-010-0153-9.Impact

Lapham, R., Lee L.-Y., Tsugama D., Lee S., Mengiste T., and Gelvin S.B. (2018) *VIP1* and its homologs are not required for *Agrobacterium*-mediated transformation, but play a role in *Botrytis* and salt stress responses. *Frontiers Plant Sci*. 9, 1-15.

Lee, L.-Y., Fang, M.-J., Kuang, L.-Y., and Gelvin, S. B. (2008) Vectors for multi-color bimolecular fluorescence complementation to investigate protein-protein interactions in living plant cells. *Plant Methods* 4, 24.

Lee, L.-Y., Wu, F.-H., Hsu, C.-T., Shen, S.-C., Yeh, H.-Y., Liao, D.-C., Fang, M.-J., Liu, N.-T., Yen, Y.-C., Dokládal, L., Sýkorová, E., Gelvin, S.B., and Lin, C.-S. (2012) Screening of a cDNA library for protein-protein interactions directly in planta. *Plant Cell*. 24, 1746-1759.

Li, J., Krichevsky, A., Vaidya, M., Tzfira, T., and Citovsky, V. (2005) Uncoupling of the functions of the *Arabidopsis* VIP1 protein in transient and stable plant genetic transformation by *Agrobacterium*. *Proc. Natl. Acad. Sci. USA* 102, 5733–5738.

Li, X., Yang, Q., Tu, H., Lim, Z., and Pan, S.Q. (2014) Direct visualization of *Agrobacterium*-delivered VirE2 in recipient cells. *Plant J*. 77, 487-495.

Li, X., and Pan, S.Q. (2017) *Agrobacterium* delivers VirE2 protein into host cells via clatherin-mediated endocytosis. *Sci. Adv.* 3, e1601528.

Liu, D., Raghothama, K.G., Hasegawa, P.M., and Bressan, R.A. (1994) Osmotin overexpression in potato delays development of disease symptoms. *Proc. Natl. Acad. Sci. USA* 91, 1888–1892.

Love, M.I., Huber, W., and Anders, S. (2014) Moderated estimation of fold change and dispersion for RNA-seq data with DESeq2. *Genome Biology*. https://doi.org/10.1186/s13059-014-0550-8

Mackintosh, C.A., Lewis, J., Radmer, L.E., Shin, S., Heinen, S.J., Smith, L.A., Wyckoff, M.N., Dill-Macky, R., Evans, C.K., Kravchenko, S., Baldridge, G.D., Zeyen, R.J., and Muehlbauer, G.J. (2007) Overexpression of defense response genes in transgenic wheat enhances resistance to *Fusarium* head blight. *Plant Cell Rep.* 26, 479–488.

Magori, S., and Citovksy, V. (2011) *Agrobacterium* counteracts host-induced degradation of its effector F-box protein. *Sci. Signal*, 4, ra69.

Mi, H., Muruganujan, A., Casagrande, J.T., and Thomas, P.D. (2013) Large-scale gene function analysis with the PANTHER classification system. *Nat. Protoc.* 8, 1551-1566.

Nam, J., Mysore, K.S., Zheng, C., Knue, M.K., Matthyssee, A.G., and Gelvin, S.B. (1999) Identification of T-DNA tagged *Arabidopsis* mutants that are resistant to transformation by *Agrobacterium*. *Mol. Gen. Genet.* 261, 429-438.

Narasimhulu, S.B., Deng, X.-B., Sarria, R., and Gelvin, S.B. (1996) Early transcription of *Agrobacterium* T-DNA genes in tobacco and maize. *Plant Cell* 8, 873-886.

Niu, X., Zhou, M., Henkel, C.V., Van Heusden, G.P.H., and Hooykaas, P.J.J. (2015) The *Agrobacterium tumefaciens* virulence protein VirE3 is a transcriptional activator of the F-box gene *VBF*. *Plant J.* 84, 914-924.

Park, S.-Y., Yin, X., Duan, K., Gelvin, S.B., and Zhang, Z.J. (2014) Heat shock protein 90.1 plays a role in *Agrobacterium*-mediated plant transformation. *Mol. Plant*. 7, 1793-1796.

Pitzschke, A., Djamei, A., Teige, M., Hirt, H. (2009) VIP1 response elements mediate mitogen-activated protein kinase 3-induced stress gene expression. *Proc. Natl. Acad. Sci. USA* 106, 18414-18419.

Robinson, M.D., McCarthy, D.J., and Smyth, G.K. (2010) edgeR: A Bioconductor package for differential expression analysis of digital gene expression data. *Bioinformatics*, *26*(1), 139–140.

Rossi, L., Hohn, B., and Tinland, B. (1996) Integration of complete transferred DNA units is dependent on the activity of virulence E2 protein of *Agrobacterium tumefaciens. Proc. Natl. Acad. Sci. U.S.A.* 93, 126-130.

Roushan, M.R., de Zeeuw, M.A.M., Hooykaas, P.J.J., and van Heusden, G.P.H. (2018) Application of phiLOV2.1 as a fluorescent marker for visualization of *Agrobacterium* effector protein translocation. *Plant J.* 96, 685-699.

Schultz, CJ., Rumsewicz, M.P., Johnson, K.L., Jones, B.J., Gaspar, Y.M., and Bacic, A. (2002) Using genomic resources to guide research directions. The arabiogalactan-protein gene family as a test case. *Plant Physiol.* 129, 1448-1463.

Sciaky, D., Montoya, A. L., and Chilton, M.-D. (1978) Fingerprints of *Agrobacterium* Ti plasmids. *Plasmid* 1, 238-253.

Sen, P., Pazour, G.J., Anderson, D., and Das, A. (1989) Cooperative binding of *Agrobacterium tumefaciens* VirE2 protein to single-stranded DNA. *J. Bacteriol.* 171, 2573–2580.

Seyfferth, C., and Tsuda, K. (2014) Salicylic acid signal transduction: The initiation of biosynthesis, perception, and transcriptional reprogramming. *Frontiers Plant Sci*. 5, 1-10.

Shi, Y., Lee L.-Y., and Gelvin S.B. (2014) Is VIP1 important for *Agrobacterium*-mediated transformation? *Plant J*. 79, 848-860.

Simone, M., McCullen, C.A., Stahl, L.E., and Binns, A.N. (2001) The carboxy-terminus of VirE2 from *Agrobacterium tumefaciens* is required for its transport to host cells by the *virB*-encoded type IV transport system. *Mol. Microbiol.* 41, 1283–1293.

Stachel, S.E., and Nester, E.W. (1986) The genetic and transcriptional organization of the *vir* region of the A6 Ti plasmid of *Agrobacterium tumefaciens*. *EMBO J.* 5, 1445-1454.

Tao, Y., Rao, P. K., Bhattacharjee, S., and Gelvin, S.B. (2004) Expression of plant protein phosphatase 2C interferes with nuclear import of the *Agrobacterium* T-complex protein VirD2. *Proc. Natl. Acad. Sci. USA* 101, 5164-5169.

Tenea, G.N., Spantzel, J., Lee L.-Y., Zhu, Y., Lin, K., Johnson, S.J., and Gelvin, S.B. (2009) Over-expression of several *Arabidopsis* histone genes increases *Agrobacterium*-mediated transformation and transgene expression in plants. *Plant Cell* 21, 3350-3367.

Thimm, O., Bläsing, O., Gibon, Y., Nagel, A., Meyer, S., Krüger, P., Selbig, J., Müller, L.A., Rhee, S.Y., and Stitt, M. (2004) MAPMAN: a user-driven tool to display genomics data sets onto diagrams of metabolic pathways and other biological processes. *Plant J.* 37, 914-939.

Tinland, B., Hohn, B., and Puchta, H. (1994) *Agrobacterium tumefaciens* transfers single-stranded transferred DNA (T-DNA) into the plant cell nucleus. *Proc. Natl. Acad. Sci. U.S.A.* 91, 8000–8004.

Trapnell, C., Williams, B.A., Pertea, G., Mortazavi, A., Kwan, G., van Baren, M.J., Salzberg, S.L., Wold, B.J., and Pachter, L. (2010) Transcript assembly and quantification by RNA-Seq reveals unannotated transcripts and isoform switching during cell differentiation. *Nat. Biotechnol*. 28, 511-515.

Trapnell C., Roberts A., Goff, L., Pertea, G., Kim, D., Kelley, D.R., Pimentel, H., Salzburg, S.L., Rinn, J.L., and Pachter, L. (2012) Differential gene and transcript expression analysis of RNA-seq experiments with TopHat and Cufflinks. *Nat. Protoc.* 7, 562-578.

Tsugama, D., Liu, S., and Takano, T. (2012) A bZIP protein, VIP1, is a regulator of osmosensory signaling in *Arabidopsis*. *Plant Physiol.* 159, 144-155.

Tsugama, D., Liu, S., and Takano, T. (2013) A bZIP protein, VIP1, interacts with *Arabidopsis* heterotrimeric G protein β subunit, AGB1. *Plant Physiol. & Biochem.* 71, 240-246.

Tsugama, D., Liu, S., and Takano, T. (2014) Analysis of functions of VIP1 and its close homologs in osmosensory responses of *Arabidopsis thaliana*. *PLOS ONE* 9, e103930.

Tsugama, D., Liu, S., and Takano, T. (2016a) The bZIP protein VIP1 is involved in touch responses in *Arabidopsis* roots. *Plant Physiol.* 171, 1355-1365.

Tsugama, D., Liu, S., and Takano, T. (2016b) VIP1 is very important/interesting protein 1 regulating touch responses of *Arabidopsis*. *Plant Sig, & Behav.* 11, e1187358.

Tzfira, T., Vaidya, M., and Citovsky, V. (2001) VIP1, an *Arabidopsis* protein that interacts with *Agrobacterium* VirE2, is involved in VirE2 nuclear import and *Agrobacterium* infectivity. *EMBO J.* 20, 3596–3607.

Tzfira, T., and Citovsky, V. (2001) Comparison between nuclear localization of nopaline- and octopine-specific *Agrobacterium* VirE2 proteins in plant, yeast and mammalian cells. *Mol. Plant Pathol.* 2, 171–176.

Tzfira, T., Vaidya, M., and Citovsky, V. (2004) Involvement of targeted proteolysis in plant genetic transformation by *Agrobacterium*. *Nature*, 431-87-92.

Tzfira, T., Tian, G.-W., Lacroiz, B., Vyas, S., Li, J., Leitner-Dagab, Y., Krishevsky, A., Taylor, T., Vainstein, A., and Citovsky, V. (2005) pSAT vectors: A modular series of plasmids for autofluorescent protein tagging and expression of multiple genes in plants. *Plant Mol. Biol.* 57, 503-516.

Van Larebeke, N., Engler, G., Holsters, M., Van Den Elsacker, S., Zaenen, I., Schilperoort, R.A., and Schell, J. (1974) Large plasmid in *Agrobacterium tumefaciens* essential for crown gall-inducing ability. *Nature* 252, 169-170.

Veena, Jiang, H., Doerge, R.W., and Gelvin, S.B. (2003) Transfer of T-DNA and Vir proteins to plant cells by *Agrobacterium tumefaciens* induces expression of host genes involved in mediating transformation and suppresses host defense gene expression. *Plant J.* 35, 219-236.

Wang, L., Song, X., Gu, L., Li, X., Cao, S., Chu, C., Cui, X., Chen, X., and Cao, X. (2013) NOT2 proteins promote polymerase-II dependent transcription with multiple microRNA biogenesis factors in *Arabidopsis*. *Plant Cell*, 25, 715-727.

Wang, Y., Peng, W., Zhou, X., Huang, F., Shao, L., and Luo, M. (2014) The putative *Agrobacterium* transcriptional activator-like virulence protein VirD5 may target T-complex to prevent the degradation of coat proteins in the plant cell nucleus. *New Phyto*. 203, 1266-1281.

Wang, Y., Zhang, S., Huang, F., Zhou, X., Chen, Z., Peng, W., and Luo, M. (2017) VirD5 is required for efficient *Agrobacterium* infection and interacts with *Arabidopsis* VIP2. *New Phyto*., doi: 10.1111/nph.14854

Wu, L., Chen, H., Curtis, C., and Fu, Z. Q. (2014) Go in for the kill: How plants deploy effector-triggered immunity to combat pathogens. *Virulence*. 5, 710-721.

Yusibov, V.M., Steck, T.R., Gupta, V., and Gelvin, S.B. (1994) Association of single-stranded transferred DNA from *Agrobacterium tumefaciens* with tobacco cells. *Proc. Natl. Acad. Sci. U.S.A.* 91, 2994–2998.

Zheng, Z., Qamar, S.A., Chen, Z., and Mengiste, T. (2006) Arabidopsis WRKY33 transcription factor is required for resistance to necrotrophic fungal pathogens. *Plant J.* 48, 592-605.

Ziemienowicz, A., Merkle, T., Schoumacher, F., Hohn, B., and Rossi, L. (2001) Import of *Agrobacterium* T-DNA into plant nuclei: two distinct functions of VirD2 and VirE2 proteins. *Plant Cell* 13, 369-383.

Zuo, J., Niu, Q.-W., and Chua, N.-H. (2000) An estrogen receptor-based system transactivator XVE mediates highly inducible gene expression in transgenic plants. *Plant J.* 24, 265–273.

FUTURE RESEARCH DIRECTIONS

We found that *VIP1* and its homologs are not necessary for *Agrobacterium*-mediated transformation, but *VIP1* may play a role in defense responses against the fungus *Botrytis cinerea*, in abscisic acid (ABA) signaling, and in growth under salt stress conditions (Lapham et al., 2018; Chapter 2 of this dissertation). Our results showed that plants lacking *VIP1* are more susceptible to *B. cinerea* infection, but the precise role of *VIP1* in response to *B. cinerea* infection is unknown. *B. cinerea* produces exogenous ABA to suppress plant defense responses (Audenaert et al., 2002; Fan et al., 2009; Sivakumaran et al., 2016) and ABA-deficient tomato plants are resistant to *B. cinerea* infection (Asselbergh et al., 2007). The *VIP1* target genes *CYP707A1* and *CYP707A3* are ABA degradation enzymes (Kushiro et al., 2004; Umezawa et al., 2006) and their activation by VIP1 may be important for defending against *B. cinerea* infection. Monitoring the expression of *VIP1* and its target genes, *CYP707A1* and *CYP707A3*, during early and late stages of *B. cinerea* infection could provide insight into their regulation and possible roles in fungal defense responses. The susceptibility of *VIP1* overexpressing plants to *B. cinerea* should also be tested. *vip1* mutant plants are more susceptible to *B. cinerea*; therefore, constitutive overexpression may help to resist *B. cinerea* infection. ABA levels within the infected plants could also be measured in both *vip1* mutant, *VIP1-SRDX*, and *VIP1* overexpressing plants throughout *B. cinerea* infection. This will help to determine if *VIP1*'s role in ABA signaling is crucial for defending against *B. cinerea* or if it participates in some other role. Finally, *vip1* mutant, *VIP1-SRDX*, and *VIP1* overexpressing plants could also be assayed with other fungal pathogens to determine if *VIP1* is important for defense against other fungal species.

We determined that cytoplasmic, but not nuclear, localized VirE2 was able to complement a *virE2* mutant *Agrobacterium* strain to restore transformation rates comparable to that of a wild-type strain (Chapter 3). We cannot rule out the possibility that a small amount of VirE2 localizes to the nucleus during transformation even if our results show that exclusive nuclear localization does not support transformation. To determine if exclusive **cytoplasmic** localization of VirE2 is required for its function or if VirE2 plays a minor role within the nucleus during transformation, plants could be generated which express VirE2-Venus tagged with a nuclear **export** signal (NES). These plants would then be tested with a *virE2* mutant

Agrobacterium strain to investigate if exclusive cytoplasmic localization of VirE2 can result in complementation of the mutant *Agrobacterium* strain as efficiently as it does with plants expressing VirE2-Venus.

Transcriptomic analyses showed that VirE2 changes the steady-state levels of certain plant RNAs, some of which are known to be important for transformation (Chapter 3). To investigate whether cytoplasmic or nuclear-localized VirE2 can mediate these plant gene expression changes, expression of genes which are up- or down-regulated in the presence of VirE2 could be measured using RT-qPCR in roots expressing VirE2-Venus (cytoplasmic-) or VirE2-Venus-NLS (nuclear-localized). This will help us determine if VirE2 must localize to the cytoplasm to modulate plant RNA levels.

Proteomic analyses revealed that certain plant proteins show increased levels in response to VirE2, and a subset of these proteins have previously been shown to be important for transformation. Overexpression of some of these proteins resulted in changes to transformation rates (Chapter 3). These overexpression lines will need to be assayed more extensively for both transient and stable transformation susceptibility to elucidate better their overall importance in transformation.

We observed that VirE2-induced changes to the plant proteome were overall more rapid than were changes to the plant transcriptome. We also found that proteins whose abundance changed at 3 hours post-induction did not exhibit any changes in the levels of their transcripts at the same time point (Chapter 3). These observations, along with the requirement for cytoplasmic localization of VirE2 to function in transformation, suggest that VirE2 mediates changes to plant RNA and protein levels post-transcriptionally. We observed that genes involved in translation are differentially expressed and enriched among genes which are up-regulated after 12 hours of VirE2 induction (Chapter 3). Some proteins involved in translation also showed changes in their steady-state levels post-VirE2 induction (Chapter 3).

The mechanism by which VirE2 modulates plant RNA and protein levels is unknown. VirE2 interacts with VIP2 (Anand et al., 2007), and VIP2 is known to be involved in miRNA biogenesis along with its homolog, At-Negative on TATA less 2a (NOT2a; Wang et al., 2013). VirE2 binding to VIP2 could inhibit or modify its function in some way. This could be investigated by performing small RNA profiling in the absence and presence of VirE2 to determine if VirE2 manipulates host miRNA abundance (Aldridge and Hadfield, 2011). The

targets of any miRNAs which show changes in response to VirE2 could be searched for within our RNA-seq and proteomics datasets. This study will allow us to identify correlations between changes in miRNA levels and changes in protein levels resulting from alterations in the translation and/or stability of their target transcripts. Transcriptional inhibitors could also be used to measure the stability of mRNAs post-VirE2 induction to determine if some transcripts are stabilized or decay faster in the presence of VirE2 (Cheneval, et al., 2010). Two different techniques can be used to determine if VirE2 affects translation of specific proteins. Ribosome profiling or Ribo-seq could be performed on inducible VirE2 plants to identify which proteins are actively translated at various time points after VirE2 induction (Ingolia, 2014). Global run-on sequencing (GRO-seq) could be used to measure which genes are actively transcribed in the presence of VirE2 since our RNA-seq analysis only allows us to measure steady-state levels of RNA (Lopes et al., 2017). These techniques would allow us to identify more accurately which transcripts or proteins may be directly versus indirectly impacted by VirE2. Finally, immunoprecipitation could be used to isolate VirE2 and any associated proteins/protein complexes. This could be done at multiple time points post-VirE2 induction to determine if VirE2 interacts with different proteins during the various stages of infection. This study would provide insight into the possible mechanism by which VirE2 impacts both plant RNA and protein levels.

VirE2 could be manipulating plant RNA and protein levels in a variety of ways. The rapid changes we observe in plant protein levels followed by more delayed changes in RNA levels, along with VirE2's cytoplasmic localization, suggest that VirE2 mediates these changes post-transcriptionally. These changes could be achieved by manipulating plant miRNA levels via VirE2 interactions with VIP2 or other proteins, increasing the stability/decay of certain mRNAs, and/or promoting or inhibiting translation of certain transcripts. Our results suggest that VirE2 manipulates both plant RNA and protein levels to facilitate transformation. The mechanism by which VirE2 achieves this will be the focus of future research.

References

Aldridge, S. and Hadfield, J. (2011) Introduction to miRNA profiling technologies and cross-platform comparison. *Meth. Mol. Biol.* 822, 19-31.

Anand, A., Krichevsky, A., Schornack, S., Lahaye, T., Tzfira, T., Tang, Y., Citovsky, V., and Mysore K.S. (2007) *Arabidopsis* VirE2 INTERACTING PROTEIN 2 is required for *Agrobacterium* T-DNA integration in plants. *Plant Cell* 19, 1695-1708.

Asselbergh, B., Curvers, K., Franc¸a, S. C., Audenaert, K., Vuylsteke, M., Van Breusegem, F., Höfte, M. (2007) Resistance to *Botrytis cinerea in sitiens*, an abscisic acid-deficient tomato mutant, involves timely production of hydrogen peroxide and cell wall modifications in the epidermis. *Plant Physiol*. 144, 1863–1877.

Audenaert, K., De Meyer, G. B., and Höfte, M. (2002) Abscisic acid determines basal susceptibility of tomato to *Botrytis cinerea* and suppresses salicylic acid dependent signaling mechanisms. *Plant Physiol*. 128, 491–501.

Cheneval, D., Kastelic, T., Fuerst, P., and Parker, C.N. (2010) A review of methods to monitor the modulation of mRNA stability: a novel approach to drug discovery and therapeutic intervention. *J. Biomol. Screen*. 15, 609-622.

Fan, J., Hill, L., Crooks, C., Doerner, P., and Lamb, C. (2009) Abscisic acid has a key role in modulating diverse plant-pathogen interactions. *Plant Physiol*. 150, 1750–1761.

Ingolia, N.T. (2014) Ribosome profiling: new views of translation, from single codons to genome scale. *Nat. Rev, Genet,* 15, 205-213.

Kushiro, T., Okamoto, M., Nakabayashi, K., Yamagishi, K., Kitamura, S., Asami, T., Hirai, N., Koshiba, T., Kamiya, Y., and Nambara, E. (2004) The Arabidopsis cytochrome P450 CYP707A encodes ABA 8'-hydroxylases: key enzymes in ABA catabolism. *EMBO J*. 23, 1647–1656.

Lapham, R., Lee L.-Y., Tsugama D., Lee S., Mengiste T., and Gelvin S.B. (2018) *VIP1* and its homologs are not required for *Agrobacterium*-mediated transformation, but play a role in *Botrytis* and salt stress responses. *Frontiers Plant Sci*. 9, 1-15.

Lopes, R., Agami, R., and Korkmaz, G. (2017) GRO-seq, a tool for identification of transcripts regulating gene expression. *Methods Mol. Biol.* 1543, 45-55.

Sivakumaran, A., Akinyemi, A., Mandon, J., Cristescu, S. M., Hall, M. A., Harren, F. J. M., and Mur, L. A. J. (2016) ABA suppresses *Botrytis cinerea* elicited NO production in tomato to influence H_2O_2 generation and increase host susceptibility. *Front. Plant Sci*. 7:709.

Umezawa, T., Okamoto, M., Kushiro, T., Nambara, E., Oono, Y., Seki, M., Kobayashi, M., Koshiba, T., Kamiya, Y., and Shinozaki, K. (2006) CYP707A3, a major ABA 8'-hydroxylase involved in dehydration and rehydration response in *Arabidopsis thaliana*. *Plant J*. 4, 171–182.

Wang, L., Song, X., Gu, L., Li, X., Cao, S., Chu, C., Cui, X., Chen, X., and Cao, X. (2013) NOT2 proteins promote polymerase-II dependent transcription with multiple microRNA biogenesis factors in *Arabidopsis*. *Plant Cell*, 25, 715-72.

VITA

EDUCATION

Ph. D., Biological Sciences, Purdue University, West Lafayette, IN **Graduation:** May 2019
Dissertation: *Role of Agrobacterium Effector Protein VirE2 in Modulating Plant Gene Expression*
GPA: 4.00/4.00

B.S., Biology, Purdue University, West Lafayette, IN **Graduation:** May 2012
Majors: Genetic Biology and Microbiology **GPA:** 3.87/4.00
Minors: Chemistry and German
Undergraduate Honors Research Program, Biology and College of Science Honors Programs

RESEARCH EXPERIENCE

Research Scientist, *Transformation Lab* (Line Manager: Kari Perez) *Calyxt, Inc.* (Roseville, MN) **Start Date: July 1st, 2019**

Graduate Research Assistant (Ph.D.), *Plant Molecular Biology Laboratory* (Advisor: Dr. Stanton Gelvin) *Purdue University* (West Lafayette, IN) **Aug. 2013-Present**

- Studied effect of virulence protein VirE2 from plant pathogen, *Agrobacterium tumefaciens*, on plant host gene expression and the plant immune system using molecular biological and Next Generation Sequencing techniques.
- Studied bacterial and host protein interactions involved in *Agrobacterium*-mediated plant genetic transformation.
- Training and mentoring of undergraduate researchers, rotation students, and research interns from Taiwan, China, Nigeria, Ecuador, India, Albania, France, Colombia, and America.
- Managed daily lab operations when my advisor was traveling (2-4 months out of the year).
- Fostered and coordinated research collaborations with laboratories in Ireland and Japan.
- Presented research findings at two international *Agrobacterium* research conferences in Europe (2016 and 2018), four national annual Crown Gall conferences meetings (2014-2017), and one American Society of Plant Biologists (ASPB) Midwestern meeting (2018).

Contractor Molecular Biology, *Molecular Biology: Trait Product Development* (Supervisor: Rodrigo Sarria and Sandra Toledo) *Dow AgroSciences through Kelly Services* (West Lafayette, IN) **Oct. 2012- Aug. 2013**

- Created *Agrobacterium* strains, screened constructs, and analyzed samples for soybean and canola transformation labs.
- Performed transformation, tissue culture, and sampling of transgenic soybean plants.

Summer Intern, *Molecular Biology: Trait Product Development* (Supervisor: Dr. Sandeep Kumar) *Dow AgroSciences through Kelly Services* (Indianapolis, IN) **May 2012-Aug. 2012**

- Designed and cloned constructs for testing of bidirectional expression promoters for use in multiple transgene stacking.
- Created *E.coli* and *Agrobacterium* strains containing the constructs for testing in *Zea mays* transformation.

Undergraduate Research Assistant, *Undergraduate Honors Research Program, Plant Cell Wall Genetics Laboratory* (Advisor: Dr. Maureen McCann) *Purdue University*
Jan. 2009-May 2012

- Co-lead a genetic research project focused on the characterization and classification of MYST gene family: a seven member plant cell wall gene family of unknown function found in *Arabidopsis*, by loss-of-function mutant analysis, phenotypic characterization, mutant rescue, and genotyping
- Presented research findings at one ASPB Midwestern Regional meeting (2011) and one ASPB National Meeting (2011).

Assistant Field Manager, *Undergraduate Research Internship, Plant Cell Wall Biochemistry Laboratory* (Advisor: Dr. Nicholas Carpita) *Purdue University* **May 2010-Aug. 2010**

- Coordinated sample collection, field upkeep (weeding, spraying, etc.), pollination, and harvest of maize.
- Organized lignin analysis in maize via chemical staining and imaging with a six-member research team.
- Prepared corn stover samples for lignocellulose analysis via pyrolysis and mass spectrometry analysis while making extensive length and diameter measurements of stover samples.

SKILLS

Professional

- Scientific writing and communication
- Organization, planning, and hosting of scientific conferences and symposia
- Teaching and training of undergraduate researchers and new employees in laboratory techniques and safety
- Writing and designing experimental protocols and scientific projects
- Teaching microbiology and genetics in a classroom and laboratory setting
- Designing and managing field trials
- Networking and managing collaborations with international researchers
- Tutoring and assisting students with learning or physical disabilities

Laboratory

- Restriction/Ligation, Gateway, and recombinant DNA cloning
- *E. coli* and *Agrobacterium* strain mobilization and transformation
- DNA and RNA extraction and analysis via polymerase chain reaction (PCR), reverse transcriptase (RT)-PCR, and Real-time (quantitative) PCR
- PCR genotyping and generation of mutant plants using CRISPR gene editing
- Analysis of RNAseq data
- Analysis of proteomics data

- Media preparation for bacterial and plant populations using sterile technique
- *Agrobacterium*-mediated plant transformation in *Arabidopsis*, tobacco, canola, and soybean
- Plant tissue culture (mostly soybean and *Arabidopsis*)
- Maintenance, care, and preparation of tobacco (BY2) protoplasts for use in recombinant fluorescent protein expression and imaging
- Fluorescent and light microscopy (Bimolecular fluorescence complementation, confocal, and wide-field epifluorescence microscopy)
- Western blot protein analysis
- Sampling and care for plant populations of *Zea mays* (maize), *Glycine max* (soybean), *Kalanchoe*, *Nicotiana benthamiana* and *Arabidopsis thaliana*

Software

- Microsoft Excel, Powerpoint, Word, and Outlook
- Programming experience in Perl, Unix, and Python
- Virtual cloning (Vector NTI) and image processing software (ImageJ)

PUBLICATIONS

Lapham, RA., L.Y. Lee, D. Tsugama, S. Lee, T. Mengiste, S.B. Gelvin. (June 2018) *VIP1 and its homologs are not required for Agrobacterium-mediated transformation, but may play a role in Botrytis cinerea and salt stress responses*. Frontiers in Plant Science.
https://doi.org/10.3389/fpls.2018.00749

Lapham, RA., L.Y. Lee, and S.B. Gelvin. (In preparation) *A novel role for the Agrobacterium virulence effector protein VirE2 in modulating plant gene expression.*

Buuck, RA., 2012. *Mapping Genomes: A Novel Gene Family in Plants may Encode Pectin-modifying Proteins* in Journal of Purdue Undergraduate Research second issue (Available at http://docs.lib.purdue.edu/jpur/).

TEACHING EXPERIENCE

Teaching Assistant, *American Society of Plant Biologists Conviron Scholars Program*
Oct. 2018-Present

- Provided feedback on student technical writing and presentation assignments.
- Maintained and updated the program website and scholar network.

Graduate Assistant, *College of Science: Summer Undergraduate Research Fellowship (SURF) Program, Purdue University* **May 2017-Aug. 2017**

- Taught students how to write literature reviews, research abstracts, and reports.
- Organized and taught workshop on how to prepare scientific research talks and posters.
- Coordinated and organized speakers for research and professional development seminars and meetings.
- Prepared the program booklet for the 2017 SURF symposium and organized student oral presentations.

Teaching Assistant, *Department of Biological Sciences, Purdue University*

Aug. 2016-May 2017

- Taught Microbiology Lab (BIOL221) under the supervision of Dr. Kiryl Datsenka (Spring 2017).
- Edited and assisted in writing a new version of the class lab manual.
- Taught General Microbiology (BIOL438) lecture course with Dr. Laszlo Csonka (Fall 2016).

Tutor and Note-taker, *Disability Resource Center*, *Purdue University* **Sept. 2013-Aug. 2017**

- Tutored students with learning disabilities enrolled in introductory biology courses
- Attended lectures and took notes for students who are hearing impaired.

Biology and Biochemistry Tutor, *Tutor Matching Service, Purdue University*
Jan. 2014-Aug. 2017

- Certified in Tutor Essentials training course provided by Purdue University
- Tutored undergraduates in a variety of courses including population genetics, molecular genetics, biochemistry, and microbiology
- Tutored high school students enrolled in Advanced Placement (AP) Biology

SCIENCE OUTREACH, PROFESSIONAL DEVELOPMENT, AND LEADERSHIP EXPERIENCE

Secretary: Purdue University Center for Plant Biology Trainee Association
November 2018-Present

- Organized and recruited the first executive board of the Center for Plant Biology (CPB) post-doctoral and graduate student trainee association (CPBTA).
- Drafted constitution for the CPBTA.
- Worked in conjunction with executive board and CPB faculty members to create career and professional development activities for all CPB trainees.

Science Advocate, Writer, and Educator: drunkphytologist.wordpress.com
May 2018-Present

- Creator of the "Daily Dose of SCIENCE" blog discussing the wonders of nature, biology, and new scientific discoveries.
- Promoted new blog posts on social media sites such as Twitter, Facebook, Discord, and LinkedIn.
- Created Youtube videos demonstrating molecular and microbiological techniques.
- Hosted monthly question and answer stream on twitch.tv/drunkphytologist, discussing various science topics and answering audience questions.

Social Media Coordinator: Purdue Cell and Molecular Biology (CMB)
August 2018-Present

- Promoted and wrote about the achievements and research of faculty, staff, and students in the CMB research group on Facebook and Twitter.

Plant Sciences Symposium Planning Committee **January 2017-December 2018**

- Planned and hosted with other graduate committee members the Purdue annual plant science symposium, sponsored by DuPont Pioneer.
- Maintained and updated social media pages to advertise the event.

Biology Graduate Student Association (BGSA): Purdue University **August 2013-Present**

- Served as **president** of the BGSA from May 2016 to May 2017.
- Coordinated and oversaw the work of the other officers.
- Planned orientation, recruitment events and the annual BGSA symposium.
- Served as "Big Sister" and mentor to first year incoming biology Ph. D students.
- Acted as the **biology graduate student representative** at faculty meetings, meetings of the Purdue Graduate Student Government, and meetings of the Deans of the Graduate School for the College of Science.

HONORS & AWARDS

Bilsland Dissertation Fellowship, *Purdue University* Feb. 2018
Travel Award, *38th Annual Crown Gall Conference 2017* Sept. 2017
American Society of Plant Biologists (ASPB) Conviron Scholar Aug. 2017
Graduate Honor Roll, *Purdue University* Apr. 2017
Yeunkyung Woo Achieve Excellence Travel Award, *Purdue University* Aug. 2016
First Year Research Foundation Research Grant, *Purdue Research Foundation* Apr. 2015
Frederick N. Andrews Graduate Assistantship, *Purdue University* Aug. 2013
Graduate Fellowship Incentive Award Nov. 2013
Kelly Services Employee Recognition, *Kelly Services at Dow AgroSciences* Aug. 2013
Outstanding Undergraduate Oral Presentation, *ASPB Midwestern Regional Meeting* Mar. 2011
Dr. Eric Dwayne Miller Memorial Scholarship, *Purdue University* Sept. 2010
Biology Outstanding Undergraduate Scholarship, *Purdue University* Sept. 2010
Golden Key International Honor Society Dec. 2009
Alpha Lambda Delta Phi Eta Sigma National Honor Society Mar. 2009
Trustee's Scholarship, *Purdue University* Aug. 2008
Valedictorian Scholarship, *Purdue University* Aug. 2008
Intellect Merit Scholarship, *Adams County Community Foundation* Aug. 2008
Valedictorian Scholarship, *Decatur Rotary Club* Aug. 2008
SSACI Hoosier Scholar Award, *State Student Assistance Commission of Indiana* Aug. 2008